Silica Export and its Relation to Nitrogen and Phosphorus in the Danube River Basin

Jessica Sara Salcedo Borda

Silica Export and its Relation to Nitrogen and Phosphorus in the Danube River Basin Jessica Sara Salcedo Borda

Propositions

1. Long residence time in reservoirs reduces silica concentrations in downstream rivers.
   (This thesis)

2. Ecological stoichiometry links earth science, chemistry, and ecology in an elegant and beautiful way.
   (This thesis)

3. Commonly used definitions of a catchment do not account for modern day water management.

4. The effectiveness of water management policy requires the application of updated science.

5. Progress can only be made with Thomas Edison's *"always trying one more time"* attitude.

6. The formal entitlement to paternity leave in a society reflects how that society sees the roles of fathers in the raising of children.

Propositions belonging to the thesis, entitled

Silica export and its relation to nitrogen and phosphorus in the Danube River Basin

Jessica Sara Salcedo Borda

Wageningen, 3 April, 2023

SILICA EXPORT AND ITS RELATION TO NITROGEN AND PHOSPHORUS IN THE DANUBE RIVER BASIN

Jessica Sara Salcedo Borda

Thesis committee

Promotor
Prof. Dr K.A. Irvine
Professor of Aquatic Ecosystems, IHE Delft Institute for Water Education
Professor of Aquatic Ecology and Water Quality Management, Wageningen University & Research

Co-promotor
Dr G.M. Gettel
Associate Professor in Aquatic Biogeochemistry, IHE Delft Institute for Water Education

Other members
Prof. Dr C. Kroeze, Wageningen University & Research
Prof. Dr T. Hein, University of Natural Resources and Life Sciences-BOKU, Austria
Prof. em. Dr B. Wehrli, ETH Zurich, Switzerland
Dr J. Garnier, Pierre and Marie Curie University, Sorbonne University, France

This research was conducted under the auspices of the Graduate School for Socio-Economic and Natural Sciences of the Environment (SENSE)

SILICA EXPORT AND ITS RELATION TO NITROGEN AND PHOSPHORUS IN THE DANUBE RIVER BASIN

submitted in fulfilment of the requirements of

the Academic Board of Wageningen University and

the Academic Board of the IHE Delft Institute for Water Education

for the degree of doctor

to be defended in public

on Monday, 03 April 2022, at 13:30 p.m.

in Wageningen, the Netherlands

by Jessica Sara Salcedo-Borda
Born in Lima, Peru

Published by:
IHE Delft Institute for Water Education
www.un-ihe.org

ISBN 978-90-73445-49-9 (IHE Delft)
ISBN: 978-94-6447-541-8 (Wageningen University& Research)
DOI: https://doi.org/10.18174/583907

To my family

ACKNOWLEDGEMENTS

First of all, I would like to express my sincere gratitude to my promotor Prof. Ken Irvine, supervisor Dr. Gretchen Gettel, and Dr. Anne van Dam in these years. You provided me with creative and innovative ideas, critical thought and advice that inspired me during my PhD research.

The work was made possible through the financial contribution through research grants from FINCyT Program, Peru (Agreement Nº 077- FINCyT-BDE-2014) and the Schlumberger Foundation Faculty for the Future. Also, thanks to Jonas Schoelynck from University of Antwerp on discussion and training on different methods to determine silica concentrations and Alessandro Amaranto for his help with R scripts.

I would like to thank the IHE-Delft laboratory staff for providing the necessary materials and the Institute of Meteorology and Climate Research Atmospheric Environmental Research (IMK-IFU) in Garmisch-Partenkirchen, Germany for the logistical support during field work.

I am grateful to Jolanda and Anique for all the administrative support. Also, there are no words to convey my feelings to all my friends in Delft for being here all this time.

I do not think I would ever get to finish my PhD without my family, my husband, and my best friend, Maurizio, my daughter Larita, and my parents Rolando and Aida. In these last years you were always there to cheer me up. My journey would not have been possible without your continuous and unlimited support and help. Thanks for your love, encouraging me in all of my pursuits and inspiring me to follow my dreams.

Jessica Sara Salcedo-Borda
IHE Delft Institute for Water Education, Delft, The Netherlands
October 2022

SUMMARY

Changes in Silica (Si) delivery to coastal systems, caused by human activities (e.g. reservoir construction, agricultural development, de-forestation, and urbanization) can cause shifts in phytoplankton community structure, with impacts through the whole aquatic food web. Although nutrient exports of nitrogen (N) and phosphorous (P), and the impacts of human activity on these are relatively well understood, the extent and potential impact on the combined effects on Si, N, and P ratios are rarely evaluated simultaneously in one basin. By using data from fieldwork and long monitoring datasets from International Commission for the Protection of the Danube River (ICPDR), I assessed the effects of natural and human controlling factors on nutrient loads and stoichiometry for Si, N, P in the Danube River and its tributaries.

The specific objectives of this thesis are *Objective 1*: Investigate the nutrient concentrations and ratios (Si, N, and P) in several high-altitude basins in the upper part of the Danube River (Austria and Germany); *Objective 2*: Describe spatial and temporal variation in dissolved Silica (DSi) loads and yields in its main tributaries and to assess the contribution of DSi from the tributaries to the Danube River and identify the controlling factors of DSi yields in the Danube River, including lithology, land use and land cover, and water infrastructure (reservoirs and waste water treatment plants); and *Objective 3*: Describe spatial and temporal variation in nutrient (DSi, dissolved inorganic nitrogen - DIN, and phosphate - PO_4) concentration, loads and ratios and to evaluate the controlling factors on the nutrient stoichiometry (N:Si:P) in the Danube River.

In the Upper Danube River Basin (Austria and Germany), 74 sites were sampled in 2015 and 2016 for dissolved Si (DSi), total dissolved nitrogen (TDN) and total dissolved phosphorus (TDP) (*Objective 1*). Concentrations of DSi ranged from 0.1 to 5.5 mg L^{-1} and were significantly lower in the streams and long-residence time reservoirs compared to run-of-the river reservoirs (RRHs) (Kruskal-Wallis; $p < 0.05$). TDN and TDP concentrations ranged from 0.09 to 1.9 mg/L and from 2 to 60 µg L^{-1}, respectively. The highest TDN and TDP concentrations were found in the RRHs (medians 0.63 mg L^{-1} and 12.29 µg L^{-1}, respectively), and were significantly greater than in inlets and reservoirs with long residence time (Kuskal-Wallis post-hoc test; $p < 0.001$). DSi yield (tonnes km^{-2} $year^{-1}$) was related positively to % coniferous forest land cover and % metamorphic rocks (lithology). In contrast, TDN and TDP yields were both related positively to % agriculture, but not lithology or forest cover. The study showed that in natural alpine streams, there is a higher tendency for N limitation, while reservoirs with a residence ~1 year tended to Si and P limitation, and river systems lower the catchment which are influenced by agricultural activities showed higher P limitation, and were not strongly affected by retention in the run-of-the river reservoirs.

In order to analyse Si together with N and P in the whole Danube River Basin, loads and yields were calculated from nutrient concentration and discharge data for years 1998 – 2017, which were available from the ICPDR long-term monitoring database (*Objective 2*). DSi loads in the mainstem of the Danube Basin ranged from 0.001 to 378 kt $month^{-1}$ (1 kt = 1000 metric tonnes), with loads generally increasing from upstream to downstream. There was an abrupt increase in loads to the Danube River after the entry of the Sava and Tisza tributaries, due to their high discharge, which was register in Bazias station. Using a statistical mixed modelling approach, I showed that land use was the most important factor controlling DSi yield. Specifically, DSi yield was negatively impacted by the ratio of agricultural and forest areas, and the proportion of grasslands in the catchment. I attribute this negative effect to the uptake and harvest of Si which removes plant biomass, specifically that which contains phytoliths, which leads to a subsequent reduction of soil recycling Si and further export to surface water.

Nutrient ratios in the overall Danube basin showed a general trend for Si and P limitation for phytoplankton communities when compared to Redfield and Dupas ratio (N:P:Si = 16:15:40) (*Objective 3).* In the mainstem, the DIN:DSi ratios were above the threshold value of N:Si =~1 showing Si limitation. DSi:PO_4 ratios were mostly higher than the threshold value Si:P =~16, while all DIN:PO4 ratios were higher than N:P =~16, which both indicate P limitation. DIN:DSi and DSi:PO_4 were related positively and negatively to the proportion of agriculture and forest, respectively. DSi:PO_4 was related positively to the proportion grassland area, while DIN:PO_4 was positively related to the proportion of the catchment covered by artificial land cover and negatively to wastewater treatment plant density.

The overall findings of this thesis indicate that LULC is the major controlling factor for Si export and its ratios with N and P at a basin scale, and that this factor tend to maintain overall P limitation in the basin. Moreover, analysis of data at Reni monitoring station just upstream from the Danube Delta showed that there has been a decrease in DIN and DSi loads from the entire Danube over time (since 2000), indicating a high risk of eutrophication in the Black Sea due to DSi reduction.

SAMENVATTING

Veranderingen in het transport van silicium (Si) naar de kust, die veroorzaakt worden door bijvoorbeeld de constructie van stuwdammen, landbouwontwikkeling, ontbossing of verstedelijking kunnen de oorzaak zijn van verschuivingen in de soortenverhoudingen van fytoplanktongemeenschappen en gevolgen hebben voor het gehele aquatische voedselweb. Alhoewel redelijk goed bekend is hoe het transport en de export van stikstof (N) en fosfor (P) beïnvloed worden door menselijke economische bedrijvigheid is het gezamenlijke effect van veranderingen in de verhoudingen van Si, N en P in een stroomgebied zelden onderzocht. Door gebruik te maken van gegevens uit veldmetingen, in combinatie met langere tijdreeksen uit de database van de Internationale Commissie voor de Bescherming van de Donau (International Commission for the Protection of the Danube River, ICPDR) heb ik een schatting gemaakt van de effecten van zowel natuurlijke als anthropogene factoren die de nutriëntenvracht en stoichiometrie van Si, N en P in Donau en zijn zijrivieren beïnvloeden.

De doelstellingen van dit proefschrift waren: Doelstelling 1. De concentraties van nutriënten (Si, N, P) en hun verhoudingen onderzoeken in een aantal hooggelegen stroomgebieden in het bovenstroomse deel van de Donau in Oostenrijk en Duitsland; Doelstelling 2. De variatie in ruimte en tijd beschrijven van de hoeveelheden opgeloste silicium (DSi) in de belangrijkste zijrivieren van de Donau en hoeveel deze bijdragen aan de totale hoeveelheid DSi in de Donau, en het bepalen van de factoren die deze totale DSi-vracht bepalen zoals bijvoorbeeld de lithologie, landgebruik, en waterinfrastructuur (reservoirs en waterzuiveringsinstallaties); Doelstelling 3. De variatie in ruimte en tijd beschrijven van concentraties, totale hoeveelheden en verhoudingen van nutriënten (DSi; DIN, oplosbare stikstof; en PO_4, fosfaat) in de Donau zelf, en ophelderen welke factoren de stoichiometrie van N, Si en P beïnvloeden.

In 2015 en 2016 werden in het bovenstroomse gebied van het Donaubekken (in Oostenrijk en Duitsland) 74 locaties bemonsterd voor opgeloste silicium (DSi), totale opgeloste stikstof (TDN) en totaal opgelost fosfaat (TDP) (Doelstelling 1). De concentraties DSi varieerden van 0.1 to 5.5 mg/L en waren significant lager in kleine riviertjes en stuwdammen dan in rivierwaterkrachtcentrales (RRHs) (Kruskal-Wallis test; $p < 0.05$). De concentraties TDN en TDP varieerden van 0.09 tot 1.9 mg/L, respectievelijk 2 to 60 µg/L. De hoogste TDN en TDP concentraties werden gevonden in de RRHs (mediaan respectievelijk 0.63 mg/L en 12.29 µg/L), en waren significant hoger in de inlaten van de stuwdammen en de stuwdammen zelf (Kruskal-Wallis post-hoc test, $p < 0.001$). De specifieke DSi-vracht (in tonnes km^{-2} year^{-1}) toonde een positief verband met de percentages naaldbossen in het landgebruik en metamorfe gesteente in de lithologie.

Daarentegen vertoonden de specifieke TDN- en TDP-vracht beide een verband met het percentage landbouw in het landgebruik, maar niet met lithologie of bosbedekking. De resultaten lieten zien dat in natuurlijke alpine rivierstromen N-limitering de overhand heeft, terwijl in stuwdammen met een hydraulische retentietijd van ongeveer 1 jaar Si- en P-limitering belangrijker zijn. Lager gelegen delen van het riviersysteem die meer onder invloed staan van landbouwactiviteiten vertoonden meer P-limitering, en ondervonden nauwelijks invloed van de riviercentrales.

Met het oog op een analyse van Si in samenhang met N en P in het gehele stroomgebied van de Donau werden de totale en specifieke nutriëntenvrachten berekend op basis van de nutriëntenconcentraties en afvoerdebieten in de jaren 1998-2017, die beschikbaar waren in de ICPDR database met monitoringgegevens (Doelstelling 2). De total DSi-vracht in de hoofdtak van de Donau varieerde tussen 0.001 en 378 kt/maand (1 kt = 1000 ton), waarbij de vracht over het algemeen toenam in de benedenstroomse richting. Waar de Sava en Tisza met de hoofdtak samenkomen nam de DSi-vracht abrupt toe als gevolg van de hoge afvoer van deze zijrivieren, zoals in het station Bazias kon worden waargenomen. Door middel van een gemengd statistisch model ("mixed model") kon ik aantonen dat landgebruik de belangrijkste factor was die de specifieke DSi-vracht bepaalde. De specifieke DSi-vracht werd negatief beïnvloed door de verhouding landbouw:bosareaal, en door het percentage grasland in het landgebruik van het stroomgebied. Dit negatieve effect verklaar ik uit de opname en vervolgens verwijdering van Si in plantaardige biomassa, in het bijzonder biomassa die fytolithen bevat, waardoor de Si vervolgens niet meer in de bodem terechtkomt en uitstroomt in het oppervlaktewater. In vergelijking met de Redfied en Dupas ratio's (N:P:Si = 16:15:1) wezen de verhoudingen in nutriënten in het gehele stroomgebied van de Donau op een trend in de richting van Si- en P-limitering voor fytoplanktongemeenschappen. In de hoofdtak waren de DIN:DSi verhoudingen grotendeels hoger dan de drempelwaarde N:Si = ~1, hetgeen Si-limitering betekent. De DSi:PO_4 verhoudingen waren meestal hoger dan de drempelwaarde Si:P = ~16, terwijl de DIN:PO_4 verhouding altijd boven de N:P = ~16 waren, hetgeen allebei duidt op P limitering. DIN:DSi was positief, en DSi:PO_4 negatief gerelateerd aan de verhouding landbouw:bosareaal. DSi:PO_4 toonde een positieve relatie met het percentage grasland in het landgebruik, terwijl DIN:PO_4 positief gerelateerd was aan het percentage "kunstmatig" landgebruik, en negatief aan de dichtheid van waterzuiveringsinstallaties.

Concluderend laat het onderzoek in dit proefschrift zien dat landgebruik en grondbedekking de belangrijkste regulerende factor is voor transport en export van Si en voor de verhoudingen van Si met N en P in het stroomgebied, en dat dit de algehele P-limitering in het stroomgebied in stand houdt. Een analyse van gegevens voor het monitoring station in Reni, vlak voor het begin van de Donaudelta, laat zien dat sinds het jaar 2000 de DIN en DSi vrachten in de Donau gestaag afnemen. Daardoor ontstaat er een hoog risico op eutrofiëring van de Zwarte Zee door de afname van DSi.

CONTENTS

Acknowledgements ... **vii**
Summary ... **viii**
Samenvatting ... **x**
Contents ... **xiii**
1 Introduction ... **1**
1.1 The importance of silica to ecosystems ... 2
1.2 Controlling factors of Si and nutrient export ... 3
1.3 Case Study ... 5
1.4 Significance of the study ... 11
1.5 Objectives ... 12
1.6 Hypotheses of the study ... 13
1.7 Outline of the thesis ... 13
2 Control of Si export and nutrient (N, P) stoichiometry in hydropower reservoirs and headwater rivers of the Danube River Basin ... **15**
2.1 Introduction ... 16
2.2 Methods ... 18
2.2.1 Study Area ... 18
2.2.2 Sampling ... 19
2.2.3 Si, N, P and Cl concentrations ... 20
2.2.4 Phytoplankton identification and counting ... 20
2.2.5 LULC and lithology analysis ... 22
2.2.6 Hydrological factors ... 22
2.2.7 Statistical analysis ... 24
2.3 Results ... 25
2.4 Discussion ... 35
2.5 Conclusions ... 45
3 Dissolved Silica in the Danube River Basin ... **47**
3.1 Introduction ... 48
3.2 Methods ... 50
3.2.1 Study area ... 50
3.2.2 Water quality and discharge data ... 50
3.2.3 LULC analysis ... 52
3.2.4 Lithology analysis ... 52

3.2.5 Major water infrastructure ... 52
3.2.6 Data analysis ... 53
3.3 Results ... 54
3.3.1 Spatial and temporal variation of monthly silica loads ... 54
3.3.2 DSi load contribution of tributaries to the Danube River ... 55
3.3.3 Annual DSi yields of tributaries to the Danube River ... 57
3.3.4 Influence of land use, lithology and water infrastructure on DSi yields in the Danube basin ... 57
3.4 Discussion ... 61
3.5 Conclusions ... 74
4 Nutrient stoichiometry of nitrogen, phosphorus, and silica in the Danube River and its tributaries ... 75
4.1 Introduction ... 76
4.2 Methods ... 78
4.2.1 Study area ... 78
4.2.2 Nutrient concentrations and discharge data ... 80
4.2.3 Land use and land cover ... 81
4.2.4 Lithology ... 81
4.2.5 Major water infrastructure ... 81
4.2.6 Annual loads and nutrient ratios ... 82
4.2.7 Indicator for coastal and freshwater eutrophication potential – ICEP and IFEP 82
4.2.8 Data analysis ... 83
4.3 Results ... 84
4.3.1 Seasonal variation of nutrient concentrations and ratios in the tributaries 84
4.3.2 Annual nutrient loads in mainstem and tributaries ... 85
4.3.3 Annual nutrient ratios in mainstem and tributaries ... 89
4.3.4 Controls of nutrient ratios: model results ... 93
4.3.5 Indicators of Eutrophication IFEP and ICEP ... 93
4.4 Discussion ... 96
4.4.1 Mainstem Danube ... 96
4.4.2 Tributaries ... 96
4.4.3 Basin eutrophication potential ... 98
4.4.4 Danube Mouth ... 99
4.5 Conclusions ... 99
5 Discussion and Conclusions ... 101
5.1 Synthesis of main findings ... 102
5.2 Importance of controlling factors ... 104

5.3 Danube basin application and future outlook 106
5.3.1 Importance of ICPDR data reliability and availability........................... 106
5.3.2 Management/policy of the basin and reflection on land use importance in basin 107
References... 109
Appendixes 125
List of acronyms 159
List of Tables.. 161
List of Figures 163
About the author.. 167

1

INTRODUCTION

1.1 THE IMPORTANCE OF SILICA TO ECOSYSTEMS

Most nutrient studies in freshwater systems have focused on the roles of nitrogen (N) and phosphorus (P) in controlling primary production and as agents of eutrophication in aquatic ecosystems, with many looking at limitation and the effects of N:P ratio on phytoplankton growth and composition. While these studies go back as early as the late 1970s (e.g. Schindler 1977), it is more recently recognized that silicon (Si) and its relationship with N and P also plays an important role in aquatic primary production and eutrophication. Si is crucial for the growth of some phytoplankton taxa that are important for both food web structure and carbon storage, including the Bacillariophyta diatoms and silico-flagellates. These organisms take up dissolved silica (DSi) and deposit it in an amorphous form known as biogenic silica (BSi) to construct structural components, including spicules, scales, solid plates, granules, and frustules (Ehrlich et al. 2010). Diatoms contribute up to 40% of the total marine primary production (Nelson et al. 1995) and are considered the main contributors to the global carbon cycle (Smetacek 1999).

Si is also used by a wide variety of terrestrial plants (Epstein 1999), which in turn is important to understanding how landcover and land use affect Si export to aquatic ecosystems. Si serves a number of purposes for plants and crops, such as the alleviation of biotic and abiotic stresses, including protection from infectious disease and herbivory and support during cell division to maintain structure against the pull of gravity (Epstein 1999, 2009; Guntzer et al. 2012). In plants, Si is taken up and converted to biogenic Si and then stored in leaves, stems, and roots in the form of phytoliths. When plants die or experience leaf fall, the stored biogenic Si is recycled in the soil or exported (Conley 2002; Struyf et al. 2009). Phytolith dissolution is estimated to release twice the amount of dissolved Si (DSi) as mineral weathering (Alexandre et al. 1997). Conley (2002) estimated that the annual rate of Si fixed on land by plants is the same order of magnitude as in the oceans (~200 Tmoles), suggesting that the terrestrial silica cycle is an important factor in controlling DSi export to aquatic ecosystems.

The ratio of Si availability to N and P has important implications for phytoplankton growth and community structure. Often referred to in ecology as nutrient stoichiometry, the fundamental idea is that phytoplankton communities require a certain proportion of N, P, and Si, and that the availability of these nutrients affects both the identity of the limiting nutrient and influences the abundance of diatoms (requiring Si) or N_2-fixing cyanobacteria (able to fix N from the atmosphere when N supply is limiting and often contributing to harmful algal blooms). The stoichiometric requirement for phytoplankton that is broadly used to define N and P limitation is the Redfield ratio (N:P = 16:1 on a molar basis) (Redfield 1958; Ptacnik et al. 2010), with a ratio below Redfield indicating N limitation. Similarly, a ratio for Si was developed based on the nutrient requirements for diatoms. However marine and freshwater diatoms have different Si requirements because freshwater diatoms have a higher silicon content (e.g. Conley et al. 1989; Lynn et al. 2000). The latest nutrient ratio adjusted for freshwater diatoms is the one presented by Dupas et al. (2015) (N:P:Si = 16:1:40), which shows a higher Si requirement than the Brzezinski ratio (N:P:Si = 16:1:16) determined earlier from a study of 27 marine diatom species (Brzezinski 1985). Values below the Dupas ratio (N:Si > 0.4, Si:P < 40) suggest Si limitation for freshwater diatom growth. Changes in nutrient stoichiometry of N, Si, and P availability therefore lead to alteration of aquatic food web structure and ecosystem functioning including biomass production, consumer-driven nutrient recycling, and of nutrient and energy fluxes in food webs.

1.2 CONTROLLING FACTORS OF SI AND NUTRIENT EXPORT

Si, the second most abundant element (28.8% by weight) after oxygen in the Earth's crust (Wedepohl 1995), originates from the weathering and breakdown of silicate-containing minerals, such as siliciclastic sedimentary rocks, acid volcanic rocks, acid plutonic rocks, and unconsolidated sediments (Hartmann et al. 2012). Therefore, lithology is considered to be a "master variable" controlling Si mobilization at a global scale (Beusen et al. 2009; Figure 1.1). However, weathering is a slow process, and mineral silica is considered to be 10^2 to 10^4 times less soluble than BSi (Fraysse et al. 2009). Therefore, even though lithology is considered to be the major natural source of Si, BSi and the recycling processes in terrestrial vegetation and soils, along with hydrological variables controlling runoff, are major factors in the transmission of Si from land to water (Figure 1.1).

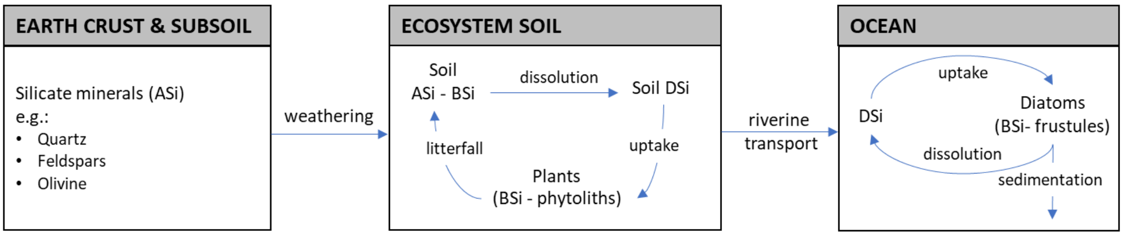

Figure 1.1. Schematic view of Si cycle and its forms (adapted from Struyf et al. 2009). ASi (Amorphous Silica), DSi (Dissolved Silica), and BSi (Biogenic Silica).

Many studies have demonstrated the influence of land use and land cover (LULC) on river water quality (Hill 1981; Osborne and Wiley 1988; Allan et al. 1997; Johnson et al. 1997; Smart et al. 1998; Sliva and Williams 2001; Turner and Rabalais 2003; Ahearn et al. 2005). The effects of LULC on N and P dynamics have been more frequently studied than that of Si (Carey and Fulweiler 2012). However, more recent studies demonstrate a growing appreciation that humans are also affecting terrestrial Si cycling and subsequent hydrological export by LULC change, and by altering sediment dynamics, erosion rates, and hydrological transport (Struyf et al. 2010; Vandevenne et al. 2012; Clymans et al. 2011; Clymans et al. 2015; Maavara et al. 2020a). The combined effect of these human influences likely alter the stoichiometry of N:P:Si in different ways, but these are not yet fully understood, particularly at basin scales. Furthermore, the importance of these human influences relative to lithology, weathering, or hydrological controls is not clear.

In natural intact forests, weathering is the main source of P and Si, while atmospheric deposition and N_2 fixation comprise the main source of N. These ecosystems tend to have low nutrient export. Low N loading usually leads to low N:P ratios and low N:Si ratios in forest streams (Vanni et al. 2011). This results in an overall pattern that at broad scales, natural landscapes are highly influenced by weathering rates, the state of the climax community, and hydro-meteorological conditions. These controls are highly altered in human-dominated landscapes, and therefore may cause differential effects on the nutrient exports compared to un-impacted systems.

Agricultural development tends to cause increases in both N and P inputs to surface waters due to application of fertilizers and animal manure (Vitousek et al. 1997; Galloway 1998; Smil 2000). In contrast, agricultural areas can cause the reduction of Si export. Si is accumulated in the phytoliths, and harvesting activities lead to the depletion of soil phytolith pools and, consequently, reduced Si export (Struyf et al. 2010). The reduction of Si export to rivers could result in high N:Si ratios, with one study documenting N:Si ratios from streams draining agricultural catchments between 1.1 and 3.5 (Carey et al. 2019). Based on the potential impacts of agriculture on nutrient ratios, agricultural land use would lead to increasing Si limitation relative to N and P, and agriculture would likely be more important than lithology in controlling Si export.

In comparison with agriculture areas, the effect of urbanization on Si export is less well studied, but increases in N and P from urban areas can also be expected (Morée et al. 2013). The main sources of Si from urban areas are detergents and discharge from paper production processes (van Dokkum et al. 2004; Dürr et al. 2011). Human waste also contributes to Si export, with one example in the Seine River basin showing that waste water treatment plants (WWTP) caused an 8% increase in DSi export (Sferratore et al. 2006). Because urbanization seems to lead to an increase in the export of all nutrients, and because urban areas tend to comprise relatively small areas at basin scales compared to other types of land use, the effect of urbanization on N:Si:P ratios is much less clear and more difficult to predict.

Reservoir construction has a profound impact on riverine discharge globally, altering the hydrology of most of the world's major rivers (Vörösmarty et al. 2004) and causing as much as a 30 - 40% reduction of suspended matter transport (Vörösmarty et al. 2003). Due to the increase of residence time, reservoirs enhance removal of both P and Si through sedimentation, which stimulates N fixation by cyanobacteria (Akbarzadeh et al. 2019). Consequently, it is common to observe higher N:P ratios in the outflow of reservoirs than in the inflows (Akbarzadeh et al. 2019), with a consequential increase of N:P and N:Si ratios in downstream river systems (Maavara et al. 2020a).

This study focused on the Danube Basin in order to understand the relative importance of these types of human-altered landscapes on the both the magnitude of DSi export and its relationship with N and P. This topic is not only important for understanding controls of nutrient export in altered river basins, generally, it is also a unique opportunity for the Danube Basin itself. Other studies have focused on understanding DSi dynamics in the basin, specifically on the role of reservoirs in DSi retention and export to the Black Sea (Humborg et al. 1997; Garnier et al. 2002). No other studies, however, have addressed the role of other types of human impacts (agriculture, urban areas) on DSi export, or looked explicitly at nutrient stoichiometry taking into account LULC effects on DSi. Because the Danube has a well established monitoring programme that divides the basin into well characterized sub-basins with a wide range of variation in controlling factors (e.g. reservoir density, agriculture and urban areas, and in lithological classes), the Danube basin is well suited to an examination of the relative effects of human impacts compared with lithology and discharge on these important macronutrients.

1.3 Case Study

The Danube River Basin is Europe’s second largest river basin and is home to more than 81 million people (Figure 1.2). The European Commission recognizes the Danube as the single-most important non-oceanic body of water in Europe (ICPDR 2015). It is the most international river basin in the world covering the territories of 14 countries. The Danube River flows from the Black Forest (Germany) and passes through the most important agricultural regions in Europe to finally discharge into the Black Sea. The main land uses and land cover of the basin are agriculture (48%), forest (40%) and urban areas (5%). The basin´s geology is characterized by the presence of the five lithology classes: siliciclastic sedimentary (38%), carbonate sedimentary (18%), unconsolidated sediments (17%), mixed sedimentary rocks (14%), and metamorphic (10%).

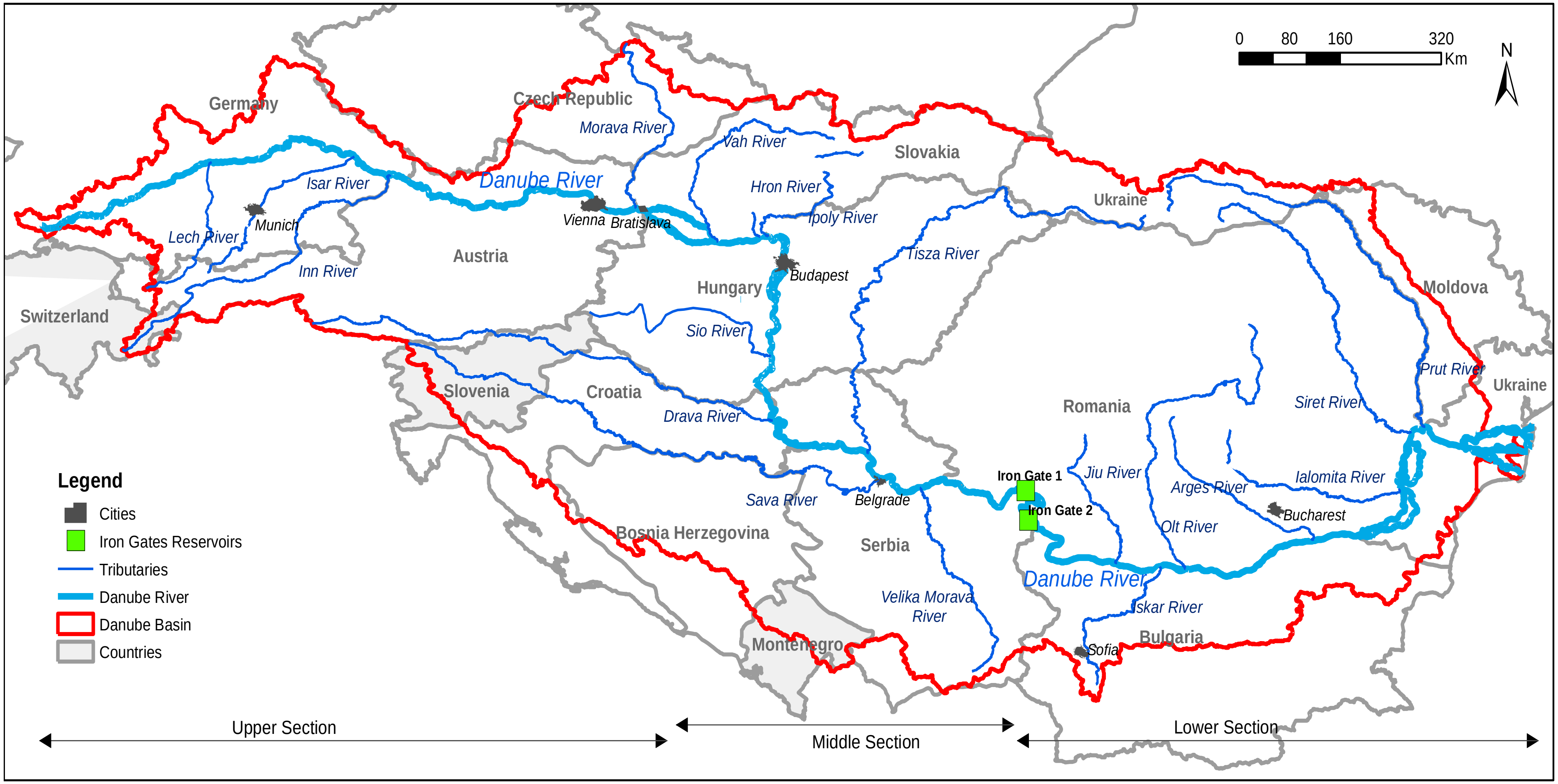

Figure 1.2. Map of the Danube River Basin, with its tributaries.

Figure 1.3. Reservoir in the Danube River Basin.

Figure 1.4. Reservoir in the Danube River Basin.

Figure 1.5. Agriculture activities in the upper part of the Danube River Basin

The Danube River Basin analysis report (ICDPR 2015), required by the Water Framework Directive (WFD 2000/60/EC) (European Commission 2000), identified hydro-morphological alterations (e.g. reservoirs), pollution by nutrients, pollution by organic substances, and pollution by hazardous substances as the four most significant pressures in the river basin. Hydrological alterations in the Danube River have occurred mainly due to the river's considerable natural elevation gradient which is ideal for building hydropower plants (ICPDR 2015) (Figure 1.3 and 1.4). The first hydropower plant was built in 1927 at Vilshofen (lower Bavaria, Germany) (WWF 2002). There are 59 dams along the river's 1,000 kilometres from the source to Gabcikovo Dam downstream of Bratislava. This means that the flow regime and river connectivity of the upper Danube is, on average, interrupted every 17 km (Zinke 1999). The largest hydropower dam and reservoir system (Iron Gates Dams I and II) along the entire Danube is located at the 117-km-long Djerdap Gorge. This system consists of two dams, jointly operated by Romania and Serbia. There are further plans (Zarfl et al. 2015) for the construction of new dams for hydropower plants in the Danube River basin in order to implement the new Renewable Energy Directive (2018/2001/EU). This directive set the objective of reaching 32% of the EU’s energy consumption through renewable energy sources by 2030. Therefore, in the Danube River Basin, planning for the construction of dams is under discussion for the Sava, Mura, Drava and Tisza Rivers and for the Danube itself between Romania and Bulgaria (ICPDR 2015).

Pollution by N and P has led to eutrophication of the Danube, with -agricultural activities and untreated or insufficiently treated wastewater as the main sources (ICPDR 2015). Agricultural land use comprises about 50% of the Danube Basin, which is the major agricultural region in Europe (Figure 1.5) producing crops like maize, soybeans, sunflowers and cereals. The application of fertilizers led to excessive addition of nutrients in the 1970s and 1980s (Popovici 2014). The implementation of the Water Framework Directive of the European Union, in combination with the economic changes in Eastern Europe after the fall of the Iron Curtain, led to a reduction of nutrient inputs into surface waters since the 1990s (Cociasu and Popa 2005; Kroiss et al. 2006). However, fertilizers continue to be used in agricultural areas to support crop production. The countries with the highest fertilizer application per cropland area in the Danube Basin for the period 2002 – 2017 were Germany, Slovenia and Croatia for nitrogen fertilizer (7,645 – 27,826 kg N km^{-2} $year^{-1}$), and Slovenia, Croatia and Servia for phosphorus fertilizer (1,400 – 10,345 kg P km^{-2} $year^{-1}$) (Ritchie et al. 2022) (Figure 1.6).

Another source of nutrient pollution in the Danube are emissions from untreated or insufficiently treated wastewater. In the western countries of the basin (e.g. Germany and Austria) almost 100% of the wastewater is collected and treated. In the eastern countries this percentage is lower. Serbia has the highest percentage (70%) of untreated wastewater with, consequentially, the highest emission among the riparian states of N and P from point sources. In total almost 16 million population equivalents of wastewater are neither collected nor treated (ICPDR 2015).

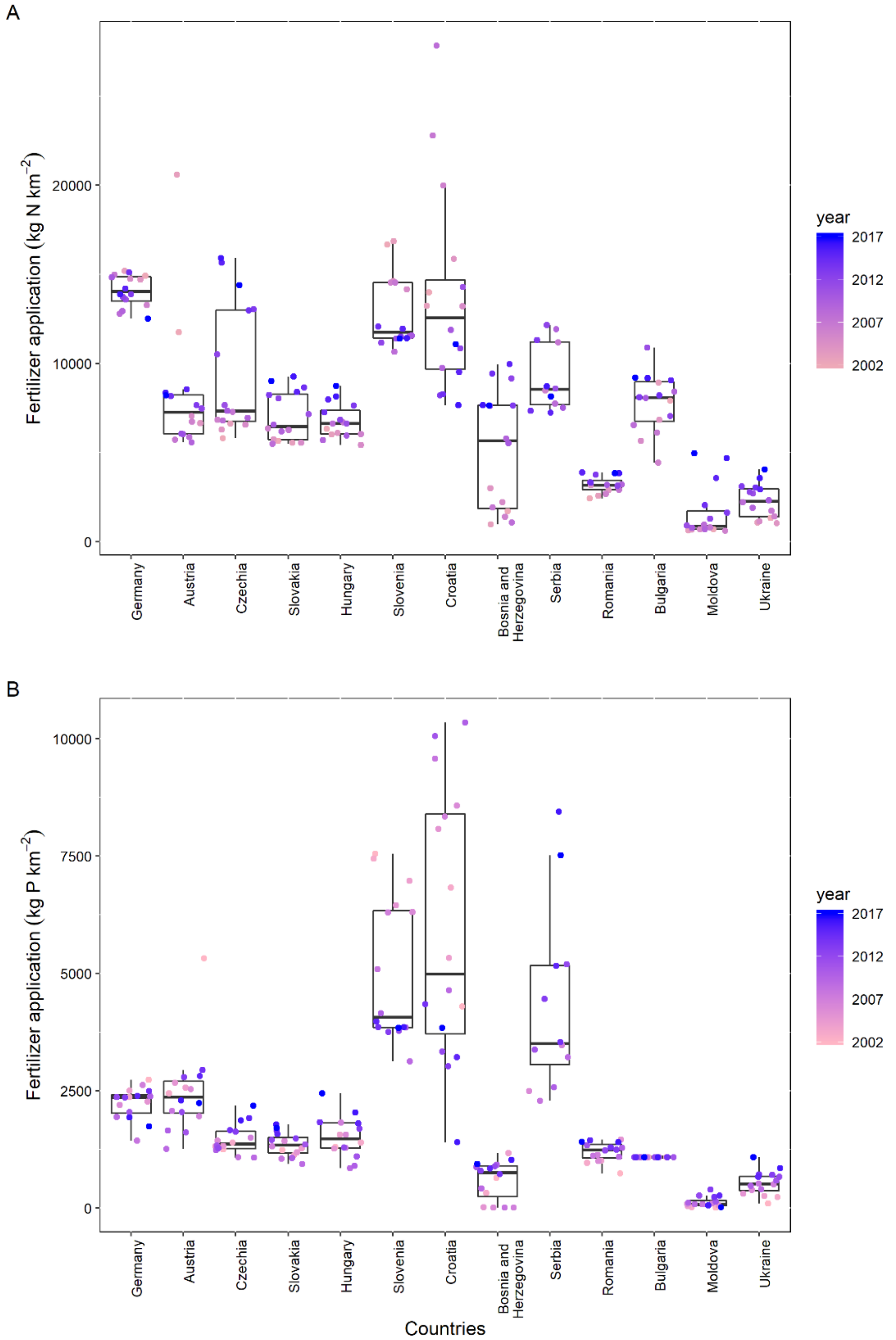

Figure 1.6. Nitrogen(A) and Phosphorus(B) Fertilizer application per area cropland from 2002 to 2017

1.4 SIGNIFICANCE OF THE STUDY

In the Danube River Basin, DSi export has been declining since 1975, with a decrease of mean DSi concentrations to the Black Sea from 8.5 in 1960 to 3.5 mg/L in 1990 (Humborg et al. 1997). This reduction of DSi export has led to a shift in phytoplankton community structure from diatoms to flagellates (Humborg et al. 2000). The reduction of DSi was originally attributed to the construction of the large reservoirs of the Iron Gates Dam, which has a short residence time (ca. 6 days) (Humborg et al. 1997). Two other studies using sediment cores concluded that the reduction in DSi started before the Iron Gate dam was constructed in 1970 (Friedl et al. 2004; Teodoru et al. 2006). Friedl et al. (2004) also mentioned that the water residence time of about six days of the Iron Gate was not long enough to cause the DSi decline reported by Humborg et al. (1997). Later findings showed that reservoirs with short residence times have an effect on Si (Humborg et al. 2006; Humborg et al. 2008) and the reduction of DSi in the Danube can be due the large number of reservoirs located in the upper part of the Danube Basin (Friedl et al. 2004; Humborg et al. 2006).

Studies that predict N, P, and Si exports are usually based on global and basin-scale models (see Table 3.2; chapter 3). N and P prediction models at basin-scales are relatively more common than those for Si. In the Danube Basin, a process-based model (Riverstrahler) was applied to predict Si loads (Garnier et al. 2002; Sferratore et al. 2005). In this model, lithology alone determines Si inputs, while LULC determine N and P inputs, resulting in Si export partially being controlled by P availability and eutrophication processes in the basin (Garnier et al. 2002). Due to the increase of primary production during the excess of nutrient inputs, including P, Si uptake by diatoms is higher, and ultimately results in deposition and storage in the sediments, resulting in an overall reduction of Si in the water column (Conley et al. 1993). Other well-known models use statistical approaches. For example, the global-scale News-DSi model (Beusen et al. 2009) uses multiple linear regression to conclude that lithology (volcanic rocks), slope, and precipitation were important predictors for riverine DSi export. The authors underlined that the global News-DSi model is different from other statistically based basin-scale models which showed that LULC or other factors can be important in addition to lithology (Carey and Fulweiler 2012; Humborg et al. 2004).

Despite the scientific advances of these previous studies, the prediction of nutrient exports in the Danube River using process-based or statistical models remains affected by a number of sources of uncertainty (e.g. model structure, calibration) (Garnier et al. 2002; Beusen et al. 2009). In this thesis, empirical data were used, collected from fieldwork campaigns and observations from the International Commission for the Protection of the Danube River (ICPDR) database (www.danubis.icpdr.org). Moreover, this study includes nutrient (N and P) and Si measurements collected from alpine systems of the upper part of the Danube Basin (Austria and Germany), which was not specifically addressed in previous studies, but was hypothesized to be potentially responsible for a high retention of DSi due to the high density of hydropower reservoirs. These measurements were done in pristine mountain streams and high-elevation reservoirs with both long (>1 year) and short (~1 day) residence times, providing a novel contribution to the assessment of reservoir influence on nutrient exports and yields in mountain systems. A synoptic sampling approach, conducted in the upper part of the Danube in 2015 and 2016, was developed for 74 number of sites across different LULC so that the importance of both natural (lithology and forest cover) and human factors (LULC and reservoirs) in controlling DSi export and nutrient ratios could be assessed.

These controlling factors (lithology, LULC, and reservoirs) with the addition of waste-water-treatment plant density were also tested in the whole Danube basin using the ICPDR database. This database includes physical and chemical variables (e.g. nutrients, discharge) from 1998 to 2017, and comprises 133 monitoring stations, of which 49 are on the mainstem of the Danube River and 84 on 20 of the main tributaries. These data were used in a mixed-modelling approach to analyse spatio-temporal and seasonal variation of DSi, N, and P export in the Basin. Together with the new field data collected in the upper part of the basin (that were not part of the ICPDR database), this study is relevant for future implementation of water and land-use management plans, allowing to target e.g. priority regions, mitigation or source-reduction measures, and/or to identify the priority nutrient that would contribute most to reducing eutrophication risks.

1.5 Objectives

This research aimed to assess the effects of natural and human controlling factors on nutrient loads and stoichiometry for N, P, Si in the Danube River and its tributaries. The specific objectives were to:

1. Investigate the nutrient concentrations and ratios (Si, N, and P) in several high-altitude basins in the upper part of the Danube River (Austria and Germany).
2. Describe spatial and temporal variation in DSi loads and yields in its main tributaries and to assess the contribution of DSi from the tributaries to the Danube River using a mass balance analysis.
3. Identify the controlling factors of DSi yields in the Danube River, including lithology, land use and land cover, and water infrastructure (reservoirs and waste water treatment plants).
4. Describe spatial and temporal variation in nutrient (DSi, DIN, and PO_4) concentration, loads and ratios and to evaluate the controlling factors on the nutrient stoichiometry (N:Si:P) in the Danube River.

1.6 HYPOTHESES OF THE STUDY

One of the main problems related to agriculture in the Danube Basin and globally, is the use of fertilizers, which causes alteration in the N and P balance in basins and an increase in their concentrations in soil and water. Although the input of fertilizers in the Danube Basin has declined since 1990, there are still diffuse sources of N and P in the catchment. Especially, after decades of manure and fertilizer application above crop requirements, agricultural land use keeps a legacy of accumulated P. On the other hand, agriculture activities reduce Si through plant harvesting and the reduction of Si inputs to the soil pool. Therefore, high N:Si, and low Si:P ratios where agricultural land use is high, can be expected.

Based on the land use classification in the Danube River Basin, high N:P and N:Si ratios are likely to be more prevalent in the upstream Danube River Basin and will decrease with the decrease in forest land cover and corresponding increase in agricultural land use. This overall pattern can be altered by the presence of water infrastructure such as wastewater treatment plants (WWTP) and reservoirs. Based on ICPDR (2015), there is not an adequate management or treatment of wastewater, especially in countries located in the middle basin such as Croatia, Bosnia-Herzegovina, Serbia, and Montenegro. WWTP are considered to be the main source of P in the basin compared to N and Si; therefore, we expect that N:P and Si:P may decrease in the middle section of the basin. On the other hand, reservoirs will restrict the natural transportation of nutrients downstream. Reservoirs will have more effect on Si and P, because N can be compensated by the process of N fixation. This will result in lower Si in reservoirs with long residence time compared to those with short residence time.

1.7 OUTLINE OF THE THESIS

This thesis is organized into five chapters:

Chapter 1 introduces the research background and objectives of this thesis. From this, the chapter presents the rationale for this study and defines its objectives.

Chapter 2 discusses nutrient yields and stoichiometry in the upper Danube River (Austria and Germany) across three types of systems (inlets, reservoirs and run-of-river reservoirs). The impacts of basin land cover and land use, lithology, and reservoirs on nutrient ratios were examined. This analysis is based on two fieldwork campaigns.

Chapter 3 analyses data available from ICPDR to describe spatial and temporal variation in DSi loads and yields in the main tributaries of the Danube River and uses a mixed linear regression model to evaluate the effect of human and natural variables controlling

Si export, including lithology, land use and land cover, reservoirs, and wastewater treatment plants.

Chapter 4 evaluates the effects of land use and land cover, lithology, reservoirs and wastewater treatment plants that may influence nutrient loads and ratios (N:P:Si) in the Danube Basin by using data from 26 monitoring stations in the Danube River and 12 in its tributaries in the period 1996 – 2017.

Chapter 5 describes the conclusions of this thesis and provides recommendations for further research and implementation of policies.

2

Control of Si export and nutrient (N, P) stoichiometry in hydropower reservoirs and headwater rivers of the Danube River Basin

2.1 INTRODUCTION

Silicon (Si), together with other macronutrients nitrogen (N) and phosphorus (P) play an important role in determining the community composition of phytoplankton assemblages, which are critical to the functioning of aquatic ecosystems. Si is required by diatoms; however, there is a difference in Si requirement based on diatoms species. Marine diatoms generally required smaller amounts of Si than freshwater diatoms (Conley et al. 1989). The latest nutrient ratio adjusted for freshwater diatoms is the one presented by Dupas et al. (2015) (N:P:Si = 16:1:40), which shows a higher Si requirement. When Si availability is low relative to N and P (below N:P:Si = 16:1:40), diatom abundance can decline, which in turn can affect aquatic food web structure (Humborg et al. 2000; Parsons et al. 2002; Lynam et al. 2017).

Low N:P ratios also play a role, with ratios below 16:1 (molar basis; Redfield, 1958) causing N limitation, which can stimulate N_2-fixing cyanobacteria, a component of harmful algal blooms (e.g. Paerl et al. 2001). The biogeochemical cycles and riverine exports of Si, N, and P have all been considerably altered by anthropogenic activities (e.g. Beusen et al. 2016; Maranger et al. 2018; Mavaara et al. 2020; Royer et al. 2020; Senath et al. 2022). with significant impacts on aquatic ecosystems, including increased eutrophication (e.g. Garnier et al. 2010).

In non-impacted river systems, Si supply to terrestrial ecosystems is controlled by the geological settings (lithology) and weathering rates, and its losses via leaching and runoff is mediated by soil processes and vegetation dynamics (Farmer et al. 2005; Cornelis et al. 2011; Struyf and Conley 2012). Plants store Si in the form of phytoliths (biogenic silica, BSi), which are retained in soil until mobilised through dissolution (dissolved Si, DSi), which makes it available for re-uptake or loss via hydrologic pathways (e.g. Cornelis et al. 2011; Struyf and Conley 2012). BSi is several orders of magnitude more soluble than mineral silicates (Farmer et al. 2005) and is usually considered the primary source of exported DSi (Bartoli 1983; Farmer et al. 2005; Cornelis et al. 2011). Phytoliths from different types of vegetation can vary in their solubility due to their morphology and moisture and aluminum content (Bartoli and Wilding 1980), perhaps with phytoliths from forest land cover as much as 10 to 15 times less soluble than those from grasslands (Wilding and Drees 1974).

Leading hypotheses for the alteration of Si, N, and P and their ratios are agricultural development, afforestation and deforestation, urbanization, and reservoir construction; however these factors do not affect each nutrient in the same way (Billen et al. 2007; Maranger et al. 2018; Carey et al. 2019; Maavara et al. 2020b). Relatively few studies examine the combined effects of reservoirs together with changes in land use and land cover (LULC) on N:P:Si stoichiometry, and these tend to be at global scales (e.g. Maranger et al. 2018; Maavara et al. 2020b). Those that are focused on specific basins generally focus on either LULC (e.g. the Seine River – Billen et al. 2007; the Mississippi – Carey et al. 2019; the Mincio – Pinardi et al. 2018) or on reservoirs (e.g. Garnier et al. 1999; Cook et al. 2010). In addition, the geological settings, which can also be important for Si and P availability (and rarely for N; Houlton et al. 2018) are sometimes, but not consistently included.

It is rather well understood that agriculture and urbanization result in increased riverine N and P export (e.g. Beusen et al. 2016; Vilmin et al. 2018), but the anthropogenic effects on Si export are different, and relatively recently appreciated (e.g. Sferratore et al. 2006; Struyf et al. 2010; Clymans et al. 2011; Vandevenne et al. 2012; Carey and Fulweiler 2016). In contrast to N and P, crop agriculture leads to a reduction in DSi export due to the depletion of phytolith pools in soil through harvesting (e.g. Struyf et al. 2010; Clymans et al. 2011; Guntzer et al. 2012; Vandevenne et al. 2012). This may counter the effects of animal agriculture on DSi which is likely to increase the mobility of DSi through higher inputs and dissolution rates of digested phytoliths in manure (Vandevenne et al. 2012; Pinardi et al. 2018). This dynamic is complicated in pastures, however, because grazing tends to increase silica plant uptake for defenses (e.g. McNaughton et al. 1985; Ryalls et al. 2018) and to increase aboveground productivity, both which could lead to more sequestration in plant biomass (Melzer et al. 2010).

Like N and P, urbanization seems to lead to increases in DSi export, with point-sources from waste-water treatment plants which includes human waste (from ingestion of Si in diet (e.g. Sferratore et al. 2006), detergent, pharmaceuticals, and other household products (van Dokkum et al. 2004; Dürr et al. 2011). Urban infrastructure can also lead to increases through storm-water runoff (e.g. Maguire and Fulweiler 2016). Another study in contrast showed no effect of urbanization on export (Conley et al. 2000) likely because urban areas comprised a relatively small area of the watershed.

Reservoir construction along the river continuum tends allows for biological processes and sedimentation (e.g. Vörosmarty et al. 2003; Syvitski et al. 2005; Harrison et al. 2009 and 2012; Maavara et al. 2014, 2015, 2020b; Akbarzadeh et al. 2019); but the retention processes for Si, P, and differ, leading to potential changes in export nutrient stoichiometry (Maranger et al. 2018; Maavara et al. 2020b). P appears to be preferentially retained compared to Si and N when the residence time is relatively long (i.e. longer than ~1 year) whereas Si seems to be preferentially retained at shorter residence times. The difference could be due to persistent P-limitation of primary production and opportunity for sedimentation in the longer residence-time reservoirs, whereas diatoms can establish communities quickly and are more successful in turbulent and light-limited environments that are more common in low residence-time reservoirs (Maavara et al. 2020b). In contrast with Si and P, N-fixation can accommodate for losses that occur via denitrification, which results in a less N sequestration in comparison (e.g. Maavara et al. 2020b). In river systems in general, there tends to be an increase in the N:P ratio with longer residence times as the balance shifts from N-loss via denitrification to P loss via sedimentation (Maranger et al. 2018).

Here we study the combination of lithology, LULC, and reservoirs in controlling Si export and its ratios with N and P in several high-altitude basins that form the headwaters of the Danube River. The Danube is a heavily altered river (on average a reservoir every 17 km in the upper catchment) and contributes about 60% of the total hydrological riverine input and is major source of nutrients to the Black Sea (Popa 1993; Venohr et al. 2011). It has been postulated that the Danube's reservoirs caused a decline of Si load and an increased N:Si delivery to the Black Sea, resulting in a shift in phytoplankton community structure from diatoms to flagellates (Humborg et al. 2000). However, increasing N and P input from development in the basin could also contribute to the increase in N:Si (Strokal and Kroeze 2013). Conflicting results from different studies make it unclear whether DSi export is primarily reduced by larger reservoirs like the Iron Gates Dam, located in the lower part of the basin and having a short residence time (ca. 6 days), or by the many reservoirs in the upper part of the Danube, many of which have much longer residence times (~1 year) (Humborg et al. 1997, 2006, 2008); or that the reduction in DSi started before the Iron Gate dam was constructed in 1970 (Friedl et al. 2004; Teodoru et al. 2006).

The objective of this study was to examine the combination of landscape-scale controls on Si, N, and P exports in the upper, Danube River basin, specifically with respect to natural and anthropogenic land use and land cover (LULC) and a comparison of systems across different residence times (unimpounded streams and rivers, long-residence time reservoirs and run-of-the-river hydropower systems). Specifically, we assessed: 1. The effect of LULC and lithology on concentrations and yields of Si and P; 2. The influence of LULC on N concentrations; and 3. The combined effect of all these factors on N:P:Si ratios. Finally, we assess the potential ecological impacts by examining the relationship of Si and diatom abundance and chlorophyll *a* in the reservoir systems.

2.2 METHODS

2.2.1 Study Area

Three different types of systems were sampled for this study in order to assess the effect of residence time on nutrient concentrations and ratios: 1) High-altitude reservoirs (reservoirs with long residence time ≥ 1 year); 2) River and streams forming inlets (IN) to these reservoirs (short residence time); and 3) Run-of-the-river hydropower systems (RRH) (reservoirs with short residence time < 1 day). Sites were located in the Lech and Inn River sub-basins of the upper Danube River in western Austria and southern Germany (Figure 2.1). Both are mountainous sub-basins, covering an area of 1,422 km^2 and 26,100 km^2, respectively, with high-residence time reservoirs at elevation 859 – 2257 m.a.s.l., which are fed mainly by glacial and snow-melt streams (kryal and rhithral runoff regimes) and mountain springs (krenal runoff regimes) which generally run through coniferous, peat, and mixed forest areas, before passing through pasture areas. Maximum Pardé coefficients (Pardé 1933), ratio between monthly and annual flows, are observed in summer (June-July), and lowest values during the winter months. With increasing flow distance towards the Danube, the regime curve is flattened with a deceased amplitude due to the influence of more precipitation driven tributaries.

Cities located at lower elevations in the Lech sub-basin include Schongau (population ~12,000 at 696 m.a.s.l.), Landsberg (population ~28,000 at 590 m.a.s.l.), and Augsburg (population ~286,000 at 485 m.a.s.l.). The main urban center in the Inn River basin is Innsbruck (population 308,290 at 574 m.a.s.l.). The long residence time reservoirs of typically more than 1 year have an average depth of 12 m (Demmer 1991). They have relatively small sub-basins (4 – 145 km^2), dominated by coniferous forest, bare rock area and glaciers. Most of these reservoirs are located in Inn River and its tributary Salzach (Figure 2.1). RRHs (elevation 300 – 780 m.a.s.l.) comprise a series of structures designed to generate hydropower while rivers run through in-river turbines. These structures lie ~10 river km apart and were sampled one after another consecutively. RRHs were located on the Lech River in two sections (hereafter Lech 1 and Lech 2; Figure 2.1) and in the lower-elevation parts of the Inn River in two stretches (Inn 1 and Inn 2; Figure 2.1). RRHs have larger sub-basin areas (1,609 – 26,253 km^2), with some populated centers. Land cover is dominated by grasslands, coniferous forest and agriculture (Appendix 1).

2.2.2 Sampling

There were 11 reservoirs and 38 inlets and 25 RRH sites. A synoptic sampling approach was designed to capture spatial variation in LULC. Sampling was conducted in September, 2015 and July-August, 2016. In reservoirs, water samples for nutrient concentrations (Si, N, and P), chloride (Cl) and chlorophyll a were collected using a van Dorn sampler at the surface and at depths 0, 1, 3, 5, 8, 12 m. When reservoirs were deeper than 12 meters, samples were taken every 4 m and 1 meter above the sediment at the bottom of the reservoir. For statistical analysis, we used the average concentrations from the depth profile, because there was no clear stratification in the reservoirs. For phytoplankton, a composite sample was collected in the photic zone between 0 and 5 m using a plankton net of 40 cm diameter and mesh size 70 µm. While the use of a 70 µm mesh size for collection of phytoplankton with net hauls is a little larger than the 50 µm mesh recommended by Bellinger and Sigee (2010), this provides a compromise, reducing effects of net clogging and loss of efficiency of sampling through net resistance. The consequence is a possible underestimate of smaller algae such as chlorophytes, while larger and colonial cells will be mostly retained. Phytoplankton community estimates should be viewed as a qualitative indicator that supports the nutrient and chlorophyll a estimate made on bulk samples. Phytoplankton samples were transferred to a 125 ml HPDE bottle and preserved with 0.5 ml of Lugol's solution. For inlets and RRHs, only surface water was collected for nutrient concentrations. Samples for nutrient concentrations were collected in pre-leached, acid-washed 120 ml HDPE bottles, placed on ice in a cool-box and transported to the laboratory for filtration for analysis. Dissolved oxygen (DO), pH, conductivity and temperature were measured using Hydrolab (HL4 sonde) appropriate meters during each sampling.

2.2.3 Si, N, P and Cl concentrations

Samples were filtered for analysis of total dissolved nitrogen (TDN), total dissolved phosphorus (TDP), and dissolved chloride (DCl) using pre-combusted (500 °C for 4 h) GF/F filters (0.45 µm nominal pore size; Whatman International Ltd., Maidstone, England). TDN concentrations were determined using a Shimadzu TOC-V-CPN with a coupled total nitrogen analyzer (TNM). TDP was analyzed using the acid spectrophotometric method (APHA, 1998). We chose to use TDN and TDP as the best measure of available N and P, as inorganic concentrations were extremely low (often at or below detection limit), and oligotrophic systems are known to recycle organic forms of N and P efficiently (Berman and Bronk 2003; Björkman and Karl 2003). DCl was determined with an Ion Chromatography (ICS-1100, Dionex - Thermo Scientific). Samples for DSi were filtered using polycarbonate membrane filters (0.4 µm pore size) and using HDPE vacuum flasks in order to prevent contamination from glassware. DSi concentration was determined using the molybdosilicate method (APHA, 1998). We analyzed silica in the dissolved form because that is the form that is taken up by phytoplankton (Amo and Brzezinski 1999).

2.2.4 Phytoplankton identification and counting

The standard Sedimentation Technique of Centrifugation (STC) was performed to concentrate the phytoplankton samples, which was required as phytoplankton concentration was generally very low. The technique involves centrifuging a 10 ml sample for 25 minutes at 2500 rpm. Each sample was examined using an inverted microscope (SZX 10 from Olympus) with 60X magnification and identified at the phylum level (Belcher and Swale 1976).

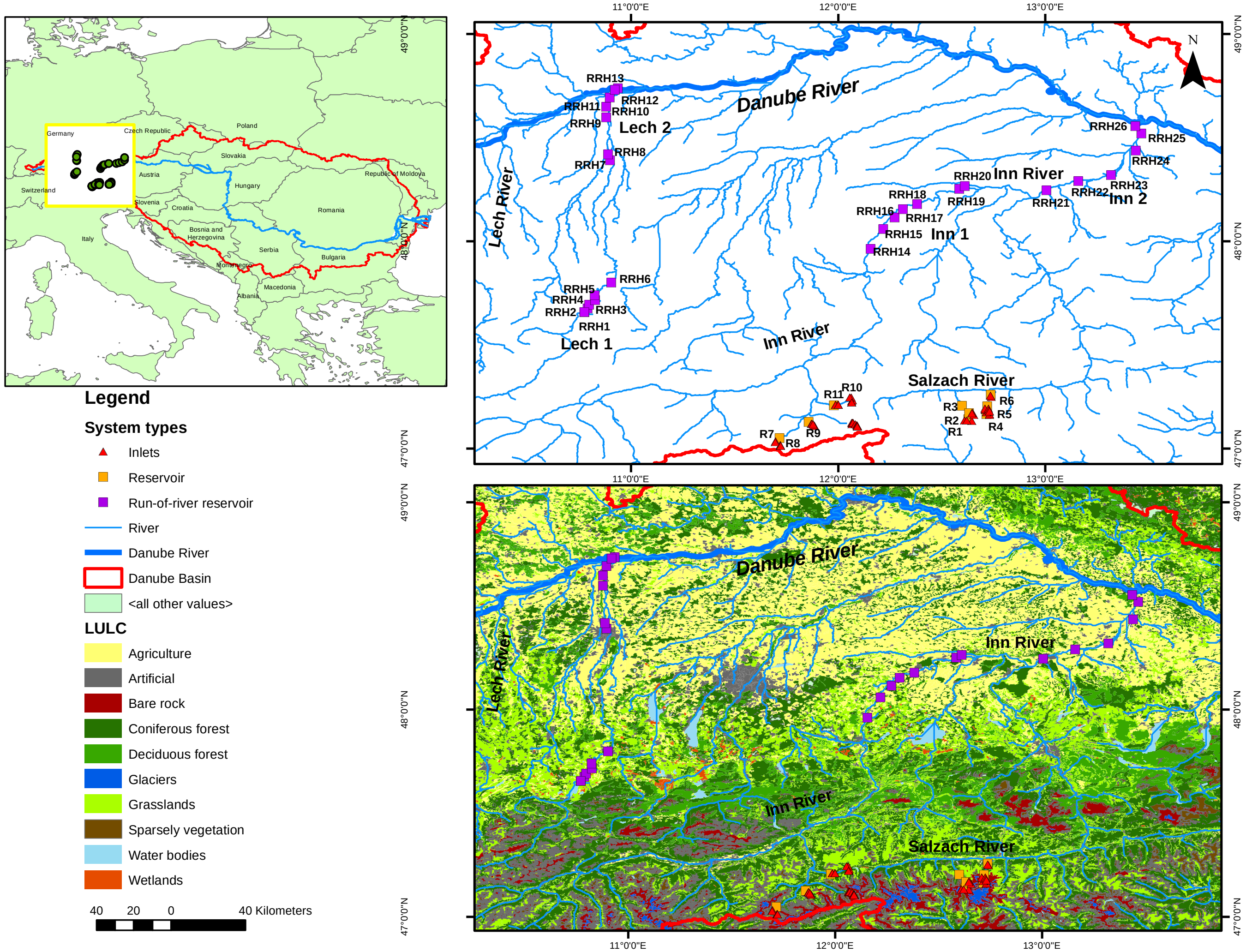

Figure 2.1. Location of sampling sites in the upper Danube River basin.

2.2.5 LULC and lithology analysis

The sub-basin area for each sampling point was delineated based on a Digital Elevation Model (DEM) with 90 m resolution, obtained from the Shuttle Radar Topography Mission (SRTM). Arc Map 10.5.1 (Esri 2017) and its spatial analyst toolsets (hydrologic function) were used to model the water flow and direction. Within each sub-basin, the area (and relative proportion) for LULC was determined using the CORINE 2012 dataset of the European Environment Agency (EEA). We considered the following classes: artificial (included urban and industrial areas), agriculture (included arable land, permanent crops, and heterogeneous agricultural areas), grasslands, coniferous and deciduous forest types (included mixed forest and broad-leaved forest), glaciers, bare rocks, sparse vegetation, wetlands, and water bodies.

The percentage of each lithologic class was determined based on shapefiles from the Global Lithological Map database - GLiM project (Hartmann and Moosdorf, 2012) with Spatial analyst tool, Extract and Statistics functions of ArcMap 10.5.1. The lithological classes present in our study area were acid volcanic rocks (AV; 72.8 % Si content by weight), acid plutonic rocks (AP; 67.8% Si), carbonate rocks (SC; 7.2% Si), metamorphic rocks (MR; 65.9% Si), mixed sedimentary rock (MR; 52.3% Si), and siliciclastic sedimentary rocks (SS; 60.3% Si) (Hartmann et al. 2012). For each sub-catchment, the percentage of each lithological class was calculated (ArcMap 10.5.1, spatial analyst tool, extract and statistics function). Of these classes, metamorphic rock (MR) was the most evenly distributed across all sites compared to the other rock types (ranging from 0 to 100%), and also represented one of the higher Si-content lithological type in the dataset. Therefore, we used this variable in our data set to assess the effect of lithology on Si. We did not consider that lithology was important in determining N export, since N is present only in sedimentary rocks of biological origin (Houlton et al. 2018), and were not present in the study area.

2.2.6 Hydrological factors

Because Si, N, and P concentration can be affected by discharge in ways that would obscure the effects of LULC and lithology, we used hydrological regionalization techniques and conservative tracer methods to take this into account. For the inlet sites located in the headwaters of the Lech and Inn Rivers, it is difficult to directly obtain discharge data (modelled or measured) because all of them are un-gauged, and the gauged stations downstream represent highly regulated flow due to the hydropower reservoirs upstream. Therefore, we used a geospatially downscaled estimate based on average long-term discharge from the HydroRIVERS Version 1.0 dataset (Lehner & Grill, 2013), acknowledging there are significant uncertainties, particularly in the snow or glacier-dominated areas. The average annual discharge values for headwater catchments were regionalized to each of the sampling points using a simple area-ratio approach. We then estimated the proportion of the long-term annual discharge that occurred during the sampling month (July or September) by a using the average long-term hydrological flow regimes (ratio of monthly/annual flow) of three upstream stations in the area, which were not regulated by hydropower-generating reservoirs (Neukaser 1976-2016, Persal 1971-2016, and Schwendberg-Aue 1996-2016; Hydrographisches Jahrbuch von Österreich 2016 (BMI, 2019)).

For the run-of –the river sites which are further downstream, we were able to obtain more reliable estimates of discharge from measured values for four stations in the Inn River (Rosenheim o.d. Mangfallmündung, Wasserburg, Eschelbach, Passau Ingling), and two stations in the Lech (Lechbruck, Augsburg u. d. Wertachmündung), provided by the Bayerisches Landesamt für Umwelt, Gewässerkundlicher Dienst (LfU-Bayen, 2020). Using the area-ratio approach described above, we calculated average daily discharge values for each of the sites for the month we sampled, which we used to calculate load and yield for each nutrient. We assumed that the concentration we measured was representative of the average monthly concentration, an assumption which is supported by our current analysis of the larger Danube-Basin data set (Chapter 3), which shows no relationship between nutrient concentrations and discharge in the region. Because of the complex dam operation rules, we were not able to estimate discharge values or residence times for the reservoirs, as these data are proprietary and not available.

Because our modelled estimates of Q are fraught with assumptions and functionally reduced our dataset by not including reservoirs, we took an additional second approach to account for hydrology, which was to use chloride as a biologically conservative tracer which, when used as a molar ratio with Si, N, or P, could indicate dilution or concentration relative to its hydrological source. This method works well for the inlet and reservoir sites as Cl was not correlated with any other LULC or lithological variable, but was more difficult for the run-of-the river sites, where we find a higher proportion of agricultural land use, which was correlated with Cl (Appendix 6). On the other hand, the run-of-the-river sites had the most reliable Q estimates due to the proximity of gauging stations. We therefore used both approaches to develop statistical models to fully account for the possible effects of hydrology on our conclusions: 1. We used yields of Si, N and P and their ratios in relationship to LULC and lithology for inlets and run of the river sites ($n = 76$); and 2. We calculated the nutrient:Cl ratios (molar basis) for the entire data set, including the reservoirs ($n = 87$).

2.2.7 Statistical analysis

Our overall approach to analyze this data set was to start with simple system-type comparisons and bi-variate correlations which served to visualize and understand results from the more complex multivariate and mixed linear effects models that we ultimately constructed as a way to transparently show relationships and the possible confounding variables common in catchment studies. First, we compared nutrient concentrations, yields, and ratios among system types (inlets, reservoirs, and RRHs). Because the variables were not normally distributed, a non-parametric one-way Kruskal-Wallis ANOVA with a Dunn post-hoc test was performed. In addition to the system comparisons, bi-variate scatter plots of DSi, nutrient concentrations and ratios and land use (% forest and agriculture), lithology (% metamorphic rock) and elevation (m) were created, and Spearman rank correlation coefficients (rho) were calculated for each system type separately.

Linear mixed effects models (Seilheimer et al. 2013; Harrison et al. 2018) were used to further define relationships between nutrient and anion concentrations, ratios and yields (as response variables) and basin properties (predictor variables). Nutrient and anion ratios were natural-log transformed as recommended for statistical analysis of stoichiometric ratios (Isles 2020). The predictor variables were the ten LULC classes determined by the above analysis (artificial, agriculture, grasslands, coniferous, deciduous, glaciers, bare rocks, sparse vegetation, wetlands, and water bodies; all expressed as a percentage of total area in each sub-basin); the lithological class, % metamorphic, and the three system types (inlet, reservoir and RRH) as a categorical independent variable. From the predictor variables, we systematically developed the most parsimonious models generally following procedures described by Zuur et al. (2007; 2009). We used R version 3.6.0 (R Core Team, 2019) and R Studio version 3.6.0 (RStudio Team, 2015). We started with a conventional multiple linear regression (MLR) model (Model 1 in Tables 2.1 and 2.2) by systematically trying individual combinations of predictor variables that gave the highest R^2 and eliminating non-significant variables. This was done manually. Multi-collinearity of predictor variables was avoided by not combining predictor variables with correlation coefficients greater than 0.5, and by checking the impact of variables on each other in case of doubt. Since elevation was correlated to many of the predictor variables, we improved Model 1 by using mixed models which took elevation into account in different ways. Elevation was divided into five classes, each representing 500 m.a.s.l. Model 1 was then improved with either a variance structure that allowed for individual variation at each elevation class (using the function 'gls()' and the varIdent variance structure of the R software package 'nlme') (Model 2 in Tables 2.1 and 2.2); or a linear mixed effects model using the elevation class as a random effect using the 'lme()' function in package 'nlme' (Model 3 in Tables 2.1 and

2.2). This accounted for possible dependencies of multiple measurements within elevation classes. From the three models, the best-fit model (generally Model 2 or Model 3) was selected based on the model that gave the lowest value of the Akaike Information Criterion (AIC) and the most homogeneous and normally distributed residuals (Burnham and Anderson, 2002).

To analyze the effect of RRH systems on DSi yields, we did a simple linear regression analysis of DSi yields with river distance in the four RRH sections of the Inn and Lech Rivers (Inn 1, Inn 2, Lech 1, and Lech 2). The relationships between nutrient concentrations from reservoirs and abundance of different phytoplankton taxonomic groups (cells/ml) was also investigated using simple linear regression analysis. The data are presented in supplementary Appendix 1 (land use), Appendix 2 (lithology), Appendix 3 (physical water quality parameters and nutrient concentrations), Appendix 4 (means and standard error of nutrient concentrations and ratios for the three different system types) and Appendix 5 (correlation results).

2.3 RESULTS

Physical-chemical parameters. Corresponding with higher elevations, reservoir and inlet sites had lower temperatures (4 to 16 °C) in comparison with RRH sites (15 to 21 °C; Figure 2.2a). Specific conductivity for reservoirs and inlets was lower (medians 38 and 36 µS/cm, respectively) in comparison with RRH systems (253 µS/cm; Figure 2.2b). Dissolved oxygen (DO) concentrations were not significantly different among the three system types (median DO 9.5 mg/L; Figure 2.2c). pH was significantly higher in RRH systems (median 8.2) than in the reservoirs and inlets (median 7.9 and 7.8, respectively; Figure 2.2d).

Nutrient concentrations and ratios. DSi concentrations ranged from 0.1 to 5.5 mg/L, with inlet streams showing the greatest variability (Figure 2.3a). Despite this variability, there was a significant difference in DSi among system types, with RRHs showing a significantly higher DSi concentration (median 3.38 mg/L) than inlets and reservoirs (medians 1.38 and 1.10 mg/L, respectively) (Figure 2.3a; $p < 0.001$). Cl was significantly higher in RRH (median 5.65 mg/L) compared to inlets and reservoirs (median 1.22 and 1.28 mg/L respectively) (Figure 2.3j). DSi:DCl for inlets (ranged from 0.06 to 2.61) showed the high variability and was significant higher than RRH (ranged from 0.11 to 0.44). DSi:DCl in the reservoirs ranged from 0.23 to 0.79 (Figure 2.3b). TDN and TDP concentrations ranged from 0.09 to 1.9 mg/L and from 2 to 60 µg/L, respectively. The highest TDN and TDP concentrations were found in the RRHs (medians 0.63 mg/L and 12.29 µg/L, respectively), and were significantly greater than in inlets and reservoirs (Kuskal-Wallis post-hoc test; $p < 0.001$) (Figure 2.3e, 2.3g) (Appendix 3)

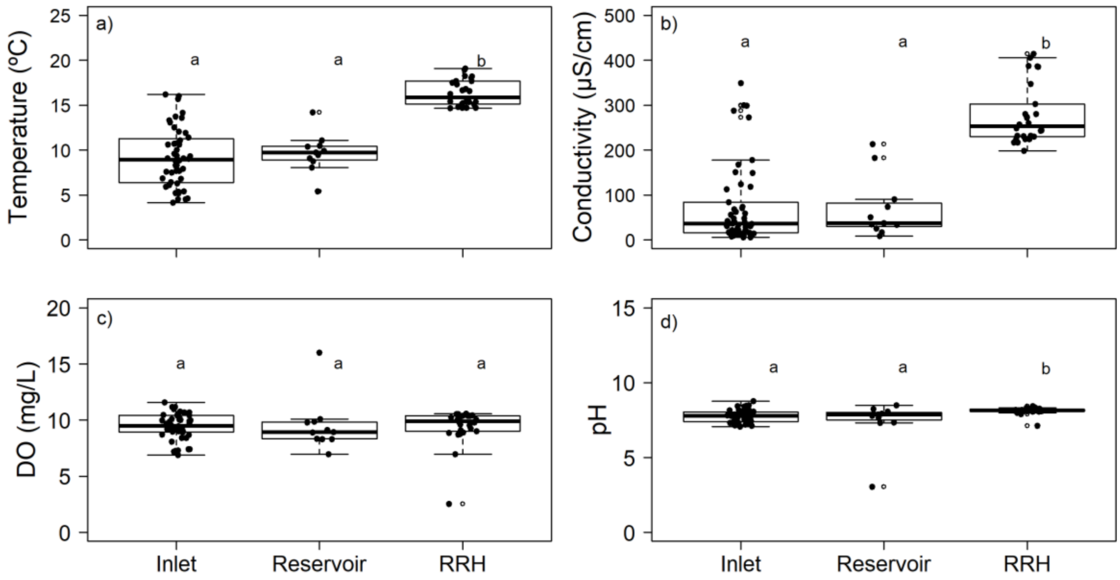

Figure 2.2. Temperature (a), electrical conductivity (b), dissolved oxygen (b) and pH (d) of inlets (n = 50), reservoirs (n = 11) and run-of-river hydropower systems (n = 26). System types sharing the same letter were not significantly different (Kruskal-Wallis ANOVA and post-hoc test, p < 0.001).

For TDN:DCl and TDP:DCl ratios, RRH ranged from 0.20 to 0.39 and 0.0014 to 0.0048 respectively and were significantly lower than inlets (0.13 – 0.82 for TDN:DCl; 0.002 – 0.011 for TDP:DCl) and reservoirs (0.32 – 0.67 for TDN:DCl; range 0.003 – 0.012 for TDP:DCl) (Figure 2.3f, 2.3h). TDN:TDP was > 16 in the three system types (28 – 197) with the highest TDN:TDP ratios occurring in the RRHs (Figure 2.3i). TDN:DSi ranged from 0.1 to 5, with lower values in inlets (median 0.55) than in reservoirs and RRHs (1.06 and 0.89 respectively; $p<0.001$) (Figure 2.3c). There was no significant difference in DSi:TDP among system types (11 – 451; Figure 2.3d).

Controls of nutrient concentrations, yields and ratios. Here we describe the mixed model results, which in most of the cases were consistent with the bi-variate scatter plots, which are included for interpretation of overall patterns shown in the mixed models (Figure 2.4 and 2.5). For DSi yields, the most parsimonious multivariate model (Model 2) included % metamorphic rock, % coniferous cover, and system types (Model 1: R^2 = 0.53, Model 2: AIC = 441.61) (Table 2.1) with DSi yields positively related to both % metamorphic rock, and % coniferous land cover. These variables were also shown for RRH and inlet systems in the bi-variate correlations (Figure 2.4a, rho = 0.63 for inlets; and Figure 2.4c; rho = 0.86 and 0.30 for RRH and inlet respectively). There was a significantly lower intercept for inlets than for RRH systems (Table 2.1).

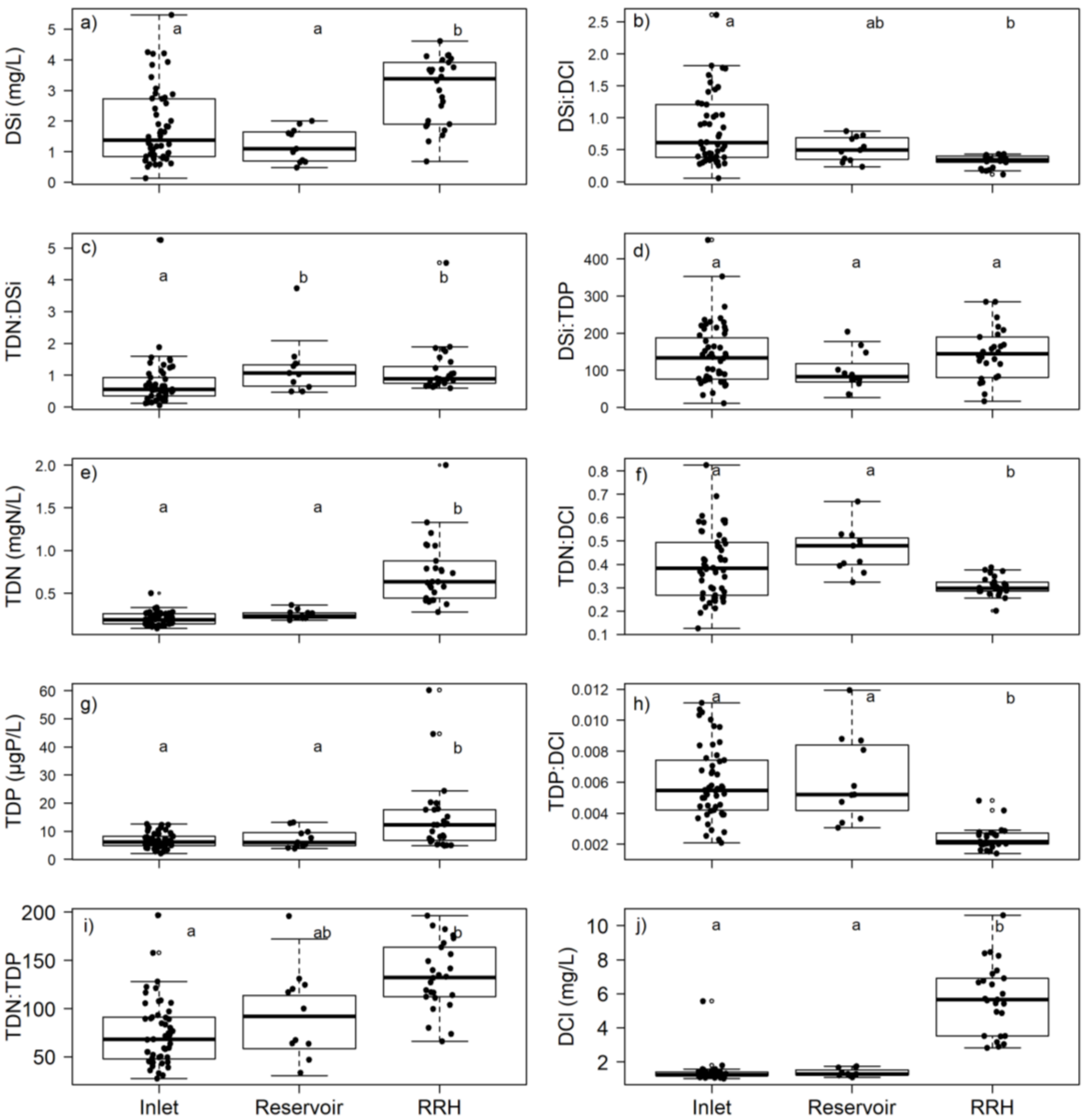

Figure 2.3. Dissolved silica (DSi) concentration (a), DSi:DCl ratio (b), TDN:DSi ratio (c), DSi:TDP ratio (d), total dissolved nitrogen TDN (e), TDN:DCl ratio (f), total dissolved phosphorus TDP (g), TDP:DCl ratio (h), TDN:TDP ratio (i), and dissolved chloride (DCl) concentration (j) of inlets (n = 50), reservoirs (n = 11) and run-of-river hydropower systems-RRH (n = 26). All nutrients ratios are expressed in molar units. System types sharing the same letter were not significantly different (Kruskal-Wallis ANOVA and post-hoc test, p < 0.001).

*Table 2.1. Results of the best-fit regression models for silica concentration (DSi), and silica ratios with Cl, N, P (n = 87 for RRH, Reservoirs and Inlets) and for DSi yield (n= 76 for RRH and Inlets). Model 1 is the best-fit multiple regression model following the model-development procedure (see Methods), which includes % coniferous, % metamorphic rock and system type; Model 2 includes a covariance structure for elevation class; and Model 3 is a random intercept model for each elevation class. Significance of slopes are indicated with * (p < 0.05), ** (p< 0.01), and *** (p< 0.001), and differences among system types (intercepts) are represented by different letters.*

	Dependent variables									
	DSi		**DSi:DCl**		**TDN:DSi**		**DSi:TDP**		**DSi yield**	
Model comparison:										
R^2 (Model 1)	0.56		0.58		0.33		0.21		0.53	
AIC (Model 1)	231.27		-37.66		30.29		164.09		509.67	
AIC (Model 2)	**207.44**		**-35.66**		**30.29**		**148.50**		**441.64**	
AIC (Model 3)	215.47		-70.88		30.98		160.61		471.91	
Best-fit model result										
Fixed effects:										
- Intercept										
RRH	2.52	b	0.07	a	0.92	b	4.58	a	21.73	b
Inlet	0.78	a	0.35	b	0.69	a	4.51	a	2.24	a
Reservoir	0.43	a	0.25	b	0.79	a	4.31	a		
-Slopes										
% coniferous	2.86	***	0.67	***	-0.66	***	0.78	***	7.65	***
% metamorphic rock	0.80	***	0.17	***	-0.07	ns	0.38	**	2.09	**
Residual Std. Error	1.59		0.11		0.13		0.47		17.27	

Similar results were found in the DSi concentration model (Model 1: R^2 = 0.56, Model 2: AIC = 207.44.2; Table 2.1) and DSi:DCl model (Model 1: R^2 = 0.58, Model 2: AIC = -35.66), which also showed that DSi concentrations and DSi:DCl ratio were positively related to both % coniferous land cover and % metamorphic rock. For the DSi concentration model, there was a significantly lower intercept for inlets than for RRH systems (Table 2.1), which is also seen in Figure 2.3a and supported by the results of the Kruskal-Wallis test (Figure 2.3a).

The TDN and TDP yield models both showed relatively good model fits (R^2 = 0.74 and 0.62 respectively, with Model 2 showing the best-fit mixed model (AIC = 125.47 and -372.77 respectively; Table 2.2). The TDN and TDP yield and concentration models all showed a positive relationship with % agriculture (Table 2.2), and these results are consistent with the bi-variate correlations shown in Figure 2.5b and 5e (rho = 0.74 for RRH and rho = 0.36 for inlets) and Appendix 7b and Appendix 7e (rho = 0.86 for RRH and rho = 0.24 for inlets). TDN yield and concentration models showed no significant relationship with % coniferous land cover, while TDP showed a positive relationship (Appendix 7d and 7l). The best fit model for TDN:DCl and TDP: DCl (Model 2: AIC = -178.42 and -776.81 respectively; Table 2.2), showed lower model fits (R^2 = 0.16 and 0.41 respectively; Table 2.2) and the same positive effect from % agriculture, which is also shown in the bi-variate plots for TDP:DCl (Appendix 7k). Percent coniferous land cover showed a negative effect on TDN:DCl and a positive effect on TDP:DCl (Table 2.2), although in this case the bi-variate plots were not consistent with these results (Appendix 7g and 7j).

For the silica:nutrient ratio models (TDN:DSi and DSi:TDP), the overall model fits were lower, with R^2 values 0.33 and 0.21, respectively (Table 2.1). Percent coniferous land cover was a highly significant predictor in both models. In Figure 2.4e and 2.4i showed the bi-variate plots of TDN:DSi (rho = -0.53 for RRH, rho = -0.64 for inlets and rho = -0.73 for reservoirs) and DSi:TDP (rho = 0.73 for RRH and rho = 0.50 for inlets) with % coniferous. The % of metamorphic rock had a significant effect in the DSi:TDP model (Figure 2.4k; rho = 0.60 for RRH), but was not significant in the TDN:DSi model.

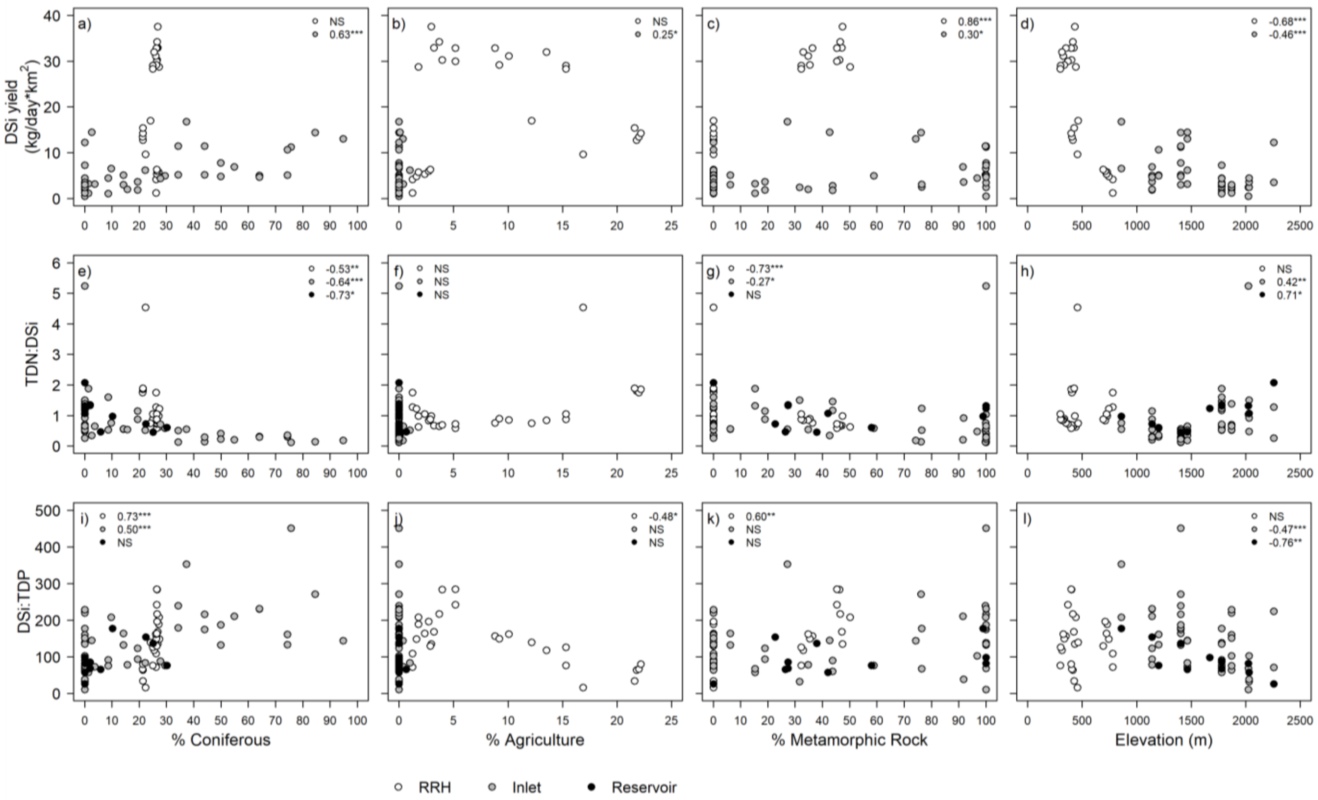

*Figure 2.4. Relationship between DSi yield and the ratios of DSi with TDN and TDP and the main controlling factors (% coniferous, % agriculture, % metamorphic rock and elevation) for the three system types: inlets, reservoirs, and run-of-the-river hydropower systems (RRH). Numbers indicate Spearman rank correlation coefficients for each system type. Significance is indicated with * ($p < 0.05$), ** ($p < 0.01$), *** ($p < 0.001$) or NS (not significant).*

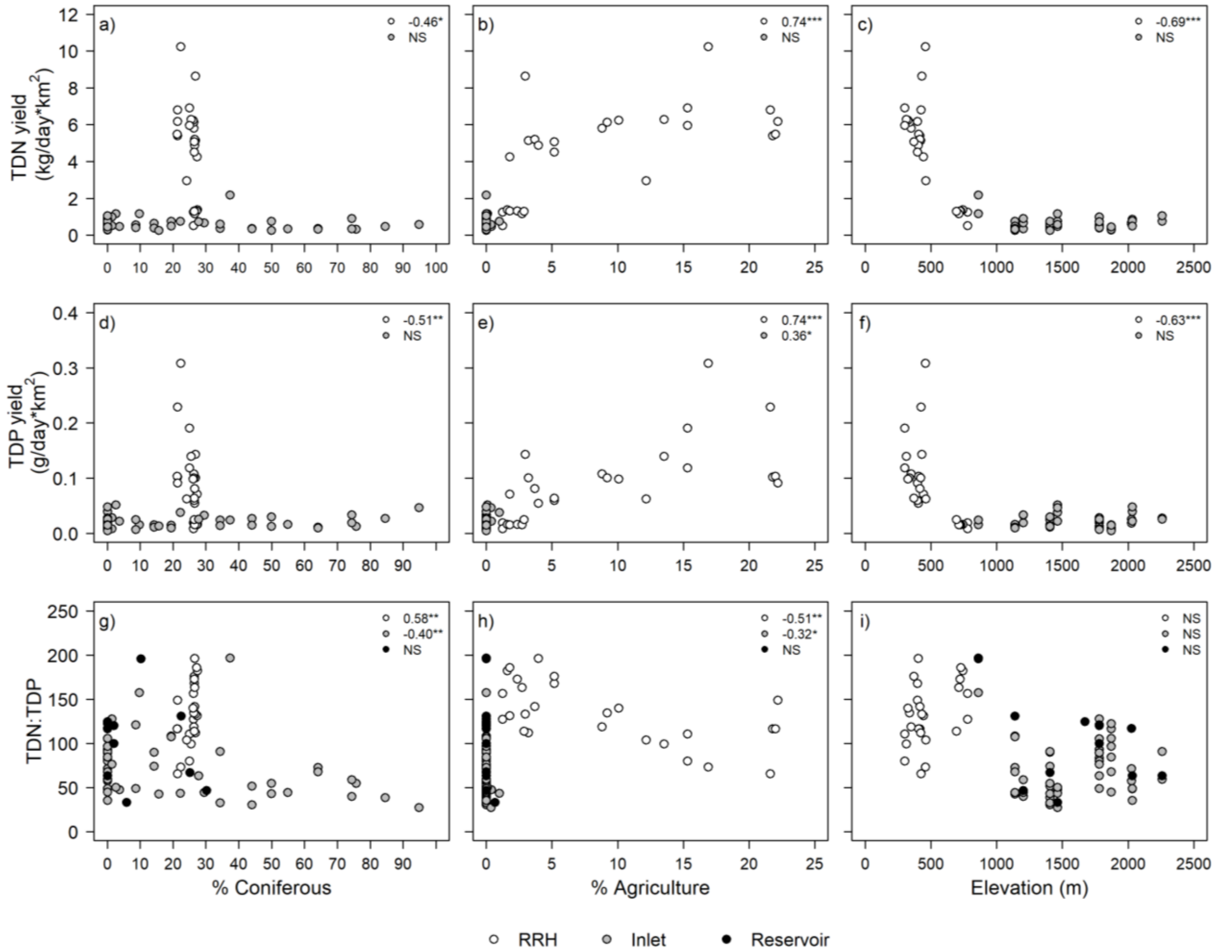

*Figure 2.5. Relationship between nutrient yields and their ratio (TDN, TDP and TDN:TDP) and the main controlling factors (% coniferous, % agriculture and elevation) for the three system types: inlets, reservoirs, and run-of-the-river hydropower systems (RRH). Numbers indicate Spearman rank correlation coefficients for each system type. Significance is indicated with * (P < 0.05), ** (p < 0.01), *** (p < 0.001) or NS (not significant).*

*Table 2.2. Results of the regression models for nitrogen (TDN) and phosphorus (TDP) concentration and their ratios with Cl with total no. of observations was 87 (RRH, Reservoirs and Inlets); TDN and TDP yield with total no. of observations was 76 (RRH and Inlets). Detailed results of the best fit model, with the lowest AIC-value (indicated in bold) are presented. Significance of intercepts are indicated with * (p < 0.05), ** (p< 0.01), and *** (p< 0.001).*

	Dependent variables													
	TDN		**TDN:DCl**		**TDP**		**TDP:DCl**		**TDN:TDP**		**TDN yield**		**TDP yield**	
Model comparison[a]:														
R^2 (Model 1)	0.79		0.16		0.52		0.41		0.44		0.74		0.62	
AIC (Model 1)	-57.26		-152.64		534.83		-754.90		90.23		250.53		-270.52	
AIC (Model 2)	**-130.08**		**-178.42**		**452.98**		**-776.81**		87.43		**125.47**		**-372.77**	
AIC (Model 3)	-55.26		-151.26		536.83		-756.17		**71.92**		208.51		-273.91	
Best-fit model result														
Fixed effects:														
Intercept														
RRH	0.35	b	0.26	a	2.06	a	0.0011	a	4.70	a	0.87	a	-0.0011	a
Inlet	0.19	b	0.34	b	5.25	b	0.0049	b	4.57	a	0.61	a	0.0165	b
Reservoir	0.24	ab	0.38	b	5.70	b	0.0050	b	4.68	a				
Slopes														
% agriculture	4.09	***	0.147	***	122.27	***	0.0076	***	-2.20	*	31.50	***	0.77	***
% coniferous	-0.01	ns	-0.063	*	4.74	***	0.0027	*	-0.39	ns	-0.23	ns	0.01	*
Random effects:														
intercept s.d.[b]									0.47					
residual s.d.[c]									0.30					
Residual s.e.[d]	0.12		0.10		1.35		0.0012				0.71		0.0046	

[a] Model 1: multiple linear regression model with % agricultural land use and % coniferous land cover as independent variables and no random effects; Model 2: variance structure model with same fixed independent variables as Model 1 that allowed different variances for each elevation class; Model 3: random intercept model for elevation class, with same independent variables as Models 1 and 2. [b]Intercept standard deviation. [c] Residual standard deviation. [d]Residual standard error.

The best fit model for the TDN:TDP ratio ($R^2 = 0.44$) was Model 3 (AIC = 71.92; Table 2.2), which showed a negative relationship with % agriculture and no effect of % coniferous land cover. which were consistent with bi-variate plots in Figure 2.5h (rho = -0.51 and -0.32 for RRH and inlets). The negative impact on TDN:TDP ratio suggests that agriculture had stronger impact on phosphorus than on nitrogen.

Correlations of controlling factors with silica:nutrient ratios followed mostly the effects on DSi and nutrients. Percent coniferous cover was related to decreased TDN:DSi ratios and increased DSi:TDP ratios, because of the positive relationship with DSi in inlets and RRH (Figure 2.4e and 2.4i). Agriculture had no significant correlation with TDN:DSi (Figure 2.4f), but a negative correlation with DSi:TDP in RRH systems (Figure 2.4j); indicating that the impact of agriculture was stronger for TDP than for TDN. This was confirmed by the negative correlation of agriculture with TDN:TDP in RRH and inlets systems (Figure 2.5g). The strong impact of % metamorphic rock on DSi in RRH systems was reflected in the negative and positive correlations, respectively, with TDN:DSi and DSi:TDP ratios (Figure 2.4g, 2.4k).

Longitudinal regression analysis. DSi yield was higher in Inn River (31.5 kg/day*km^2) than a Lech River (9.5 kg/day*km^2). Regression analysis between DSi yield and the distance between RRH in the four sections of the Inn and Lech Rivers (Inn 1, Inn 2, and Lech 2) showed that regression coefficients were not significantly different from zero ($p > 0.05$). Results showed that there was no significant difference of DSi yield between RRHs in those four river sections (Figure 2.6).

Phytoplankton abundance and chlorophyll a concentration. Diatoms, green algae and cyanobacteria were the major phytoplankton groups in the reservoirs, while Rhodophyta, dinoflagellates and Chrysophyceae were found in minor proportions (data not shown). Linear regression showed DSi had a positive relationship with diatom abundance ($p < 0.05$, $R^2 = 0.39$) (Figure 2.7a). No significant relationship was found between cyanobacteria or other phytoplankton taxonomic group and nutrient concentration and ratios. Additionally, estimated chlorophyll *a* concentration in the reservoirs ranged from 0.2 to 1.9 µg/L, with an exception of 22 µg/L in reservoir RE11 located downstream of the city of Gmund. Chlorophyll *a* concentration was only significantly related to DSi concentration ($R^2 = 0.51$, $F = 11.43$, $p < 0.001$) (Figure 2.7b).

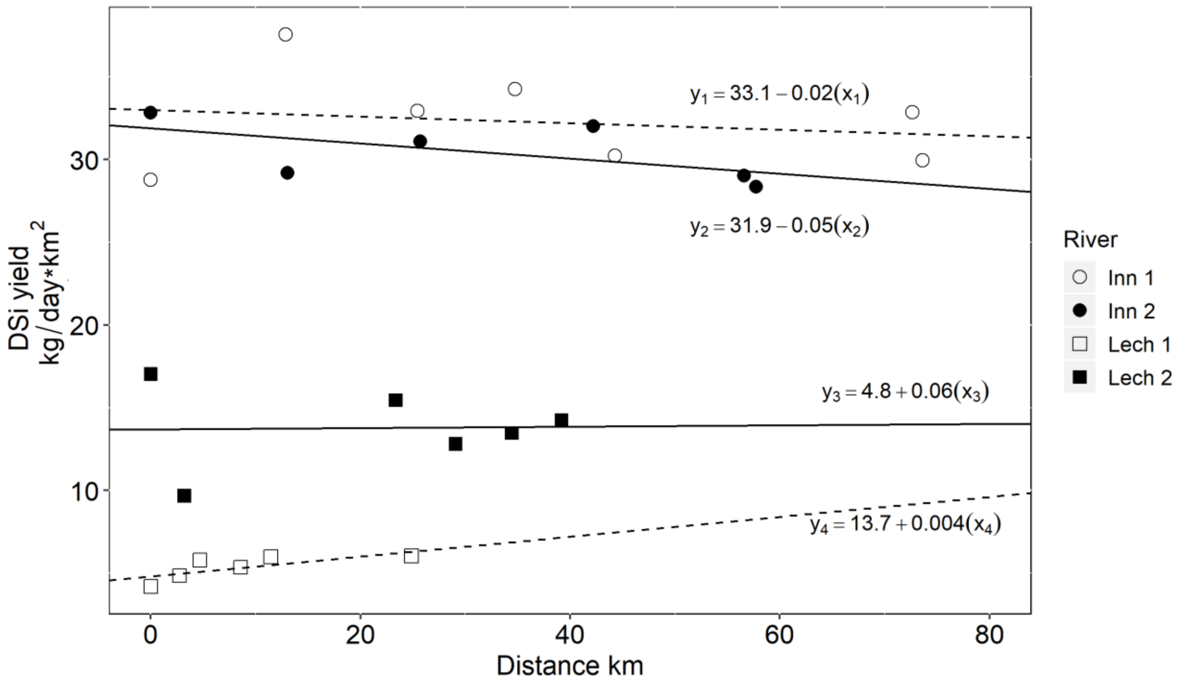

Figure 2.6. Longitudinal trend of DSi yield for two rivers Inn and Lech with presence of RRH. The two rivers were divided in four sections: Inn 1 - upstream (y_1) (R^2= 0.03), Inn 2 – downstream (y_2) (R^2= 0.4), Lech 1 – upstream (y_3) (R^2= 0.6), Lech 2 – downstream (y_4) (R^2= 0.001).

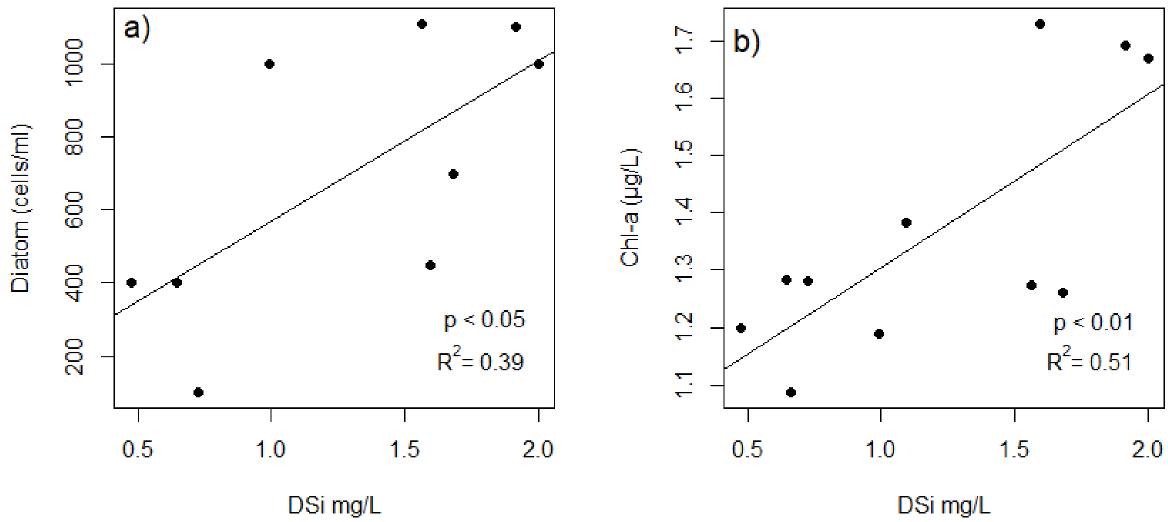

Figure 2.7. a) Relationship between DSi and diatom abundance in the reservoirs (n = 9). The estimated regression line equation is y = 130.7x + 438.4. b) Relationship between DSi and chlorophyll a concentration in the reservoirs (n = 11) and the estimated regression line equation is y = x + 0.30. Lines indicate linear regression relationships.

2.4 DISCUSSION

In this paper we were able to use estimate the contribution of lithological class, LULC variables and residence time (system types) to DSi export and DSi ratios with TDN and TDP. We controlled for hydrological variation by scaling each nutrient with a conservative ion (chloride) and also estimated yields through applying a discharge model. These three approaches (concentrations, nutrient:chloride ratios, and yields) gave us similar statistical outcomes and conclusions.

Landscape controls of dissolved silica, nitrogen, and phosphorus. Our results show that DSi concentrations and yields in surface water of the upper Danube basin are controlled by lithology (% metamorphic rock) and % coniferous forest land cover whereas TDN and TDP yields are predominately controlled by % agriculture and % coniferous forest land cover types. None of the other predictor variables we tested (% artificial areas, % deciduous, % grasslands, and other types of lithology) were significant or gave stronger explanatory power in the overall multivariate mixed models. A closer look at the bi-variate correlations (Figure 2.4 and Appendix 6) reveal more detailed understanding of the differences between these controls in reservoirs, inlets, and run-of-the-river hydropower systems for all three nutrients.

Silica. For reservoirs and inlet systems, coniferous forest cover shows stronger correlations for DSi yield and concentrations than for run-of-the-river systems (Figure 2.4) where DSi concentration and yield is most strongly related to % metamorphic rock. Other studies (Dürr et al. 2011; Beusen et al. 2009) have suggested that lithological differences may play a stronger role in describing Si export in larger catchments, e.g. >10,000 km^2. However, these studies also argue that at local and regional scales, factors such as LULC and human impacts should be considered and that the importance of these factors likely vary depending on climate conditions among other factors. The catchments involved here are relatively small (0.2 – 26,250 km^2), and the weaker correlation of DSi with lithology in the upper-elevation systems may be due to the diversity in the types of inlet rivers, which comprise largely krenal (groundwater-fed) and rhithral and kyral (glacial- and snowmelt-fed) streams (Brown et al. 2003), with krenal streams showing higher DSi concentrations compared to rhithral streams (2.6 vs. 1.3 mg/L in our study; Table 2.3). Other studies have also shown different relationships DSi concentration with lithology (Table 2.4), ranging from negative (with % carbonate rocks; Humborg et al. 2004 or sandstone; Onderka et al. 2012), positive (with marls; Onderka et al. 2012) and no relationship (with % carbonate rocks; Carey and Fulweiler 2012). These results show the potential importance of the typology of the river systems in understanding controls on and sources of DSi export in alpine systems, and that the relative importance of lithology and landcover may vary depending on the types of systems involved.

In addition to system-type, the scale and region may also be important in determining the relative importance of lithology and LULC characteristics, as most other regional-scale studies find significant relationships of lithology on DSi concentration or export along with LULC – although these results are also variable, ranging from positive, negative, or no relationship (Table 2.4; Humborg et al. 2004; Carey and Fulweiler 2012; Onderka et al. 2012; Chen et al. 2014). One study in the Upper Mississippi Basin found that lithology (limestone and shale) and water residence time and *not* LULC were most important in controlling silica concentration in the Upper Mississippi Basin (USA) (Carey et al. 2019). This basin is the largest basin summarized in Table 2.4 (490,000 km^2), and the authors hypothesized that the importance of lithology is due to the wide range of variation within the catchment area relative to the variation in LULC. The variability of the lithological classes used in the studies summarized in Table 2.4 and their different levels of significance highlight the importance of considering lithology as well as the LULC variables at local and regional scales in understanding controls on DSi export, as the relative importance of these variables will depend on specific basins.

Coniferous forest cover positively contributed to DSi concentration and yield, which is consistent with Humborg et al. (2004), who assessed landscape controls on DSi concentration in Swedish rivers, which are, like our study, characterized by coniferous forests in relatively unperturbed areas with little agriculture or urban development. Two studies (Carey and Fulweiler, 2012 and Chen et al. 2014; Table 2.4) in contrast, showed negative relationships with forest cover, but the reasons for this difference are unclear. The authors interpreted the relationship to be due to Si storage in plant biomass, which can be important especially in aggrading forests (Fulweiler and Nixon 2005; Struyf et al. 2010). The forests in our study are mostly undisturbed and generally in a climax state and less likely to retain (re)mobilized Si and therefore be more susceptible to hydrological losses through soil-processes (Struyf et al. 2010). The forests in the Carey and Fulweiler (2012) and Chen et al. (2014) studies also comprised mixed coniferous and hardwood forests (in southern New England (USA), and in southern China, respectively). The solubility of phytoliths of different types of trees may also play a role. Phytoliths from coniferous trees are apparently less soluble than deciduous trees owing to differences in Si/Al ratios, surface area, and water content (Bartoli and Wilding, 1980; Bartoli 1985), suggesting that the relative importance of tree species in mixed stands may be important in understanding overall how forest cover affects DSi export, and may point to the need to discern these types when using remote sensing to model DSi export. Taken together, it seems that forest dynamics (age and type) are more important in controlling Si export in the more natural catchments than in more developed systems, which also tend to be located at lower elevations, especially in these particular alpine catchments.

DSi concentration was not affected by agriculture or artificial areas, which adds to the mixed results from the literature (Table 2.4). This differs from findings related to other types of agriculture in which harvesting removes phytoliths (especially of cereal crops) and ultimately a reduction in DSi export (Guntzer et al. 2012; Vandevenne et al. 2012). Agriculture in the study region is dominated by livestock production rather than crop-production systems, which may be harvested for hay or grazed. Grazing increases the mobility and turnover Si through manure deposits, as digestion breaks down organic matrices and makes DSi more easily accessible to soil processes (Vandevenne et al. 2013), including for plant re-uptake. Further study is needed to understand how and over which time-scales grazing and crop systems affects DSi export in agricultural systems, and further highlights the need to carefully assess how remote sensing data is classified with respect to land use for modeling DSi export.

Urban land use was not a significant predictor that affected DSi concentration in this study area. Previous studies have been mixed (Table 2.4), showing that urban land use either has no effect (Conley et al. 2000) or a positive effect (Sferratore et al. 2006, Carey and Fulweiler, 2012, Onderka et al. 2012). Onderka et al. (2012) and Carey and Fulweiler (2012) analyzed a range of urban areas in different sub catchments in Luxembourg (0 - 20% urban area) and Massachusetts and Connecticut (USA) (0.2 - 69.5% of developed areas) respectively, covering a much larger range of urban area than our study (only up to 6%). Sferratore et al. (2006) showed that the urban discharge from wastewater treatment plants (WWTP) near Paris comprised 8% of DSi input in the Seine river basin. These studies suggest that urban areas are important when they include densely populated areas or a significant percentage of the catchment area, with potential sources including artificially produced zeolith used for paper production and pharmaceuticals and detergents (Dürr et al. 2011, van Dokkum et al. 2004). In our study, urban systems are mainly characterized by small populated centers, and appear to be unimportant points sources of Si compared with the natural sources from lithology and forest land cover.

Nitrogen and phosphorus. Of all the landscape variables considered, TDN and TDP concentrations across all the sites were influenced only by agricultural land use (Table 2.2), which in the study region is likely the result of manure deposition from livestock and/or manure spreading. This was visible particularly in RRH systems, with significantly higher median nutrient concentrations that were clearly correlated with agricultural land use and in the inlet systems (Figure 2.5), located where traditional high-altitude grazing lands are maintained therefore showing a large range of % agricultural land use across all the sites (Figure 2.5).

Differences in system types and longitudinal variation in stoichiometry.
Silica. There are very few other studies that report on Si concentration in high alpine regions, but the stream inlet results were similar to results from the Italian and Swiss Alps (0.1 – 1.2 mg/L) (Table 2.3), and as much as 5 times lower than main-stem sites in the

Danube River at lower elevations (ICPDR; Table 2.3). Long-residence time reservoirs had the lowest DSi concentrations of all three systems, and on average a much lower concentration of DSi than the inlet systems. These was only one other study from a mountain lake in Italy also showing a low concentration in the range of our values (Table 2.3). The low DSi:Cl ratio in the reservoirs compared to inlets (Figure 2.3) suggests Si sequestration and subsequent reduction of DSi transport (and variability) to downstream systems compared to what would have been formerly free running rivers. The high-elevation, long-residence time reservoirs are oligotrophic and may not seem to support high production that would lead to increased sequestration; however oligotrophic lakes and reservoirs can sequester significant amounts of DSi, e.g. 20 – 90% (Harrison et al. 2012). Further work should include seasonal monitoring for e.g. spring and fall diatom blooms, more precise understanding of residence time and outflows, and using sediment cores to further understand the potential sequestration in these reservoirs.

Table 2.3. Overview of published literature and monitoring stations reporting the DSi (mg /L) for the Danube River. DSi values represent medians for the period reported with the range in parentheses. [a]Mean. [b]Statndard error

Station/system name	**Country**	**Elevation m.a.s.l.**	**River**	**Year**	**DSi (mg/L)**	**Reference**
Haut Glacier d'Arolla	Switzerland	3030	Switzerland	1993 – 1994	1.0[a] (0.8 – 1.1)	Tranter et al. 2002
Lillet lake western Italian Alps	Italy	2087 - 2765	Po Italy	2008	0.7[a] (0.1 – 1.2)	Tiberti et al. 2010
Reservoirs	Austria	859 - 2024	Inn and Lech (upper basin)	2015 – 2016	1.2[a] (0.5 – 2.0)	This study
Krenal Inlets	Austria	859 - 2030	Inn and Lech (upper basin)	2015 – 2016	2.6[a] (0.8 – 5.5)	This study
Rhithral Inlets	Austria	1140 - 2024	Inn and Lech (upper basin)	2015 – 2016	1.3[a] (0.1 – 3.4)	This study
Run-of-the-river hydropower	Austria and Germany	300 - 780	Inn and Lech (upper basin)	2015 – 2016	3.0[a] (0.7 – 4.6)	This study
Inn 4.2	Austria and Germany	308	Inn	August 2007	4.1	ICPDR
Inn 0.6	Austria and Germany	300	Inn	August 2001	3.4	ICPDR
Bratislava	Republic of Serbia	128	Danube	2007 – 2017	5.8[a] ± 0.1[b] (1.1 - 13.9)	ICPDR
Batina	Croatia	86	Danube	2008 – 2017	4.9 [a] ± 0.2[b] (0.1 – 17.2)	ICPDR
Bogojevo	Republic of Serbia	80	Danube	2002 – 2017	5.6[a] ± 0.2[b] (0.3 - 13.4)	ICPDR
Banatska Palanka	Republic of Serbia	70	Danube	2002 – 2017	5.8[a] ± 0.2[b] (0.4 – 12.1)	ICPDR
Reni-Chilia/Kilia arm	Romania	5	Danube	2001 – 2017	5.3[a] ± 0.1[b]	ICPDR

					(0.4 – 21.4)	
Vylkove	Ukraine	1	Danube	2007 – 2017	$3.2^{a} \pm 0.2^{b}$ (0.6 – 10.8)	ICPDR
Sulina arm	Romania	1	Danube	2001 – 2011	$6.4^{a} \pm 0.2^{b}$ (0.4 – 18.7)	ICPDR
Sulina arm	Romania	1	Danube	1979 – 1992	3.5^{a} (0.4 – 6.6)	Humborg et al. 1997

Table 2.4. Summary of peer-reviewed literature that statistically examined landscape controls on DSi, with studies showing either a positive (+), negative (-) or no relationship (nr). Blanks show that the study didn't consider the variable.

Reference	**Geology/lithology[a]**							**LULC[b]**								**Dams**	**Impoundment[c]**	**Remarks**
	cb	vc	mf	sd	mr	sa	gr	fo	co	de	df	ag	art	gr	wet			
DSi concentration in Rivers																		
Jordan et al. 1997												–						Basin area 0.53 - 32 km^2 in Chesapeake Bay (USA).
Conley et al. 2000								nr				+	nr					River mouths in Sweden and Finland.
Humborg et al. 2004	–	+							+	–					nr			Basin area from 34 to 39000 km^2 in Sweden.
Sferratore et al. 2006													+					Urban discharge in the Seine River. France.
Conley et al. 2008											+							Basins 0.11 - 0.36 km^2 at the Hubbard Brook Experimental Forest USA.
Carey and Fulweiler, 2012	nr		+	+			nr		–	–		nr	+					Basin area from 27 to 11450 km^2 Southern New England USA.
Chen et al. 2014							+		–			+				–		Jiulong River, basin area is 14,741 km^2. Located in southeastern China.
Carey et at. 2019				+													+	Upper Mississippi River System – USA, basin area 490,000 km^2.
DSi yield in Rivers																		
Struyf et al. 2010								+						–				Scheldt basin (Belgium).
Onderka et al. 2012					+	–		+				nr	+	–				Basin area from 0.47 to 1091 km^2 Luxembourg.

BSi in Soil		
Clymans et al. 2011	–	All sites were located in southern Sweden
Vandevenne et al. 2012	–	Between 0.46 – 0.70 kg BSi $km^{-2}year^{-1}$ is removed from the soil by harvest in Belgium.
Guntzer et al. 2012	–	Experimental crop areas at Rothamsted Research (UK).
Carey and Fulweiler, 2016	+	Data from the United Nations Food and Agricultural Organization (FAO).

[a] *Geology categories cb: carbonate rock, vc: acid volcanic rocks, mf: mafic, sd: sedimentary rock, mr: marl, sa: sandstone, gr: granite rocks.*
[b] *LULC: fo: all forest, co: coniferous forest, de: deciduous forest, def: deforested area, agr: agriculture, art: artificial areas, gra: grasslands, wet: wetlands.*
[c] *Rt: Residence time.*

The RRH sites in the mainstem of the Inn and Lech Rivers had higher DSi yields by factors of two to four respectively (Table 2.1), suggesting that these reservoirs were not likely retaining Si in the same rate as the longer residence time reservoirs upstream. The longitudinal trends in DSi yields in the four different RRH sequences over 5 – 12 km of river length (Figure 2.6) showed no significant change in DSi yields, also suggesting that residence time, which is ~ 1 day, is not as important as in the upper-elevation reservoirs.

This conclusion, however, is not 100% straightforward, as we cannot fully understand the effect of loading and discharge in both places, as we are not able to calculate exact discharge from the long residence time reservoirs (see methods), and the method of using the DSi:Cl ratios is also not reliable in the downstream section of the study area because the concentration of Cl is significantly higher (Figure 2.3), likely as a result of increased agricultural influence and/or road-salt application. RRH reservoirs also contain higher concentrations of N and P than the long-residence time reservoirs and may therefore have higher Si uptake, even though we don't detect a net storage in this data set.

Nutrient ratios. We hypothesized that different controls of N and P compared to DSi would lead to changes in nutrient ratios and differences in limitation in different systems. If DSi were being preferentially stored at faster rates in either the long-residence time or RRH reservoirs, we would predict lower DSi:TDP ratios, and possible DSi limitation (i.e. DSi:TDP < 40). In fact the DSi:TDP showed a strong P limitation (DSi:TDP ratios ranging from 100 –145). Despite this, DSi was the only nutrient that was related (positively) to chlorophyll *a*, a response that is likely due to the diatom taxa, which comprised on average 25% of the phytoplankton community in the reservoirs we sampled (data not shown). Furthermore, the synoptic survey approach did not allow us to capture seasonal dynamics in phytoplankton community structure or nutrient loads, and the fact that we did not include dissolved organic fractions of P or BSi, both which may be efficiently recycled in these oligotrophic systems and may therefore be more bioavailable that using the inorganic nutrients would suggest (Van Cappellen 2002; Thingstad et al. 2005).

Despite the different controls on DSi and TDP, the DSi:TDP remains relatively constant along the longitudinal gradient. In downstream sections, agricultural land use contributed to increased TDP, while lithology contributed to an increase DSi. The end result is that these different controls did not lead to differences in DSi and P ratios (or DSi or P limitation) between system types or along the longitudinal gradient. This somewhat contradicts other findings of that suggest that processing in the "freshwater pipe" should result in changes in nutrient stoichiometry, particularly with preferential sequestration of P (Maranger et al. 2018). In this case, we show that the riverine systems are certainly not a pipe, but that the different controlling factors on these two elements do not necessarily result in altered stoichiometry or changes in Si vs. P limitation from upstream to downstream in this case.

The TDN:TDP ratios in all the systems in this study also indicates strong P limitation for the phytoplankton overall (ranging 27 - 197), but with a greater incidence of low N:P ratios in the inlet streams (Figure 2.3i). The phytoplankton community counts in the long residence time reservoirs did not contain high numbers of N-fixing cyanobacteria (data not shown), so there was no strong evidence for compensatory N fixation. The TDN:DSi ratio shows for all three system types, Si limitation relative to N (TDN:DSi were > 0.4). The TDN:DSi ratios overall tended to increase from upstream to downstream from inlets to RRH (Figure 2.3; Appendix 4). This relative increase in N availability from upstream to downstream was due to the increase in agricultural contributions of N over the elevation gradient (Table 2.2), while the long-residence time reservoirs appear to preferentially sequester DSi. This is evidenced by the low DSi:DCl and low concentrations of DSi in the long-residence time reservoirs compared to the inlet streams. Taken together, these results show human alteration of the catchment and river flow (reservoirs and agricultural land use) together with the decreasing control of coniferous forest on DSi yield along the elevation gradient in this system results in more DSi and P limited systems downstream and drives shifts in phytoplankton assemblages in surface waters away from diatoms.

Understanding the implications of the three different nutrient ratios highlights the need to consider both controls on nutrient emission from landscapes as well as the in-river processes, and the combined effect of human impacts. In this study, we see Si limitation in the high-altitude reservoirs, and more likely P limitation in the run-of-the-river reservoirs, while N appears not to be strongly limiting, even in the high altitude inlet streams. Ultimately, it appears that sequestration of silica in the long-residence time reservoirs is important, but that the concomitant increases in Si contribution from lithological sources downstream compensate for the storage, so that the increased contribution of N with increasing agriculture maintain the rivers in the lower elevations in P-limited status.

Humborg et al. (1997, 2006) documented an overall shift in N:Si from 2.8 to 42 in the Black Sea and attributed this to the preferential sequestration of Si in the large number of dams in the Danube River. Our study shows that this dynamic appears to start in the headwaters of the Danube, but that the story is more complicated when taking into account other controlling factors, including LULC and the contribution of lithology. These factors need to be included holistically in assessment of nutrient exports in order to fully understand the effect of human activities on nutrient ratios, nutrient limitation, and impacts on downstream ecosystems.

2.5 CONCLUSIONS

This study analyses DSi, N and P yield and molar ratios in alpine systems in the Alps, which are characterized by a large number of hydropower reservoirs and run-of-the-river hydropower systems. Specifically, controls related to reservoir system types (short and long residence time) as well as landscape and lithological variables were evaluated. Results show that in relatively unimpacted systems at high-elevation, forest cover and lithology are main controlling factors of DSi yields, while human impacts - specifically agriculture and long-residence time reservoirs conspire to limit Si and P from upstream to downstream systems. This in turn has consequences for phytoplankton community structure and the functioning of aquatic ecosystems. Further work will need to consider seasonal dynamics, better constrained estimates of fluxes, and more detailed work on LULC classes (grazing vs. crop agriculture and forest types). Further analysis of the Danube Basin will help to further clarify the causes for the changes in the delivery of Si and nutrients to the Black Sea.

3

DISSOLVED SILICA IN THE DANUBE RIVER BASIN

3.1 INTRODUCTION

Silicon (Si) is an essential element for the growth of siliceous algae, the preferred food of many grazers and the basis for many productive fisheries (Conley et al. 1993). Changes in Si delivery to coastal systems, caused by human activities including reservoir construction, agricultural development, de-forestation, and urbanization, can cause shifts in phytoplankton community structure, with impacts through the whole aquatic food web (Humborg et al. 2000). The Danube River is one relatively well studied river system that has shown a reduction in DSi concentration (– i.e. from 800 x 10^3 tonnes year^{-1} in 1960 to 230 – 320 x 10^3 tonnes year^{-1} in 1990 (Humborg et al. 1997)). Over the same period, shifts in dominant phytoplankton from diatoms to flagellates have been observed in the Black Sea (Humborg et al. 2000). This reduction was hypothesized to be due to the construction of dams used for hydropower production and flood control (Humborg et al. 2000), but other effects including agriculture and urbanization have not yet been explored. Almost 50% of the Danube Basin territory is under agriculture land use, especially in eastern countries (ICPDR 2005). Emissions from waste-water treatment plants are could also play a role (ICPDR 2015).

Si export in natural ecosystems is controlled by bedrock geology and weathering rates (Hartmann et al. 2010; Cornelis et al. 2011), with recycling mediated by soil processes and vegetation cover (type and productivity) (Conley 2002; Struyf and Conley 2012). However, human activity has altered Si cycling in several ways (e.g. Carey and Fulweiler 2012; Maguire and Fulweiler 2016; Sferratore et al. 2006; Struyf et al. 2010; Vandevenne et al. 2012). Agricultural development generally leads to a reduction in hydrologic Si export (Vandevenne et al. 2012), with ~210 – 224 million tonnes of Si removed per year from cultivated soil (Matichenkov and Bocharnikova 2001). This is of the same order of magnitude as the annual flux of dissolved silica from rivers to oceans (Berner and Berner 1996). Crops tend to take up Si at higher rates than forest and grasslands ecosystems (Guntzer et al. 2012), and crop harvesting removes plant biomass, a subsequent reduction of soil recycling, and ultimately a depletion of the phytogenic Si pool (Keller et al. 2012).

Reservoirs resulting from dam construction reduce Si export through phytoplankton uptake and sedimentation (e.g. Harrison et al. 2012; Maavara et al. 2020b). About 50% of the world's stream and river flow crosses one or more dams before reaching the oceans (Lehner et al. 2011), which removes ~ 9 – 31 million tonnes DSi per year globally, and have been identified as the main factors causing the reduction of Si export in many basins (e.g. the Baltic – Humborg et al. 2008; The Seine – Garnier et al. 1999).
The effect of urbanization on Si export is less well studied, but it seems to have the opposite effect as agriculture by increasing Si export, mainly through the construction of waste water treatment plants (WWTP) and storm-water management, which diverts water that would otherwise infiltrate (Maguire and Fulweiler 2016; Sferratore et al. 2006).

Sources of Si in waste-water include excreted Si, as well as detergents that ultimately reach the aquatic system via discharge (Dürr et al. 2011).

Basin-scale models that predict Si export are relatively uncommon compared with those for nitrogen and phosphorus. The Riverstrahler model is a process-based model and has been applied to large basins of 20 – 80 x 10^3 km^2, including the Danube (Garnier et al. 2002). In this model, lithology alone determines Si inputs, while LULC determine N and P inputs, resulting in Si export partially being controlled by P availability and eutrophication processes in the basin (Garnier et al. 2002). Other models used budget or statistical approaches (e.g. Dürr et al. 2011 vs. e.g. Humborg et al. 2008). In the global-scale News-DSi model, Beusen et al. (2009) used a multiple linear regression approach and showed that LULC was not significant, while lithology (volcanic), slope, and precipitation were important predictors. In this case, the effect of reservoirs on Si export was determined by comparing reference years of pre 1950 to more recent data. Beusen et al. (2009) noted that the global model was different than other statistically based basin-scale models, which showed that LULC or other factors can be important in addition to (or instead of) lithology (e.g. New England (USA) – Carey and Fulweiler 2012; Swedish boreal rivers – Humborg et al. 2004; Red River (China) – Le et al. 2010; and Mississippi River Basin (USA) – Carey et al. 2019).

Here we take an empirical mixed-modelling approach to quantify sources of DSi to the Danube River, including lithology, land use and land cover, and water infrastructure (reservoirs and waste water treatment plants). Mixed-effect linear models account for the possibility of co-dependencies of data in space and/or time, the possibility of random effects associated with e.g. sites, and are helpful to determine main controls and effect-sizes that can be later used in other process-based models that rely on e.g. nutrient transfers as a function of land use or other landscape features. These factors not well represented in current Si process-based models which at present rely heavily on lithology as the main input variable. We use data from the TransNational Monitoring Network (TNMN) of the International Commission for the Protection of the Danube River (ICPDR). Specifically, we: 1. Describe spatial and temporal variation in DSi loads and yields in its main tributaries; 2. Assess the contribution of DSi from the tributaries to the Danube River using a mass balance analysis; and 3. Analyse the influence of lithology, water infrastructure (reservoirs and wastewater treatment plants), and LULC on annual DSi yields in the Danube River Basin.

3.2 METHODS

3.2.1 Study area

The Danube River Basin (801,463 km^2) (Figure 3.1) transverses the territories of 14 countries, rising in the Black Forest of Germany (700 m.a.s.l.) and after a journey of 2857 km discharging to the Black Sea (0 m.a.s.l.). The Basin is commonly divided into three sections (Stancik et al. 1988) with the Upper section comprising the river from its headwaters in the Black Forest of Germany to Bratislava in Slovakia. The most important tributaries of this section in terms of discharge are the Lech, Isar, and Inn Rivers (Austria and Germany) and the Morava River (located in the Czech Republic). The Middle section is the largest of the three sub-sections, extending from Bratislava to the Iron Gates Dam on the border between Serbia and Romania. In this section, the three major tributaries are the Drava, Tisza, and Sava Rivers. The Sava is the Danube's largest tributary overall in terms of discharge and the second largest in terms of catchment area. Other smaller tributaries are the Vah, Hron, Ipel, and Velika-Morava Rivers (Figure 3.1).

The Lower section starts after the Iron Gates Dams. The tributaries in this section are Jiu, Olt, Arges, Ialomita, Siret, and Prut which are comparatively small and account for a modest portion of the total discharge (< 10%). Before reaching the Black Sea, the Danube River divides into three main branches: Chilia, Sulina, and Sf. Gheorghe, forming the Danube Delta which covers an area of 4560 km^2.

3.2.2 Water quality and discharge data

The International Commission for the Protection of the Danube River (ICPDR), which was created to implement the Danube River Protection Convention (DRPC), launched the TransNational Monitoring Network (TNMN) in 1996 in order to monitor trends in water quality in the Danube River, as well as many of the major tributaries (Appendix 8 and 9) (ICPDR 2005). TNMN comprises133 monitoring stations, 49 on the mainstem of the Danube River and 84 on 20 of its main tributaries. DSi data have been collected only in 32 stations in the mainstem and 43 stations in 15 tributaries. From the mainstem stations, DSi data from 3 pairs of stations were merged because stations had similar GPS coordinates, and the data were from different years (Appendix 8 and 9). DSi and discharge are available together with other physical and chemical variables for the period 1998 to 2017, in general with a monthly sampling frequency. For some stations, there were gaps of several years (Appendix 10 and 11). Discharge measurements were taken daily in some stations (Appendix 10 and 11).

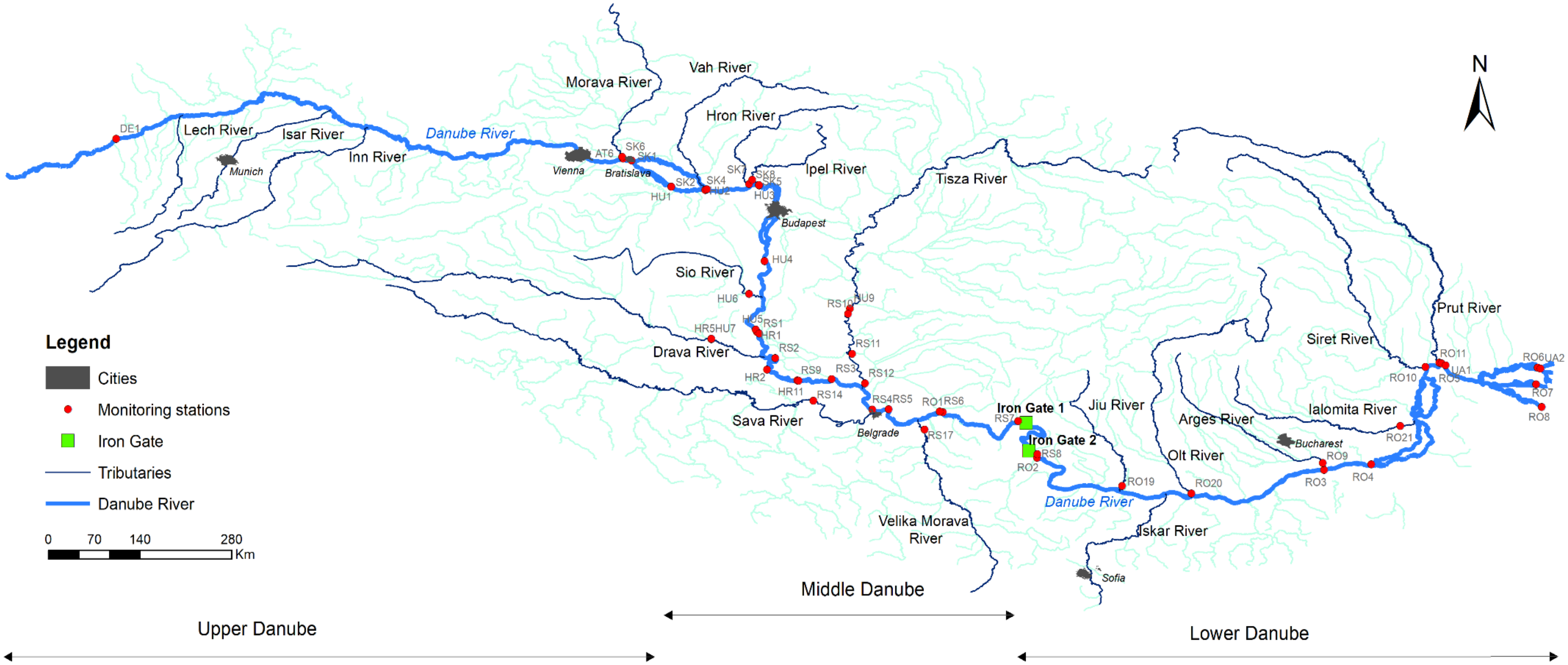

Figure 3.1. Schematic location of the tributaries and the monitoring station from the Trans-National Monitoring Network (TNMN) of the International Commission for the Protection of the Danube River (ICPDR) in the Upper, Middle, and Lower sections of the Danube Basin.

3.2.3 LULC analysis

The sub-catchment area for each monitoring station was delineated based on Digital Elevation Models (90 m resolution) obtained from the Shuttle Radar Topography Mission, publicly available on the website of the Consortium for Spatial Information of the Consortium of International Agricultural Research Centers (CGIAR) (http://srtm.csi.cgiar.org). Within each sub basin, the area and relative proportion of LULC categories for the years 2000, 2006, 2012 and 2018 were determined using the CORINE dataset of the European Environment Agency (EEA 2000; EEA 2006; EEA 2012; EEA 2018) in ArcMap 10.5.1 (ESRI Inc 2007). From 2000 to 2018, LULC change in all the categories was < 3% (Appendix 13). Therefore, the LULC in 2000 was used for the period 2000-2003, LULC2006 for the period 2003 – 2009, LULC2012 for the period 2010 – 2015 and LULC2018 for the period 2016 – 2017. We considered the following classes: artificial (includes urban and industrial areas); agriculture (arable land, permanent crops, and heterogeneous agricultural areas); grasslands (pastures and natural grasslands); forest (coniferous, deciduous, mixed forest and broad-leaved forests); glaciers; bare rocks; shrubs and herbaceous vegetation; wetlands; and water bodies.

3.2.4 Lithology analysis

The lithological classes of the study area were determined using the classification of the Global Lithological Map database - GLiM (Hartmann and Moosdorf, 2012) which consists of 16 lithological classes, with differing Si content from high (>50% based weight) (e.g. siliciclastic sedimentary (SS), acid volcanic (VA), acid plutonic (PA), metamorphic rocks (MT), mix sedimentary rock (SM), and unconsolidated sediments (SU) to lower classes (e.g. carbonate rocks (SC), basic plutonic (PB)) (Hartmann et al. 2012). For each sub-catchment, the percentage of each lithological class was calculated (ArcMap 10.5.1, spatial analyst tool, extract and statistics function) (Appendix 12).

3.2.5 Major water infrastructure

In our study, we included all the major dams from the Global Reservoir and Dam (GRanD) Database (Lehner et al. 2011). The storage capacity of the major dams, as classified in the GranD database ranged from 5 to 1230 million cubic meters. For each sub-basin, dam density (# dams/km^2) was obtained by dividing the total number of major dams in the sub-basin by the area.

Data for wastewater treatment plants (WWTPs) were collected from the open source platform Geographic Information System for the Danube River Basin (www.DanubeGIS.org) developed by ICPDR. The density of plants (# WWTP/km^2) was calculated by dividing the total number of WWTP in a sub-basin by the total area of each sub-basin. We included WWTP that handle ≥ 10,000 p.e. (population equivalents).

3.2.6 Data analysis

In the mainstem of the Danube River, DSi data from 29 stations were available: three in the Upper, 18 in the Middle, and eight in the Lower section, all from the period 1998 – 2017 (Appendix 8). For the 15 tributaries, we selected DSi data from the stations located closest to the confluence with the Danube River. There was one tributary for the Upper section, 8 for the Middle, and 6 for the Lower, from the period 2001 – 2017 (Appendix 9). Daily discharge data was collected from 1996 to 2017, but not continuously and not in all monitoring stations. In the mainstem, there are three stations without discharge data, and six stations did not have discharge data for the same years as the DSi data (Appendix 10). From the 15 tributaries, three (Jiu, Olt, Ialomita) had < 71 number of discharge observations since 2007 (Appendix 11). Therefore, only 20 stations from the Danube River and 12 from the tributaries were used here for the DSi load and yield analysis.

Load estimations. Our approach for estimating the DSi loads in the tributaries and the mainstem of the Danube Basin included the following steps: First, we used correlation and linear regression analysis to assess the relationship between DSi concentration and discharge, but no significant relationships were found for any of the monitoring stations. Therefore, we assumed that the monthly measurements of DSi concentrations were representative for the entire month, and multiplied these by the daily discharge to obtain daily loads. We then summed the daily estimates to obtain monthly DSi loads. Stations that had more than 5 days of missing discharge data were excluded from the data set. We compared our DSi load results with the loads reported by ICPDR (ICPDR 2017), which were calculated by multiplying the average monthly concentrations with the average monthly discharge. The differences between the loads calculated by ICPDR and our method is < 1%.

Mass Balance analysis. The contribution of DSi from each sub-basin to the mainstem was evaluated by calculating the percent contribution of each tributary to total DSi load to the mainstem of the Danube at the station downstream from the confluence. For this, we identified confluence sections in the Danube River for which DSi data was available from a downstream station, an upstream station, and the tributary (Figure 3.1). This resulted in six confluence sections, some of which contained more than one tributary, as follows: 1. Vah, Hron and Ipel; 2. Drava; 3. Sio; 4. Velika-Morava, Sava and Tisza; 5. Arges; and 6. Siret and Prut. To evaluate the potential error in our estimates, we compared the monthly DSi loads in the downstream station with the sum of the monthly DSi loads in the upstream and tributary stations at each confluence.

Controlling factors. To determine the effect of basin properties on DSi export, we calculated annual DSi yield (tonnes km^{-2} year^{-1}) by summing our monthly DSi loads to obtain annual estimates, and dividing by the sub basin area. If more than 3 months of load data were missing from any given station in any given year, the annual DSi yield was not calculated and was not included in the data set. We then estimated statistical models (multiple linear regression analysis and linear mixed effect models) to assess the relationship between DSi yield (dependent variable) and LULC, lithology, and water infrastructures as explanatory variables, in a series of steps. First, we developed correlation analysis among explanatory variables and DSi yield. All analyses were done using R version 3.6.0 (R Core Team 2019) and R Studio version 3.6.0 (R Studio Team 2015).

Multicollinearity of predictor variables was avoided by not including those with correlation coefficients greater than 0.5. The potential explanatory variables included all LULC variables determined by the above analysis, lithology variables (eight lithologic classes: SS, AV, AP, MR, SM, US, SC, and PB also as a percentage), the density of dams in the sub-basin (#dam/km^2), and the density of wastewater treatment plants (#WWTP/km^2). Percentage agriculture and forest were strongly so, we aggregated these by using the ratio of agriculture to forest land use (Ag:Fo ratio) to include as an explanatory variable.
From the predictor variables, we started with a conventional multiple linear regression (Model 1, using the 'lm()' function). We subsequently improved this model with either a variance structure that allowed for individual variation for each tributary to deal with heterogeneity in variance among the tributaries (Model 2, using the function 'gls()' and the varIdent variance structure in R), a linear mixed effect model using the 'lme()' function (Model 3) to estimate random slope models with tributaries as a random effect to account for possible correlation of annual yield estimates within tributaries, or a model with both variance structure and random effect (Model 4). Model 1 was developed systematically by trying combinations of predictor variables from all five categories of explanatory variables that gave the highest R^2. After determining Model 1, Models 2, 3 and 4 were estimated with the same predictor variables. The best-fit model was selected based on the lowest value of the Akaike Information Criterion (AIC) and the most homogeneous residuals (Burnham and Anderson 2002). Additionally, we evaluated the effect size of the explanatory variables by estimating standardized regression coefficients (beta-weights) from Model 1 with the 'model_parameters()' function.

3.3 RESULTS

3.3.1 Spatial and temporal variation of monthly silica loads

DSi loads in the mainstem of the Danube Basin ranged from 0.001 to 378 kt month^{-1} (1 kt = 1000 metric tonnes), with loads generally increasing from upstream to downstream (Figure 3.2A) until a drop from mean 125 ± 7 at Reni station to 46 ± 2 kt month^{-1} across the last three stations (Chilia, Sulina and Sf. Gheorghe) where river branches enter the

Delta (Figure 3.1). The loads in the Upper and Middle sections ranged from 0.01 – 87 kt DSi month^{-1} as a result of relatively low DSi concentration (mean 5.3 ± 0.9 mg L^{-1}; Appendix 15) and discharge (mean 2196 ± 17 $m^3 s^{-1}$; Appendix 16). From the Bazias station downstream to Reni-Chili stations, loads were higher (7 – 378 kt month^{-1}), a function of higher DSi concentrations (mean 6.1 ± 0.9 mg L^{-1}) and higher discharge values (mean 4771 ± 32 $m^3 s^{-1}$). The abrupt increase in load at the Bazias station is likely because it is located downstream of confluence of the largest tributaries in the basin: the Tisza and Sava. The load drops again in the Lower section where the river enters the Delta, ranging from 1 – 157 kt month^{-1} due to reduction in the flow (mean 2575 ± 23 $m^3 s^{-1}$) and relatively low DSi concentration (mean 5.4 ± 0.8 mg L^{-1}).

DSi loads in the tributaries ranged from 0.003 to 80 kt month^{-1} (Figure 3.2B). The lowest loads (0.003 – 16 kt month^{-1}) were located in the Upper and part of the Middle section from Morava to Sio tributaries. These tributaries had relatively high DSi concentrations (mean 12.2 ± 0.5 mg L^{-1}, Appendix 15) but also low discharge (mean 113 $m^3 s^{-1}$ ± 69; Appendix 16). In the Middle section, Tisza and Sava tributaries had significantly higher DSi load than other tributaries from the basin (corresponding with the high load at Bazias station in the mainstem). This is a result of high discharge (mean 1042 $m^3 s^{-1}$ ± 23) rather than a high DSi concentration which was comparable with other tributaries (mean 6.6 ± 1.2 mg L^{-1}). In the Lower section, DSi loads in the tributaries was highly variable, ranging from 0.05 to 23 kt month^{-1}, and these tributaries showed relatively high DSi concentration (mean 7.1 ± 1.0 mg L^{-1}) but low discharge (mean 127 $m^3 s^{-1}$ ± 7.4).

3.3.2 DSi load contribution of tributaries to the Danube River

We examined the effect of the tributaries on DSi load at the confluences in the mainstem of the Danube using mass balance (Figure 3.3). In general, the DSi load in the mainstem was about equal to the sum of the loads from upstream and tributary inputs, which was surprising given the uncertainty in the load estimates. There were some exceptions to this, and some temporal variation. For the sub-basin containing Ipel, Hron, and Vah tributaries, the DSi load from the tributaries and the upstream station exceeded the downstream load for most of the periods (Figure 3.3A). The downstream load for the Sio basin was underestimated in 2003 and 2004 but was relatively equivalent in 2009 and 2011 (Figure 3.3B). In the sub-basin containing Drava, Velika-Morava, Sava, and Tisza tributaries, the downstream loads were higher than the contribution from the tributaries and the upstream station in most of the periods (Figure 3.3C, 3.3D). For the years 2002 and 2003, the mainstem downstream of Siret and Prut tributaries indicated a high contribution from the tributaries, while in the later year the contribution from the tributaries decreased (Figure 3.3F). Overall, the highest contribution of loads to the Danube mainstem stations was from the upstream and not from the tributaries (61 – 99 %; Figure 3.3).

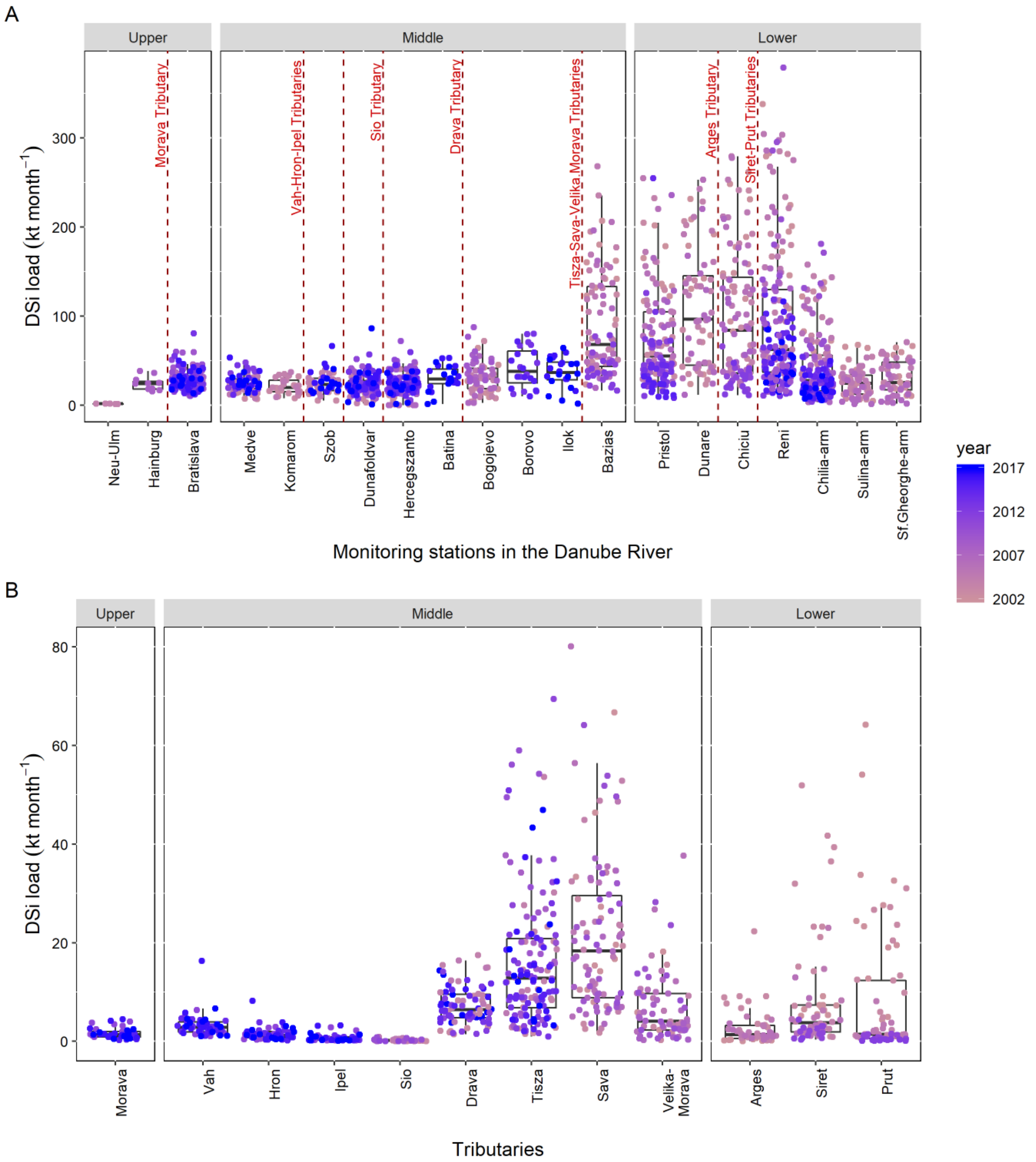

Figure 3.2. Monthly DSi loads on the Danube River (A) and its tributaries (B) for 2002 - 2017 in the Danube Basin. Dashed red lines on plot A indicates the presence of tributaries.

Comparing the tributaries, the highest contributions to the mainstem loads were from Drava and Sava (Middle section) with 21% at the confluence for each tributary. Tisza, which have similar discharge than Drava, only contributed 11% to the downstream load at its confluence (Figure 3.3D). The tributaries with the lowest contributions were distributed throughout the basin, with the Ipel and Sio (Middle section) and Arges (Lower section) contributing < 2% to the downstream flux.

3.3.3 Annual DSi yields of tributaries to the Danube River

In the tributaries, DSi yields ranged from 0.1 to 4.5 tonnes km^{-2} $year^{-1}$ (Figure 3.4). The Upper section showed rather low yields compared to the other tributaries (Morava ranged from 0.6 to 0.9 tonnes km^{-2} $year^{-1}$, while the Middle section showed the highest in the Sava, ranging from 1.4 to 4.5 tonnes km^{-2} $year^{-1}$. The Sio had the lowest yield (0.1 - 0.2 tonnes km^{-2} $year^{-1}$) (Figure 4). In 2017, DSi yields for tributaries located in the Upper section until Tisza (Middle section) were lower than in the previous years for which there were data (Figure 3.4).). In the Lower section, Arges showed an increase in the DSi yields from 2002 to 2006 (0.2 to 1.2 tonnes km^{-2} $year^{-1}$, respectively). An opposite trend was observed in the Siret and Prut tributaries, with a decrease in the DSi yields from 2002 to 2012 (from 1.5 to 0.5 tonnes km^{-2} $year^{-1}$ at Siret and from 1.1 to 0.08 tonnes km^{-2} $year^{-1}$ at Prut).

3.3.4 Influence of land use, lithology and water infrastructure on DSi yields in the Danube basin

For annual DSi yield, Model 1 (R^2 = 0.59, AIC = 149.36) retained the predictor variable included the log-transformed (base 10) agriculture:forest ratio (log Ag:Fo), % grasslands, dam density, WWTP density, and % metamorphic rock (Table 3.1). Models 2 and 3 showed more homogenous residuals compared to Model 1, but the AIC values were either higher (AIC = 153.31; Model 2) or not meaningfully lower (AIC = 148.68; Model 3). Model 4 was the best model, with a meaningfully lower AIC value than Model 1 (AIC = 145.53). In this model, logAg:Fo and % grassland had significant negative effects on annual DSi yield, with regression coefficients of -4.02 ($t = -4.93$, $p < 0.0001$) and -0.11 ($t = -2.06$, $p = 0.0451$), respectively (Table 3.1). The effects of dam density, WWTP density and % metamorphic rock, though significant in Model 2, were not significant in Model 4.

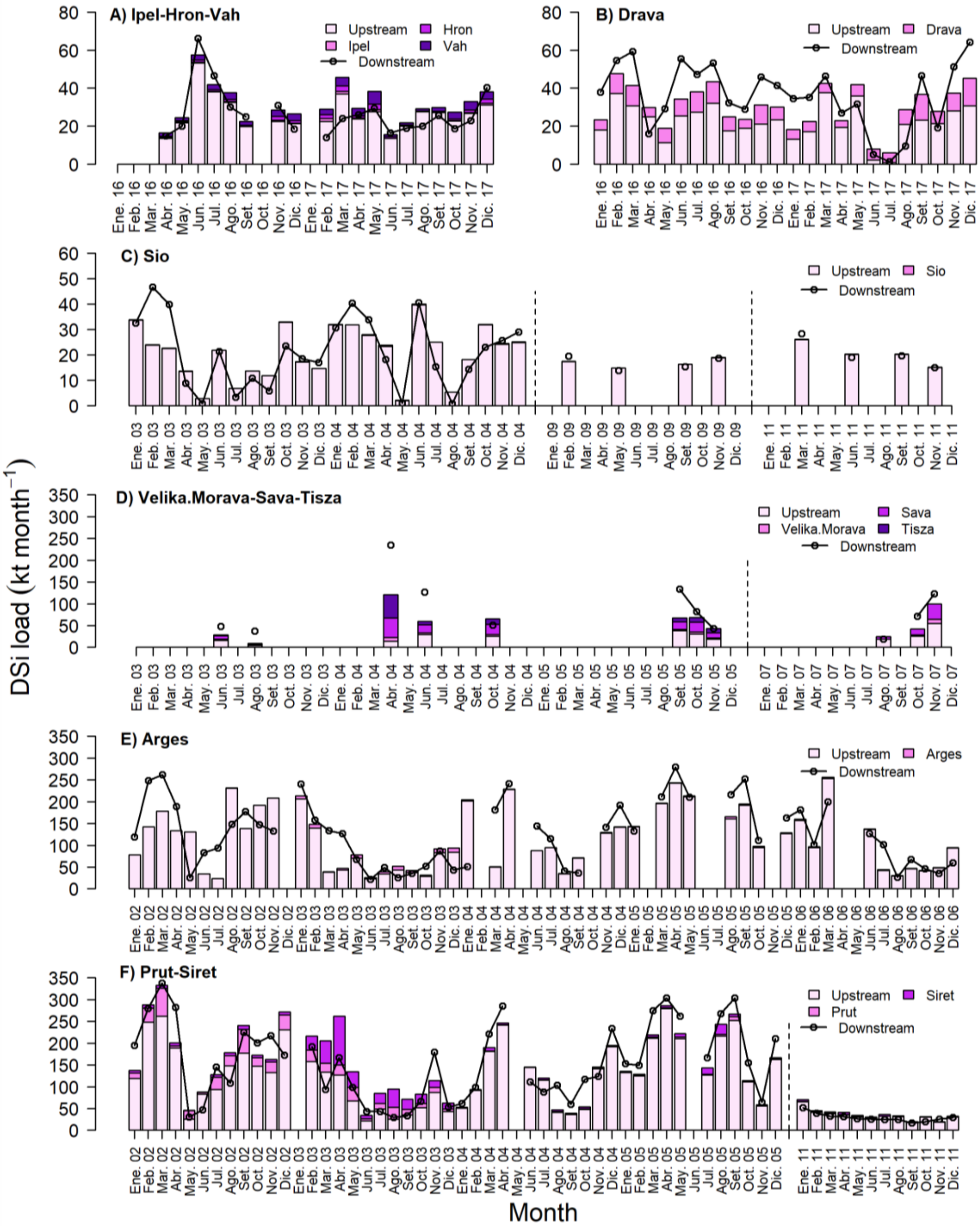

Figure 3.3. Contribution of the monthly DSi loads from upstream and tributaries, in six river sub basins over time. The bar plots showed contribution from the upstream and tributaries, while the dots showed the downstream load.

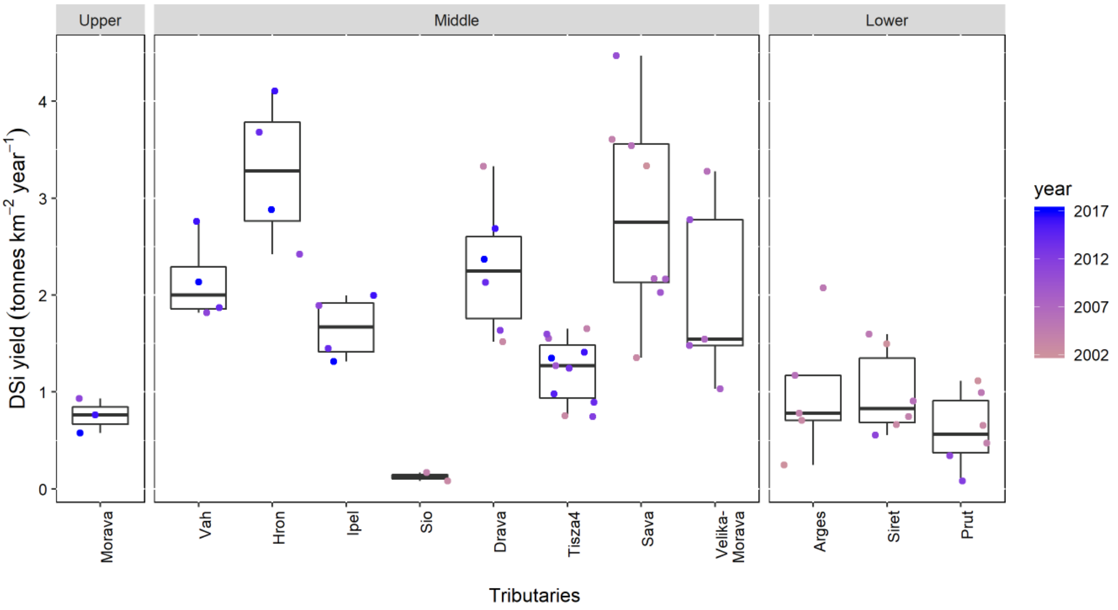

Figure 3.4. Annual DSi yields on the tributaries of the Danube Basin for different periods in the Danube Basin.

The land use variables (Ag:Fo ratio and % grasslands) consistently had significant negative effects for all four models, while the water infrastructure variables (dam and WWTP density) had a negative significant effect only in Model 2 and were not significant in the other three models. The lithology variable (% metamorphic rock) was not significant in any model. The significant effect of Ag:Fo ratio and dam density found in the models were consistent with our bi-variate correlation analysis (rho = -0.72, $p < 0.0001$ and rho = -0.24, $p < 0.05$); however, the other predictor variables (% grasslands, WWTP density and (% metamorphic rock) did not show significant bi-variate correlation.

The two land use variables explained about 60% of the variation in annual DSi yield, and this was mainly attributed to the Ag:Fo ratio. This was determined by dropping % grassland from Model 1 and observing that this resulted in a small reduction in the R^2 from 0.59 to 0.52. This consistent with the fact that we did not find a significant relationship in the bivariate correlations. The effect size of the Ag:Fo ratio on DSi yield was also larger than that of % grassland, as shown by the standardized regression coefficients of Model 1 (-0.79 compared with -0.30, respectively; Table 3.1). These effect sizes are visualised in Figure 3.5, which shows that a doubling of the Ag:Fo ratio from 1 to 2 leads to a decrease in DSi yield of about 1.2 tonnes km^{-2} year^{-1}. When Ag:Fo ratio increases from 2 to 3, this effect size is reduced 0.71 tonnes km^{-2} year^{-1} due to the logarithmic relationship. The effect size of % grassland is lower, with an increase of 10% grassland leading to a reduction in DSi yield of 1.1 tonnes km^{-2} year^{-1} (Figure 3.5).

*Table 3.1***.** *Results of the regression models for DSi annual yield (DSi, in tonnes km^{-2} year^{-1}) as dependent variable and land use, geology, dam density and wastewater treatment plant density as explanatory variables (see footnote). Significance of intercepts are indicated with ns (not significant, $p > 0.10$), ms (marginally significant, $p < 0.10$), * ($p < 0.05$), ** ($p < 0.01$), and *** ($p < 0.001$). Total no. of observations was 64.*

	Model estimates[b]								
	Model 1			**Model 2**		**Model 3**		**Model 4**	
R^2	0.592								
AIC	149.36			153.31		148.68		**145.53**	
Fixed effects[a]:									
Intercept	3.01		***	3.15	***	2.97	***	3.15	***
Slopes									
log(Ag:Fo)	-3.67	(-0.79)	***	-3.03	***	-3.86	***	-4.02	***
% Grassland	-0.097	(-0.30)	**	-0.13	***	-0.095	ms	-0.11	*
Dam/100 km^2	-8.28	(-0.14)	ns	-19.46	**	-6.20	ns	-4.25	ns
WWTP/100 km^2	0.91	(0.046)	ns	3.79	*	0.48	ns	-0.53	ns
% Metamorphic rock	-0.0090	(-0.10)	ns	-0.0022	ns	-0.0095	ns	-0.0075	ns
Random effects:									
intercept s.d.[c]	-					0.369		0.480	
residual s.d.[d]	-					0.639		0.728	
Residual s.e.[e]	0.687			0.671					

[a]Explanatory variables: log-transformed ratio of % agricultural land use and % forest land cover (logAgFo), % Grasslands, dam density (Dam/100 km^2), WWTP density (WWTP/100 km^2) and % Metamorphic rock as independent variables.

[b]Model 1: multiple linear regression model with no random effects; Model 2: variance structure model that allowed different variances for each sub-basin; Model 3: random intercept model with sub-basin as a random effect; Model 4: model combining variance structure and random intercept for each sub-basin; Model 5: same as Model 4, but excluding the non-significant explanatory variables.

[c]Intercept standard deviation; [d]Residual standard deviation; [e]Residual standard error

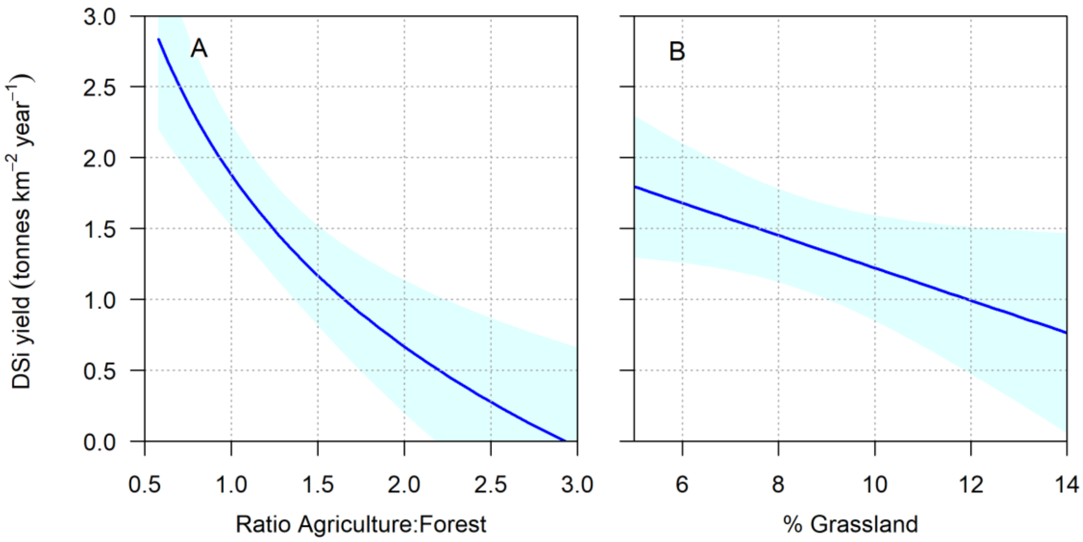

Figure 3.5. Effect plots for the effects of land use on the annual DSi yield (tonnes km^{-2} year^{-1}) in the Danube River basin. A) Agriculture:Forest ratio; and B) % Grassland. The colored bands indicate 95% confidence levels calculated using Model 4 (see Table 3.1).

3.4 DISCUSSION

Overall, our model results showed that LULC was the most important factor in controlling annual DSi yields in the Danube Basin, with the largest effect from the relative proportion of agricultural to forest land (Ag:Fo), followed by the % grassland. These effects are likely caused by a combination of differences in plant-uptake and storage, phytolith solubility, and land management. DSi is taken up by plants at different rates, with crops generally taking up Si at higher rates than forested and grassland ecosystems (Guntzer et al. 2012), particularly for those crops common in the Danube Basin which include wheat, barley, sugar beet, soybean, and tomatoes (https://www.icpdr.org). In addition to the different plant uptake rates, crop harvesting ultimately removes Si from the soil pool, reduces soil recycling and ultimately reduces Si yields to rivers (Struyf et al. 2010; Vandevenne et al. 2012). While agricultural areas tend to lead to a decrease in DSi export overall, there are mixed responses of DSi to forest areas reported in the literature (Chapter 2), depending on forest type (deciduous or coniferous), whether they are aggrading or in a climax state, and on previous disturbance and management practices (e.g. Struyf et al. 2010 and Carey and Fulweiler 2012). In the headwaters of the Danube, coniferous forests have a positive effect on DSi export (Chapter 2), a result that is also consistent with findings from the Scheldt Basin, Belgium (Struyf et al. 2010), and in forested boreal catchments in Sweden (Humborg et al. 2004). Though land use history, i.e. deforestation and/or disturbance may lead to depleted soil Si availability (Struyf et al. 2010; Carey and Fulweiler 2012) overall, forested systems represent the potential for a large pool of BSi and soil recycling (Gérard et al. 2008), with relatively soluble phytoliths compared to phytoliths in grassland systems (Wilding and Drees 1974), and appear to be relatively more important in the Danube Basin than sources from agriculture or grasslands.

In this study, grasslands behave similar to agriculture, showing a negative effect on DSi yield, a pattern that was also consistent with the Scheldt Basin in Belgium (Struyf et al. 2010). The grasslands in the Danube represent a majority grazing systems (60 – 98%), but also include haying and natural systems, so the reason behind this negative effect is less easily interpreted. On the one hand, grazing can mobilize DSi through digestion and deposition in manure (Vandevenne et al. 2013); on the other hand, haying will remove phytoliths from the soil pool. Overall, grasslands have a high sequestration rate and higher phytolith density than trees (Conley 2002; Hodson et al. 2005), in addition to relatively insoluble phytoliths and therefore appears to be responsible for the observed negative relationship of DSi export with grassland area in the Danube.

Artificial land use did not explain any variation in DSi yield, but we did observe a significant, but small, positive effect of waste water treatment plants WWTPs (shown only in Model 2). Urban or developed land has shown positive impacts in other studies (Carey and Fulweiler, 2012; Onderka et al. 2012), but mostly observed as diffuse sources. Given the relatively small area comprising urban land use in this study (2 – 9%), it makes sense that point-sources from WWTP's would be more detectable. WWTP's near Paris were shown to contribute up to 8% of Si export in the Seine River, which was consistent with Si content in a typical Parisian diet, and with detergent use (Sferratore et al. 2006; Dürr et al. 2011; van Dokkum et al. 2004). WWTP's are also typically designed to receive some amount of storm drainage, which in natural systems, would have otherwise been exported to rivers, thus reducing Si export via diffuse sources and transferring them to point-sources (MacGuire and Fulweiler 2016).

A surprising result from this study was that the effect of reservoirs (as represented by the density of large dams) on DSi yields was not very strong, and was only detected in one of the models (Model 2) and weakly detected when considered alone in a bivariate correlation (Appendix 17). Many studies have assessed the importance of dam construction on basin-scale retention of Si (and P) via primary production and sedimentation, originally known as the 'artificial-lake effect' and further developed by many studies (e.g. van Bennekom and Salomons 1981; Harrison et al. 2012; Maavara et al. 2020b; Humborg et al. 2008; Garnier et al. 1999). Previous studies in the Danube have highlighted the importance of reservoirs on DSi sequestration to overall DSi export, specifically focused on the Iron Gates Dam (Humborg et al. 1997; 2000). Similar to our study, the evidence for this effect in the Iron Gates is slightly mixed, with two studies using annual budget and evidence in sediment records showing weaker evidence for Si sequestration in Iron Gates (Teodoru et al. 2006 and Friedl et al. 2004). This led to the hypothesis that hydropower reservoirs in the headwaters with longer residence time (>1 year) may contribute to DSi sequestration (Friedl et al. 2004; Humborg et al. 2006), and evidence for this was shown in Chapter 2. Evidence from this present study shows a tendency for DSi reduction from upstream to downstream of Iron Gates Dam with a mean monthly load 89 ± 6 kt $month^{-1}$; n = 92 at Bazias station compared to 74 ± 12 kt $month^{-1}$; n = 139 at Pristol station. (Figure 3.2A), which does support the idea that the Iron Gates Dams contribute to DSi sequestration. The evidence for DSi sequestration in the longer-term reservoirs in the headwaters is based on comparing DSi yield, nutrient ratios and DSi:Cl ratios between inlet streams and reservoir outflows (Chapter 2), but this was not observed for run-of-the river hydropower dams which have a residence time of <1 day. Taken together, it seems that there is indeed evidence for DSi sequestration in the Danube Basin due to reservoirs, but the effect of this is not easily observed when compared to LULC effects, and our understanding will improve when we take into account more specifically the residence time of each reservoir.

Geochemical controls on DSi export as represented by lithological classes appeared in this study to be unimportant relative to the human influence on LULC. We used % metamorphic rock to represent DSi availability, which did not strongly co-vary with other predictor variables in the models and represented a range of DSi availability over the sub-catchments (0 to 40%). Other studies showed that Si export is related to volcanic lithology (Beusen et al. 2009; Humborg et al. 2004), which has a higher weatherability than other lithological classes (Hartman et al. 2010). In this study, % volcanic rock (acid and basic) comprised only 0 to 6 % across the tributaries, except for 2, which had 34 and 39% (Hron and Ipel tributaries respectively) and was therefore not well distributed. When tested, % volcanic rock was not significant in predicting DSi any of our models. In another study in the headwaters of the Danube (sub-catchment sizes ranging from 0.2 to 26,000 km^2; Chapter 2), % metamorphic represented a larger range (0 – 100%), and in this case did account for an increase in DSi export. Other authors have hypothesized that controls on DSi export is scale-dependent, in which lithology is more important for larger basins, while LULC and other regional factors are more important for smaller ones (Beusen et al. 2009; Carey and Fulweiler 2012). Our results point to a different result, with lithology being important for smaller headwater catchments and LULC being important at larger ones; instead, it could be that Si cycling, like other element cycles including N, P, and C, is becoming increasingly dominated by human factors.

Spatial and temporal variation in DSi yield in the Danube River

Most of the variation in DSi load along the mainstem of the Danube River appeared to be due to the input of tributaries, though our ability to determine this is sometimes limited by discrepancies in the mass balance at the confluences or lack of data availability. The section containing the Velika-Morava, Sava, and Tisza tributaries had the largest number of data gaps (Figure 3.3D) and therefore had the highest percent error (35%). For the longer-term data records, the strongest discrepancies occurred in an under-estimation of load downstream of the confluences of the Drava and Sio tributaries (Figure 3.3B and 3.3C). In the Sio, this discrepancy was particularly evident in the winter months while was more consistent for the Drava tributary. Discrepancies suggest either error in the load estimates, or unaccounted for sources of Si between the confluence and downstream the monitoring station. For the Drava, the monitoring station is 78 km upstream of the confluence, which is longer than the others, and has the potential to receive sources from e.g. the WWTPs of Osijek city. In the case of the over-estimation of the load downstream of the Sio confluence, could be a result of larger variation in discharge in winter months, or other dynamic that we were not able to capture using monthly load calculations.

Uncertainties in load estimation can arise from our relatively coarse approach to calculating load (applying one DSi concentration measured at monthly time steps to a whole month). We did not find that DSi concentration was related to discharge at any of the stations, but we do not have a good understanding of how, or whether, this lack of a relationship is related to hysteresis or other flows which may be activated more episodically or change over the course of a season, for example a storm event or spring snowmelt. These have the potential to change the relative importance of baseflow (groundwater contribution), subsurface and surface runoff or storm-drainage (e.g. Scanlon et al. 2001; McGuire and Fulweiler 2016). Given the uncertainties in our method, the mass-balances for the other tributaries are relatively good and the percentage of error ranged from 0.5 – 17% for most tributaries. The highest percentage of error was 35% for the Velika-Morava, Sava and Tisza section mainly because the gaps on the data.

At absolute values, the Tisza and Sava tributaries contributed the highest loads to the mainstem of the Danube, and the Sava and Tisza tributaries contributed the largest proportion of DSi to the overall export, as calculated at Reni station), representing 17% and 15% respectively. Both of these tributaries have high discharge (Appendix 16), though not the highest yield, indicating that loading is a function of both discharge and catchment factors that control the transfer of DSi to the river system, as well as in-river retention and cycling processes (Hartmann et al. 2010; Cornelis et al. 2011; Harrisson et al. 2012; Maavara et al. 2020b). With respect to yields, the Sava and Hron each had the highest in the basin, with (ranged from 1.4 to 4.5 tonnes km^{-2} $year^{-1}$). This is consistent with our modelling, which showed that relatively high forest cover leads to a positive DSi export, and with the suggestion that dams overall contribute to DSi retention, as both of these tributaries were nearly 50% forest (> 47%), had 33- 35 % agricultural land use, and low dam density (< 1 dam/10000 km^2). The Hron tributary also contained high volcanic rock (acid and basic) (34%; Appendix 12), which may have contributed to high yield, but was not included in the statistical analysis. In contrast, the Morava, Sio, Arges, and Prut tributaries were characterized by a high percentage of agricultural area (>50%) and also had the lowest yields (0.08 to 2.1 tonnes km^{-2} $year^{-1}$). Additionally, Arges had a high dam density (7 dam/10000 km^2). DSi yield in other rivers like Seine – France (0.04 to 1.2 tonnes km^{-2} $year^{-1}$) and Mississippi – USA (mean 0.8 tonnes km^{-2} $year^{-1}$) were low compared to Sava and Hron tributaries, which may also be related to the agricultural area in these basins (> 50%) (Goolsby et al. 1999; Billen et al. 2007). Further analysis should be developed in order to analyse how DSi behaves together with other nutrients as nitrogen and phosphorus through a stoichiometry analysis and the factors controlling them.

Model comparison and empirical approach

Our estimates of yield from the Danube Basin (0.45 – 2.93 tonnes km^{-2} $year^{-1}$) are in similar range of previous reported studies from the basin, which range from 0.18 - 4 tonnes km^{-2} $year^{-1}$ (Cociasu et al. 1996; Garnier et al. 2002; Beusen et al. 2009; Table 3.2). Overall, the Danube falls within the global average, which was estimated at ~3 tonnes km^{-2} yr^{-1} (Dürr et al. 2011; Beusen et al. 2009) and overall estimates for Europe (Dürr et al. 2011; Onderka et al. 2012; Struyf et al. 2010; Garnier et al. 2006; Table 3.2), but is smaller than the Mississippi (Goolsby et al. 1999; Table 3.2) and other rivers in Japan (Hartmann et al. 2010; Table 3.2).
Perhaps the largest difference between this study and the others conducted in the Danube is with the Riverstrahler model (Garnier et al. 2009), which is at the very lower end of our study (~0.45 tonnes km^{-2} $year^{-1}$) and is 6 – 7 times lower than our higher estimates (~2.9 tonnes km^{-2} yr^{-1}), despite the fact that it also includes particulate silica. This may be because lithology is the dominant controlling factor in this model, and only considers P availability controlling Si uptake within the river system (Garnier et al. 2002). Our results show that ignoring the impact of land use on the Si cycle can result in an inaccurate estimates of Si export. For example, using an analysis of effect size, we showed that a doubling of the proportion of agricultural land compared to forest (i.e. an increase of the ratio from 1 to 2) leads to a decrease in DSi yield of about 1.2 tonnes km^{-2} $year^{-1}$. This amount is similar to the yields observed in other river basins (e.g. the Seine and Scheldt Rivers; Table 3.2) and is therefore potentially important to include in river-basin models. The grassland effect, while smaller is also important, with a 10% increase leading to a reduction in DSi yield of 1.1 tonnes km^{-2} $year^{-1}$. Other differences among these models used for the Danube Basin may result from e.g. location of the downstream monitoring station; for example, Cociasu et al. 1996 used the DSi data from the Sulina Branch, which is within the Danube Delta and compromises wetlands and lakes which likely sequester Si compared to the measurements we used at Reni station, which is just upstream of the Delta.

In summary, we that using a mixed modelling approach gives some advantages that are helpful to other modelling efforts. First, we made use of the nested basin data representing different sub-basins and tributaries which could be analysed without violating the required assumption of independence in the statistical analysis. Second, the mixed-effect linear models account for co-dependencies of data in space and/or time using random effects associated with e.g. sub-basins. While the mixed model approach could not be used to predict scenarios, like e.g. the Global News model, it does include the possibility of analysing temporal trends, by assessing monthly and annual loads. Third, the application of the linear mixed models in the case of the Danube appear to be helpful in understanding controls and effect-sizes that can be later used in other process-based models that rely on e.g. nutrient transfers as a function of land use or other landscape features.

Table 3.2. Summary of DSi yields, modelling methods and controlling factors from the literature for other river basins worldwide.

River	DSi yield tonnes km^{-2} $year^{-1}$	Data sources and Methods	Model Name, Type, or Method	Significant controlling factors	Factors considered but not retained or found insignificant	Reference
World average	3.3	GEMSGLORI for Q; Meybeck and Ragu (1995) for DSi concentration	Information from existing models	Runoff/precipitation and lithology		Dürr et al. 2011
World average	3.1	GEMSGLORI for Q; Meybeck and Ragu (1995) for DSi concentration	Statistical analysis: Stepwise multiple linear regression.	Precipitation, area of volcanic lithology, bulk density, and slope	LULC, ice/glacial coverage, maximum elevation, agro-ecological zones, lakes/wetlands.	Beusen et al. 2009

USA (142 basins)	0.0004 – 23.1	Geological Survey National Stream Water-Quality Monitoring Networks.	Non-linear, lumped model	Lithology and runoff	Jansen et al. 2010
Mississippi River (USA)	0.69	Concentrations estimated by linear interpolation between monthly observations. The average concentration is multiplied by the total water discharge during the period to estimate flux.	No statistical analysis		Goolsby et al. 1999

Japan (516 basins)	4.5 – 85.3	Hydrochemical data of Japanese rivers for 754 locations sampled monthly from two periods: 1940/50s and 1970s. Okayama University	Bi-variate linear or nonlinear regression	Lithology, runoff, slope	Temperature	Hartmann et al. 2010
Europe	1.6	GEMSGLORI for Q; Meybeck and Ragu (1995) for DSi concentration	Information from existing models	Runoff/precipitation and lithology		Dürr et al. 2011
Alzette - Luxembourg	2.2	Data collected from 24 sub-basins outlets	Partial least square regression analysis	Positive effect from runoff, urban areas, marls and sandstone; Negative effect from slope, and grassland.		Onderka et al. 2012

Baltic Sea Basins						
Bothnian Bay Sub-basins (unperturbed boreal)	1±0.09	Monthly observations Si multiplied by discharge. Baltic Environmental Database (http://www.mare.su.se/nest/)	Regression analysis	Hydraulic load (m $year^{-1}$ as a proxy of residence time) and TOC concentration as a proxy for vegetation cover		Humborg et al. 2008
Bothnian Seas sub-basins (regulated boreal)	0.7±0.05					
Baltic Proper Sub-basins (eutrophic agricultural basin)	0.4±0.06					

Gulf Finland Sub-basins (eutrophic agricultural basin)	0.2±0.1					
Gulf of Riga Sub-basins (eutrophic agricultural)	0.4±0.01					
Scheldt River Basin (51 sub-catchments) (Belgium)	0.67 – 9.48	Multiplied observed Si concentration with calculated discharge (2007 – 2008)	Mixed multiple linear regression analysis	Forest cover	No effect from soil texture and drainage class	Struyf et al. 2010
Scheldt River (Belgium)	1.4	GEMSGLORI database, Meybeck and Ragu (1995)	Riverstrahler model	Lithology Si export partially being controlled by P availability and eutrophication processes in the basin	Land use, morphology, rainfall temperature, discharge	Garnier et al. 2006
Seine River (France)	0.8					

Danube Basin	2 – 4	GEMSGLORI database, Meybeck and Ragu (1995)	Global NEWS-DSi model	Precipitation, area of volcanic lithology, bulk density, slope	LULC, ice/glacial coverage, maximum elevation, agro-ecological zones, lakes/wetlands.	Beusen et al. 2009
Danube River	0.18 - 0.37	DSi concentration measured in the Sulina branch multiplied by water discharge measured upstream of the river before it enters the Delta. Data from 1988-1992.	No statistical analysis			Cociasu et al. 1996
Danube River	0.43(*)	GEMSGLORI database, Meybeck and Ragu (1995)	Riverstrahler model 352 kt /year, divided by the area	Lithology Si export partially being controlled by P availability and eutrophication processes in the basin		Garnier et al. 2002

Danube River (Reni station-outlet)	0.45 – 2.93	ICPDR; Monthly DSi concentration multiplied by daily measurements of Q to calculate monthly and annual loads. Data from 2002-2017	Mixed Model analysis	Relative proportion of agriculture and forest land cover, % Grassland area	Density of large dams (5 to 1230 million cubic meters), WWTP density, lithology (% metamorphic)	This study

* Total Silica, including dissolved and particulate

3.5 Conclusions

Here we used an empirical approach to analyse DSi loads and yields from the Danube Basin along the longitudinal gradient and distributed among its tributaries. This paper showed that LULC is the most important controlling factor of DSi export, and overpowers our ability to observe of lithology. Specifically, the relative proportion of agricultural land compared to forest land cover is the most important, with agriculture causing a negative effect on DSi export and forest causing a positive effect with large effects on the overall basin Si yield. The effects of reservoirs and waste water treatment plants is observable, but less strong than the effects of LULC. The main sources of Si to the overall export are the Sava and Tisza tributaries mainly due to their high loads or discharge, and Sava and Hron tributaries due to high yields which are explained on the basis of prominent controlling factors in these sub-basins, particularly the presence of agriculture and dam density. There has been an overall reduction of silica concentration and loads in the most downstream stations from the time-period studied (2000 – 2017) – a pattern that may not only be a result of sequestration by reservoirs, but also a result of agricultural land use.

4

NUTRIENT STOICHIOMETRY OF NITROGEN, PHOSPHORUS, AND SILICA IN THE DANUBE RIVER AND ITS TRIBUTARIES

4.1 INTRODUCTION

Rivers are important for transport and processing of nutrients including silica (Si), nitrogen (N) and phosphorus (P). Nutrient concentrations and ratios strongly influence the community composition of phytoplankton assemblages, with different phytoplankton species having different optimum nutrient concentrations for growth. For example, diatoms require silica as a fundamental inorganic nutrient, while cyanobacteria require more nitrogen and phosphorus. Silica requirements for diatoms vary according to species, and marine diatoms generally require less silica than freshwater ones (Conley et al. 1989). The optimum Si:N ratio for freshwater diatoms identified was 2.5 after examining their elemental stoichiometry, under various nutrient regimes (Lynn et al. 2000). This Si:N ratio requirement for freshwater diatoms was used in different studies assessing nutrient limitation (Dupas et al. 2015; Royer et al. 2020; Senath et al. 2022). Therefore, we assume a N:P:Si = 16:1:40 (Redfield 1958; Dupas et al. 2015), with imbalances in this ratio leading to nutrient limitation and a shift in phytoplankton community composition. Therefore, nutrient loading, concentrations and N:P:Si stoichiometry are strong selective forces shaping phytoplankton communities (Elser et al. 1996).

Nutrient fluxes, concentrations, and their ratios in freshwaters have been altered by human activities, including changes in land use and land cover (LULC) (Humborg et al. 2002; Maavara et al. 2020b; Struyf et al. 2010; Vandevenne et al. 2012). N and P exports have both increased with agricultural development through non-point sources such as fertilizer leaching and runoff, livestock management, and catchment erosion (e.g. Boyer et al. 2002; Howarth et al. 1998; Vilmin et al. 2018) while urbanization has increased increasing surface runoff and emissions from point sources (Carpenter et al. 1998; Howarth et al. 2011). Silica is also affected by changes in LULC, with conversion of forest to agricultural systems which reduces Si export through reduced weathering and crop harvesting, which ultimately reduces the Si soil pool (Vandevenne et al. 2012). These land use changes influence the ratios of N, P, and Si export, but the relative importance of these impacts with respect to other influences, including changes to basin residence time due to reservoir construction is not well known.

Reservoirs also contribute to the alteration of N, P, and Si ratios along the river continuum by spatial and temporal increase of residence time of river flow, enhancing the removal of P and Si through sedimentation and stimulating N fixation, thus causing N:P and N:Si ratios to increase from upstream to downstream in a river system (Maavara et al. 2020a, b). Studies so far that examine these stoichiometric changes in river systems are based often on modelling or literature review studies, with relatively few using empirical data sets or considering the potentially confounding effects of LULC, point sources, and reservoir construction on nutrient exports and their ratios (but see e.g. Carey et al. 2019 and Chapter 2). Furthermore, some basin-scale Si models do not take into account LULC, but consider lithology as the primary Si source to river systems (e.g. Garnier et al. 2002; Beusen et al. 2009), which does not take into account our current understanding of human effects on Si export. Here, we use long-term monitoring data from the Danube River to assess the combined effect of natural (lithology and forest cover) and human (agriculture and urban land use, reservoir density, and waste-water treatment plant density) impacts on nutrient stoichiometry in both the main stem and its tributaries.

The Danube River contributes about 60% of the total hydrological riverine input, and is a major source of nutrients to the Black Sea (Friedrich et al. 2002). The Danube River Basin analysis report (ICDPR 2005), required by the Water Framework Directive (WFD 2000/60/EC) (EC 2000), identified hydro-morphological alterations (e.g. reservoirs), pollution by nutrients, pollution by organic substances, and pollution by hazardous substances as the four most significant pressures in the river basin. Since 1990, there has been a reduction of nutrient inputs into surface waters (Cociasu and Popa 2005), probably as a result of the fall of the Iron Curtain (Kroiss et al. 2006) and subsequent collapse of the Soviet system in the 1990s and economic change in the eastern countries. Despite this improvement, nutrient pollution is still a concern (ICPDR 2015) with high fertilization rates remaining in Germany, Slovenia, Croatia, and Serbia countries (Ritchie et al. 2022), relatively low waste-water treatment capacity in some parts of the basin (ICPDR 2015), and hydropower construction planned in several of the important tributaries (Zarfl et al. 2015). Changes in nutrient ratios, especially with respect to the relative reduction of silica compared to N, have been hypothesized to increase the eutrophication risk of the Black Sea (Humborg et al. 1997; Friedrich et al. 2002; Ludwig et al. 2009), and further work is needed to understand how these factors affect eutrophication risk.

Eutrophication potential can be estimated in the freshwater and marine system by using an indicator of coastal eutrophication potential (ICEP) (Billen and Garnier 2007) and indicator of freshwater eutrophication potential (IFEP) respectively (Dupas et al. 2015). These indicators estimates potential risk of eutrophication to coastal zones and freshwater systems by quantifying excess loads of N or P over Si based on the limiting nutrient as determined by a balanced N:P:Si nutrient ratio, i.e. the Redfield, Conley ratio (16:1:20) (Billen and Garnier 2007) and Dupas ratio (16:1:40) (Dupas et al. 2015). ICEP and IFEP values above 0 indicate that N or P loads are higher than Si. Based on predictions from the Global-NEWs model, P–ICEP values at the outlet of the Danube River Basin were 2–5 for the period 1970 – 2000 (Garnier et al. 2010), and 5 for the year 2000 (Strokal and Kroeze 2013), indicating high eutrophication risk.

The current study analyses the nutrient stoichiometry of the Danube River basin and its controlling factors by using empirical data. Specifically, we: i) use the ICPDR database to describe spatial and temporal variation in nutrient (DSi, DIN, and PO_4) concentration and ratios; ii) estimate monthly nutrient loads in the Danube River and its tributaries, hypothesizing an increase of nutrient loads along the longitudinal gradient of the Danube River; iii) analyse the influence of lithology, water infrastructure (reservoirs, wastewater treatment plants), and LULC on nutrient ratios in the Danube River and its major tributaries, with the expectation that agricultural and urban land use would increase N:Si ratios and decrease Si:P ratios; and iv) estimate the Index of potential Eutrophication in coastal and freshwater systems (ICEP and IFEP) in the Danube River and its major tributaries. Based on previous studies (ICPDR 2015; Humborg et al. 1997), we expect that the ICEP and IFEP values would be above zero, having the potential to lead to eutrophication.

4.2 METHODS

4.2.1 Study area

The Danube River Basin (801,463 km^2) is Europe's second largest and home to more than 83 million people. It is the most international river basin in the world, including the territories of 14 countries. The Danube River starts from the Black Forest of Germany and passes through four Central European capitals - Vienna, Bratislava, Budapest, and Belgrade before entering the Black Sea where it creates the ecologically important Danube Delta. This Delta, located in Romania along the Ukraine border, became a UNESCO World Heritage Site in 1991, and is considered among the world's 200 most valuable ecological regions and Europe's largest remaining natural wetland. For these reasons, the European Commission recognizes the Danube as the single-most important non-oceanic body of water in Europe (CEC 2001).

The Danube River Basin is commonly divided into three sections based on its elevation gradient from the mountains of the Black Forest (700 m.a.s.l.) to the mouth (0 m.a.s.l.) at the Black Sea (Stancik et al. 1988). The Upper section extends from the source in Germany to Bratislava in Slovakia. Its tributaries arise from the northern side of the Alps as well as from the southern side of the Central European Highlands. Due to the steep slope of the river bed and high potential for hydropower, this sub-region contains the highest density of reservoirs in the basin, one dam every 17 km (Zinke 1999). Based on the mean annual discharge, the most important tributaries of this section are the Lech, Isar, and Inn Rivers, located in Austria and Germany, and the Morava River, located in the Czech Republic (Figure 4.1).

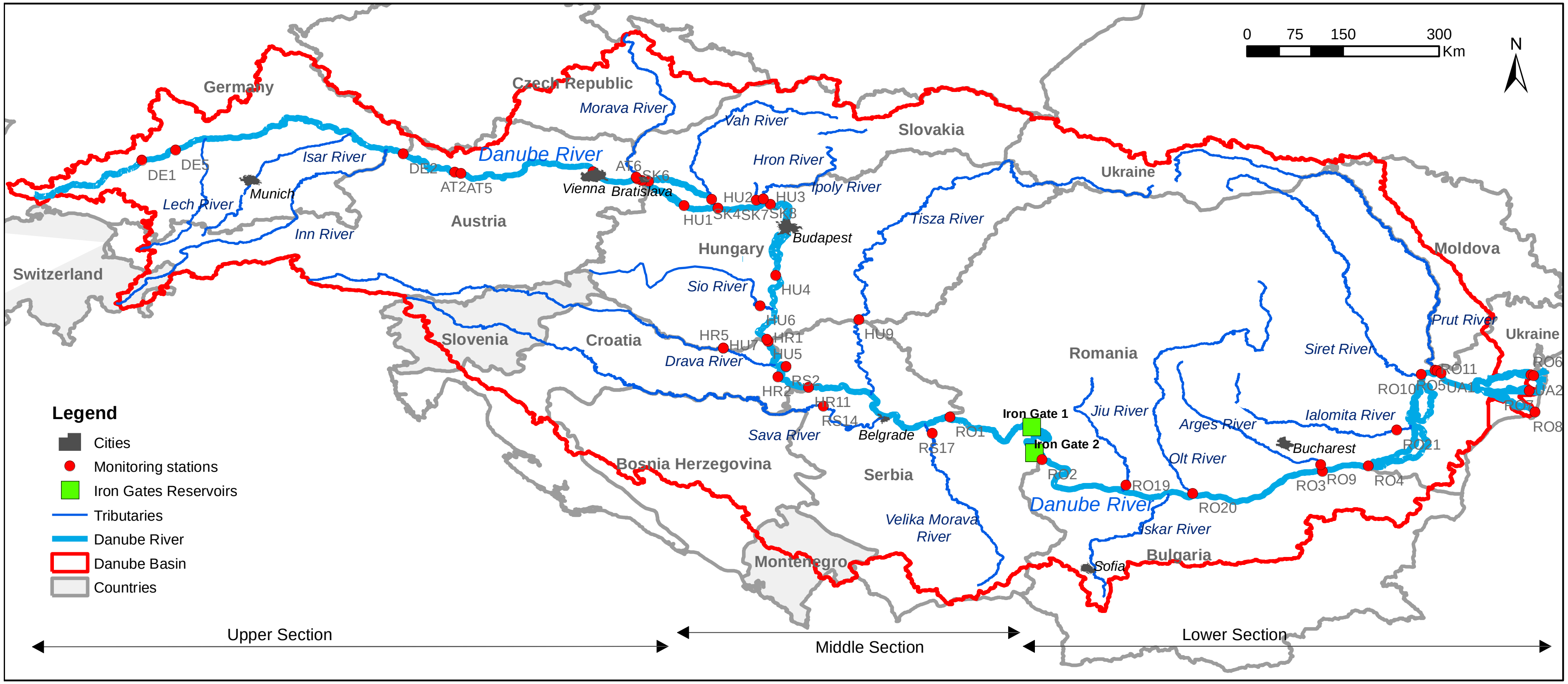

Figure 4.1. Schematic location of the monitoring stations in the tributaries and in the mainstem of the Danube River in the three sections of the basin. The detailed information of the monitoring stations from the mainstem and tributaries are in Appendix 8 and 9.

The Middle section is the largest of the three sub-sections and extends from Bratislava, Slovakia to the Iron Gates dam, on the border between Serbia and Romania. The Danube is shallower in the Middle section than in the Upper section, and has about half the water velocity, lower banks, and a riverbed that reaches a width of more than 1.5 km. In this section, the three major tributaries in terms of discharge are the Drava, Tisza, and Sava rivers. The largest tributary in terms of discharge and the second largest in terms of basin area is the Sava River. Other smaller tributaries are the Vah, Hron, Ipel, and Velika-Morava Rivers (Figure 4.1).

The Lower section starts after the Iron Gates dams where the basin is formed by the plain area of Romania and Bulgaria (Figure 4.1). Here, the river becomes shallower and broader, with several major islands, and the velocity of water slows down considerably. The tributaries that enter the main river along this section, including the Jiu, Olt, Arges, Lalomita, Siret, and the Prut, are comparatively small and, collectively, account for <10% of the total discharge. Before reaching the Black Sea, the river divides into three main channels: Chilia, Sulina, and Sf. Gheorghe, which carry 63%, 16% and 21% of the flow, respectively, forming the Danube Delta which covers an area of 4560 km^2.

4.2.2 Nutrient concentrations and discharge data

The Danube River Basin has a TransNational Monitoring Network (TNMN), established in 1996 by the Commission for the Protection of the Danube River (ICPDR) to support the implementation of the Danube River Protection Convention. Through the TNMN, the contracting parties of the ICPDR monitor trends in water quality in the Danube River, as well as many of the major tributaries.

The Trans National Monitoring Network (TNMN) includes 133 monitoring stations, 49 on the mainstem of the Danube River and 84 on 20 of its main tributaries. For this study, we considered only the stations that measured N (inorganic nitrogen (NH_4 + NO_3, DIN), and soluble reactive P (SRP, orthophosphate, PO_4) and Si (dissolved silica, DSi) concentrations. Total nitrogen (TN) and total phosphorus (TP) were not considered in the analysis, due to the large gaps in the measurements and their data availability did not correspond to the same timeline as DSi measurements. In the mainstem, there were 26 stations that reported the N and P, while only 18 stations reported Si. In the tributaries, we considered stations that were closed to the inflow to the Danube mainstem (11 stations). Nutrient data were available for the period 1996 to 2017 for N and P, and from 2002 to 2017 for Si, in general with a monthly sampling frequency. For some stations, there were gaps of several years. For other stations, discharge measurements were taken daily. In order to analyse the seasonal variation in nutrient concentrations and ratios, nutrient concentrations were considered representative for the month of measurement, and were converted to nutrient ratios using their molar masses (Appendix 18, 19).

4.2.3 Land use and land cover

The sub-catchment area for each of the 12 tributaries was delineated from the most downstream monitoring station based on Digital Elevation Models (DEM, 90 m resolution) obtained from the Shuttle Radar Topography Mission (SRTM) available in the public domain on the website of the Consortium for Spatial Information of the Consultative Group for International Agriculture Research (CGIAR) (http://srtm.csi.cgiar.org). ArcMap 10.5.1 (ESRI Inc. 2007), and its spatial analyst tool sets (hydrologic function), were used to model the water flow and direction. Within each sub-basin, the area and relative proportion of land use and land cover (LULC) categories for the years 2000, 2006, 2012 and 2018 were determined using the CORINE dataset of the European Environment Agency (EEA 2000; EEA 2006; EEA 2012; EEA 2018). From 2000 to 2018, LULC change in all the categories was < 3% (Appendix 13, and 14). Therefore, the LULC in 2000 was used for the period 2000-2003, LULC in 2006 for the period 2003 – 2009, LULC in 2012 for the period 2010 – 2015 and LULC in 2018 for the period 2016 – 2017. We considered the following classes of land use: artificial (includes urban and industrial areas); agriculture (arable land, permanent crops, and heterogeneous agricultural areas); grasslands (pastures and natural grasslands); coniferous forest; deciduous forest (mixed forest and broad-leaved forests); glaciers; bare rocks; shrubs and herbaceous vegetation; wetlands; and water bodies.

4.2.4 Lithology

Using the classification of the Global Lithological Map database - GLiM (Hartmann and Moosdorf 2012), the lithological classes of the study area were determined. We found 16 lithological classes, all with different Si content. Based on their geochemical composition in weight % of surface lithological classes, the classes with high silica content were Siliciclastic Sedimentary Rocks (SS), Acid Volcanic Rocks (AV), Acid Plutonics Rocks (AP), Metamorphic Rocks (MR), and Unconsolidated Sediments (US) (Hartmann et al. 2012). For each sub-catchment, the percentage of each lithological class was calculated (ArcMap 10.5.1, spatial analyst tool, extract and statistics function).

4.2.5 Major water infrastructure

Information on dams in the Danube River basin was collected from the Global Reservoir and Dam (GRanD) Database (Lehner et al. 2011). We included all major dams with a storage capacity from 5 to 1230 million cubic meters. For each sub-basin, dam density (in dams km^{-2}) was obtained by dividing the total number of major dams by the sub-basin area.

Data on wastewater treatment plants (WWTPs) was collected from the open source platform Geographic Information System for the Danube River Basin (www.DanubeGIS.org) developed by ICPDR. The density of wastewater treatment plants (WWTP km^{-2}) was calculated by dividing the total number of WWTP in a sub-basin by the total area of each sub-basin. We included only WWTPs with loads entering the plants of ≥ 10,000 p.e. (population equivalent).

4.2.6 Annual loads and nutrient ratios

Nutrient ratios based on annual loads were calculated both in the mainstem and the tributaries. To calculate the annual nutrient molar ratios, first we calculated the monthly loads, assuming that the monthly measurements of nutrient concentrations (DIN, PO_4, DSi) were representative for the entire month (this was based on the fact that nutrient concentrations were not significantly related to river discharge; Chapter 3). Recorded monthly concentrations were multiplied by the daily discharge measurements to obtain daily loads, and these in turn were summed to obtain monthly and annual nutrient loads. Stations with less than 25 and 10 measurements for daily and monthly loads, respectively, were excluded from the monthly and annual load calculations. Once the annual loads were determined, nutrient molar ratios were calculated for DIN:DSi, DSi:PO_4, and DIN:PO_4.

4.2.7 Indicator for coastal and freshwater eutrophication potential – ICEP and IFEP

ICEP values were calculated based on the Redfield molar N:P:Si ratios and using the equations from Billen and Garnier (2007). ICEP is expressed in carbon mass unit, in order to compare between N, P and Si; and per square kilometre of basin area, which allows comparison among rivers. For the calculation of N–ICEP and P– ICEP, only DIN and PO_4 were used because of limited availability of monthly total nitrogen and total phosphorus data.

In order to calculated the IFEP values, nutrient ratios were adjusted as freshwater diatoms have a greater silicon content (e.g. Conley et al. 1989; Lynn et al. 2000). Based on this adjustment, ICEP was modified for Dupas et al. (2015) by using a ratio of N:P:Si::16:1:40. Similar than ICEP, IFEP is expressed in carbon mass unit. Positive values of ICEP and IFEP (> 0) show that nitrogen or phosphorus fluxes are higher than silica fluxes, indicating a potential condition for eutrophication. Negative values of ICEP and IFEP (< 0) show that nitrogen and phosphorus fluxes are lower than silica and therefore there is lower risk for eutrophication.

4.2.8 Data analysis

All analyses were done using R version 3.6.0 (R Core Team 2019) and R Studio version 3.6.0 (RStudio Team 2015), with three different analyses: 1) test for seasonal variation in monthly loads in the tributaries to detect possible annual trends in nutrient loading in the mainstem; 2) determine the most important predictor variables for explaining variation in yields and their stoichiometry; and 3) determine whether the ICEP or IFEP values were significantly different from zero.

To detect seasonal patterns in nutrient concentrations, differences between months were tested using Kruskal-Wallis ANOVA in the tributaries. Bi-variate scatter plots of annual nutrient loads and years were created, and Spearman rank correlation coefficients (rho) calculated for each nutrient. To determine the effect of basin properties on annual nutrient ratios, we estimated statistical models (multiple linear regression analysis and linear mixed effect models) to assess the relationship between nutrient ratios (dependent variable) and land use, lithology, and water infrastructure (predictor variables). The potential predictor variables included all the LULC and lithology variables as described above, as well as the density of dams in the sub-basin (dam density, km^{-2}), and the density of wastewater treatment plants (WWTP density, km^{-2}). To avoid multicollinearity of predictor variables, we used correlation analysis among the predictor variables and did not include variables with correlation coefficients greater than 0.5 in the models together. Percentage agriculture and forest were strongly correlated, and we calculated the ratio of agriculture to forest land use (ratioAg:Fo) to include as a predictor variable.

We used the procedure for developing the best-fit model following Zuur et al. (2007; 2009). First, we used a conventional multiple linear regression model (Model 1 using the lm function in the R software). This model was developed manually and systematically by trying combinations of predictor variables described above that gave the highest R^2. In the combinations, we retained a representative variable of WWTP and dams as based on recent studies. These two predictor variables were important for nutrients, especially Si. Therefore, this study estimated the effect of these predictor variables together.
Once the best model was determined, we tested other models with the same combination of predictor variables to develop mixed models, including variance structures and random effects. Model 2 included a variance structure that allowed for individual variation for each tributary (the function 'gls()' and varIdent variance structure in R were used). Model 3 included a linear mixed effect model using the lme function to estimate random intercept models with tributaries as a random effect. Model 4 combined both Model 2 and Model 3 and included both variance structure and random effects. The best model among these was selected based on the lowest value of the Akaike Information Criterion (AIC) and the most homogeneous residuals (Burnham and Anderson 2002).

To determine if the medians of the ICEP and IFEP values were greater than zero, a one-sample Wilcoxon sign rank test was used.

4.3 RESULTS

4.3.1 Seasonal variation of nutrient concentrations and ratios in the tributaries

DSi concentration in the 11 tributaries ranged from 0.001 to 27.2 mg L^{-1} (Appendix 20). The tributary with the highest DSi concentration was Ipel (6.3 – 27.2 mg L^{-1}), while Sava had the lowest (1.6 – 10.9 mg L^{-1}). Generally, there was no clear seasonal trend in DSi concentrations, and differences among months were not significant. Exceptions were the Drava and Tisza Rivers, which showed lower DSi concentrations in the summer than winter months (Kruskal Wallis, $p < 0.05$, Appendix 20). DIN concentrations ranged from 0.24 to 7.79 mg L^{-1}, with the lower concentrations observed in the Drava, Tisza, Sava, and Velika-Morava Rivers in the Middle section (0.24 – 3.12 mg L^{-1}), and higher concentrations in the Lower section in the Arges tributary (0.99 – 7.79 mg L^{-1}). In contrast to DSi, the DIN concentration in almost all of the tributaries (except Sava and Arges) showed stronger seasonal variation with lower concentrations during the summer than in winter (Kruskal Wallis, $p< 0.05$, Appendix 20). PO_4 concentrations in the tributaries ranged from 0.002 to 0.54 mg L^{-1} (Appendix 20), with the Middle section (Drava, Sava and Tisza) showing the lowest (0.002 – 0.25 mg L^{-1}), and the Lower section (Arges) the highest (0.014 – 0.49 mg L^{-1}). Generally, there were no significant differences in PO_4 concentration among months, except for the Morava and Vah Rivers (Kruskal Wallis test, $p < 0.05$, Appendix 20).

DIN:DSi in the tributaries ranged from 0.1 to 4.0, with the lowest ratios in the Middle section in Hron, Ipel and Tisza Rivers (0.15 – 2.3), while the higher ratios were observed in the Lower section at Arges, Siret, and Prut Rivers (0.18 – 4.0). Most tributaries did not show seasonal variation in the DIN:DSi ratio, except Drava and Tisza which showed lower ratios in summer than in winter (Kruskal Wallis, $p < 0.05$, Appendix 21). DSi:PO_4 in the tributaries ranged widely from 0.1 to 300, with the lowest values in Morava, Vah, and Arges Rivers, and the highest in the Siret and Prut (Appendix 21). No strong seasonal variation in DSi:PO_4 was observed though there was a significant difference between September and February in the Sava River (Kruskal Wallis $p < 0.05$, Appendix 21). DIN:PO_4 ranged from 1.2 to 300, with the lowest ratio in the Hron and Ipel Rivers (3.9 – 125), and the higher ratios in in the Arges, Siret and Prut (3.8 – 300). Clear seasonal patterns in DIN:PO_4 ratios were observed in the six tributaries (Morava, Vah, Hron, Ipel, Drava, and Tisza Rivers), with lower ratios in summer than winter (Kruskal Wallis, $p< 0.05$, Appendix 21).

4.3.2 Annual nutrient loads in mainstem and tributaries

Annual DSi loads in the mainstem ranged from 11 to 2030 kt year^{-1}, generally increased from upstream to downstream, but then dropped in the Danube Delta (Figure 4.2A). From Bratislava to Ilok stations, DSi load ranged from 11 to 563 kt year^{-1}, increased between Bazias and Reni stations from 228 to 2310 kt year^{-1}, and dropped again in the Danube Delta (stations in the arms of the River at Chilia, Sulina, and St. Gheorghe stations). DIN and PO_4 loads showed a similar trend of increasing from upstream to downstream. The lowest DIN and PO_4 loads were in the Upper section (Neu-Ulm and Dillingen stations), ranging from 9.8 to 23.8 kt year^{-1} (Figure 4.2B) and from 0.1 to 0.4 ktyear^{-1} (Figure 4.2C), respectively. The DIN and PO_4 loads increased from Bazias to the Reni station, ranging, respectively, from 164.4 – 565.5 kt year^{-1} and from 3.7 to 15.9 kt year^{-1}. Before entering the Danube Delta, nutrient loads at the most downstream station (Reni station) averaged ± SE: 1108 ± 172 kt of Si, 370 ± 25 kt of N, and 9 ± 0.7 kt of P. At Reni station, DIN and DSi loads declined over the years (DIN: rho = -0.60, $p < 0.01$ and DSi: rho = -0.77, $p < 0.01$) (Figure 4.3). In contrast, PO_4 loads have stayed relatively constant (Figure 4.3).

In the tributaries, the highest loads for DSi, DIN, and PO_4 were shown for the Drava, Tisza, Sava, and Velika-Morava Rivers in the Middle section. Loads ranged from 0.03 to 392.6 for DSi (Figure 4.4A), from 8.6 to 62.6 kt year^{-1} for DIN (Figure 4.4B), and from 0.2 to 3.3 kt year^{-1} for PO_4 (Figure 4.4C). The other tributaries had lower loads, ranging from 1.1 to 73.5 for DSi, 0.4 to 23.6 kt year^{-1} for DIN and 0.02 to 0.7 kt year^{-1} for PO_4 (Figure 4.4).

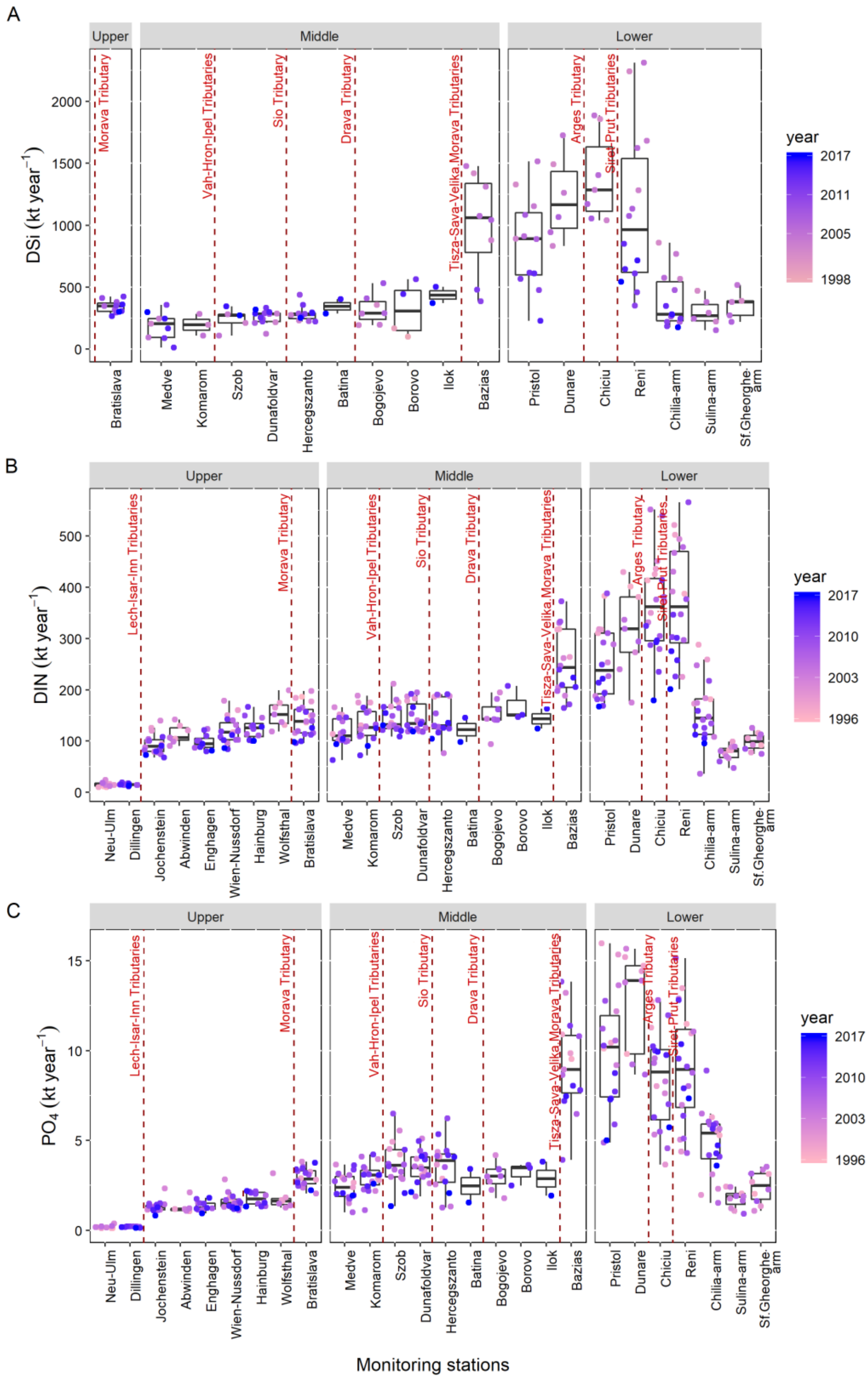

Figure 4.2. Annual nutrient loads: A) DSi from 2002 to 2017, B) DIN, and C) PO_4, from 1996 to 2017, in the three sections of the mainstem of the Danube River.

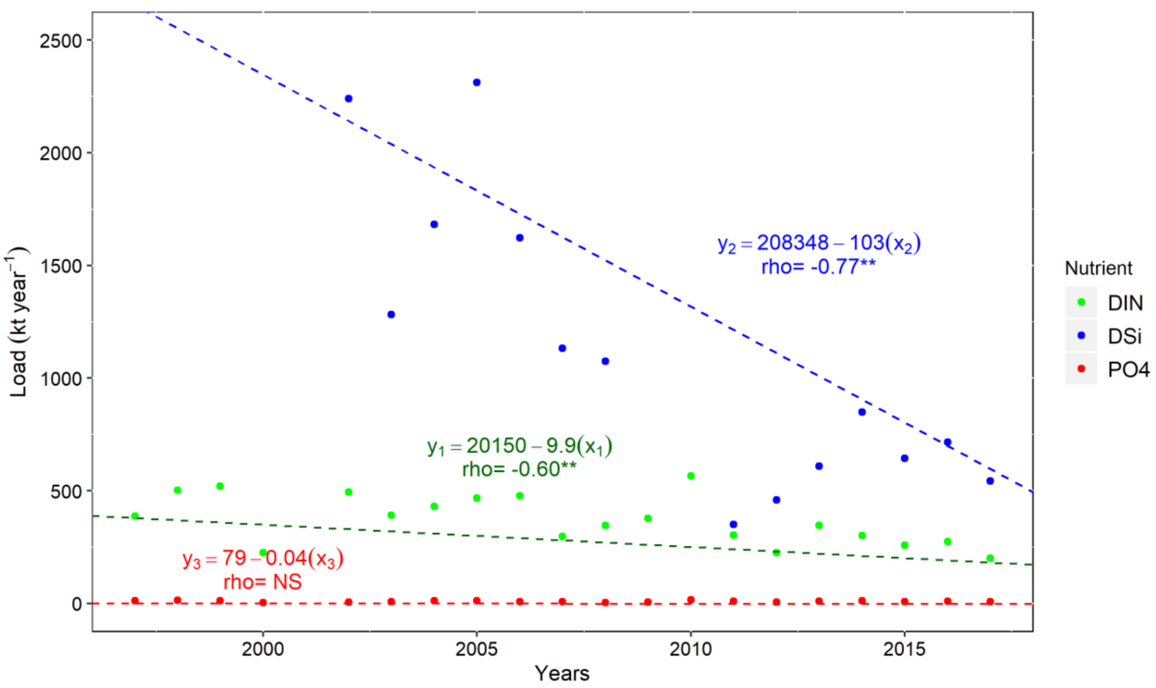

*Figure 4.3. Nutrients loads at Reni station, before entering the Danube Delta, from 1997 to 2017. Numbers indicate Spearman rank correlation coefficients (rho). Significance is indicated with * ($p < 0.05$), ** ($p < 0.01$), *** ($p < 0.001$) or NS (not significant). DIN (y_1) (R^2= 0.31), DSi (y_2) (R^2= 0.67), PO_4 (y_3) (R^2= 0.005).*

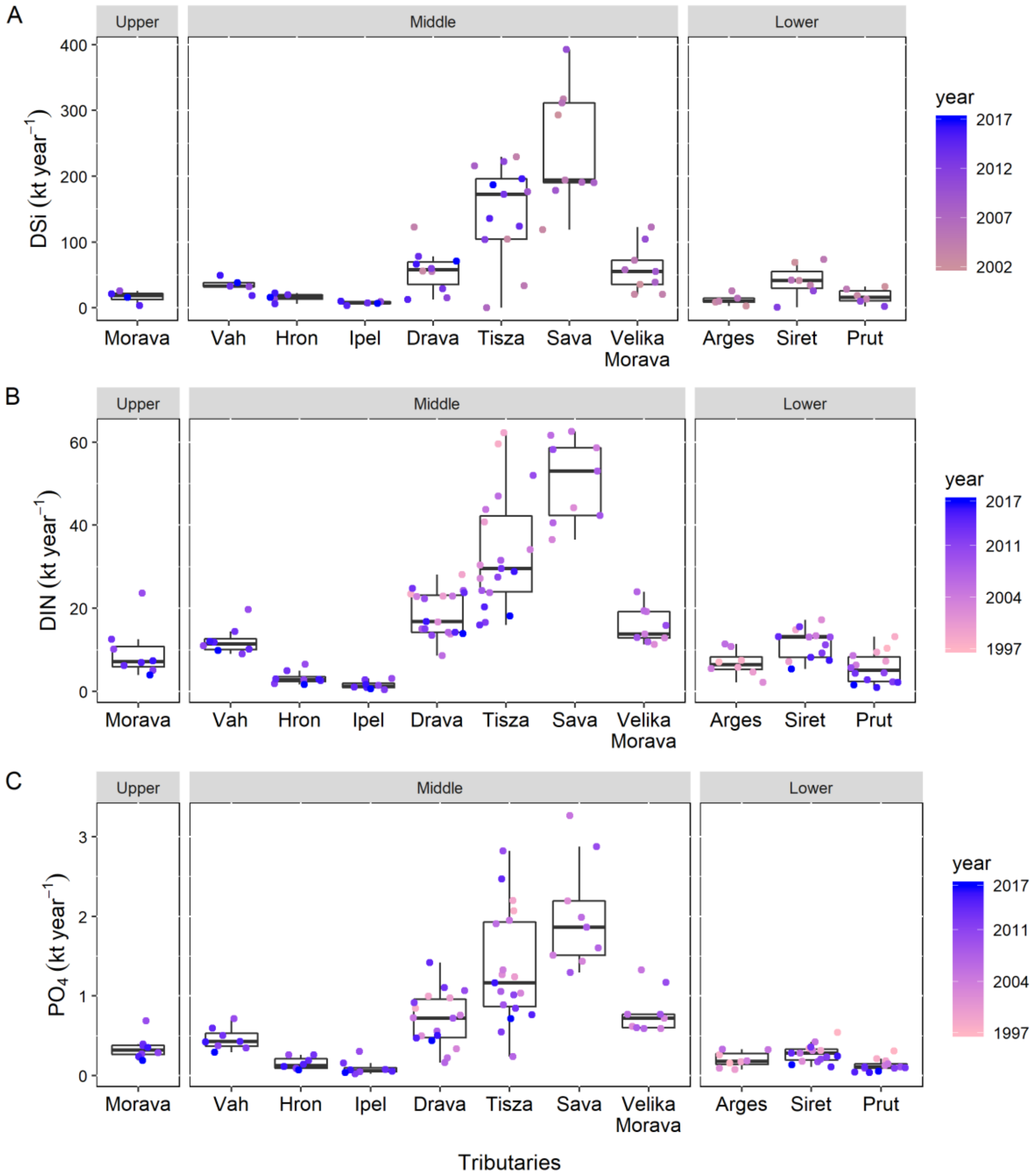

Figure 4.4. Annual nutrient loads: A) DSi from 2002 to 2017, B) DIN, and C) PO_4, from 1996 to 2017, of 11 tributaries located in the three sections of the Danube Basin.

4.3.3 Annual nutrient ratios in mainstem and tributaries

In the mainstem, the DIN:DSi of the annual fluxes were mostly above the threshold value of N:Si =~1 showing Si limitation, with values ranging from 0.7 to 3.1 (Figure 4.5). The stations above 1 were in the Upper and Middle sections from Bratislava to Ilok (1.2 – 3.2). The DIN:DSi generally declined from upstream to downstream. These, however, showed considerable variability in the Lower section and the Delta stations, although they remained mostly above 1 (0.7 – 2.8). Similar to DIN:DSi, DSi:PO_4 ratios were mostly higher than the threshold value Si:P =~16, while all DIN:PO4 ratios were higher than N:P =~16, indicating P limitation in the mainstem. DSi:PO_4 ranged from 2.4 to 129.2 and showed higher variability in the stations compared to the other nutrient ratios. DIN:PO_4 ranged from 23.1 to 244.3, the highest ratios were in the Upper section until Wolfsthal station (116.9 – 244.3), then generally decreasing in the whole Middle section (26.8 – 147.9). There was a slight increment of the ratio in the Lower section from Chiciu to Sf. Gheorghe station (48.3 – 216.6).

Similar to the mainstem, in the tributaries the three nutrient ratios (DIN:DSi, DSi:PO_4, DIN:PO_4) were mostly above the threshold value. DIN:DSi ratios ranged from 0.4 to 4.1 (Figure 4.6). The lowest ratios were found in Hron, Ipel and Tisza tributaries located in the Middle section (0.42 – 1.1), while the highest ratio were found in the Lower section (Arges and Prut range 1.3 –4.1). DSi:PO_4 ratio ranged from 2.6 to 135. The higher ratios were located in the Middle section (25.9 to 135), while the lower ratios were found in the Arges River (2.6 – 40.9) in the Lower section. DIN:PO_4 ranged from 22.8 to 211.3, the lower ratios were in the Upper and Middle sections (22.8 – 91.1), with generally increasing to the Lower section (50.6 – 211.3).

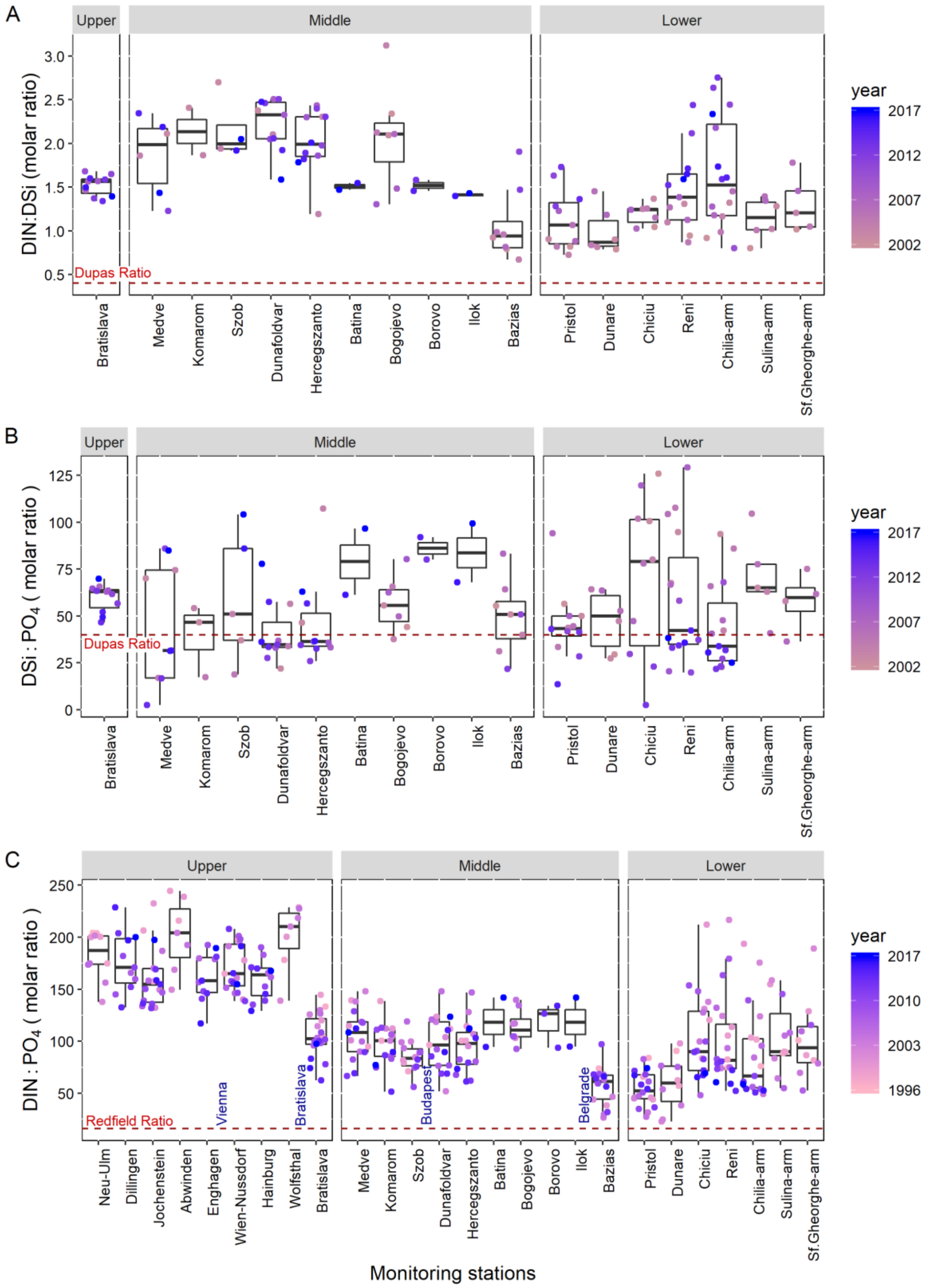

Figure 4.5. Nutrient ratios based on annual loads in the tree sections of the mainstem of the Danube River: A) DIN:DSi, B) DSi:PO_4 from 2002 to 2017, C) DIN:PO_4 from 1996 to 2017. Location of main cities are in red lyrics.

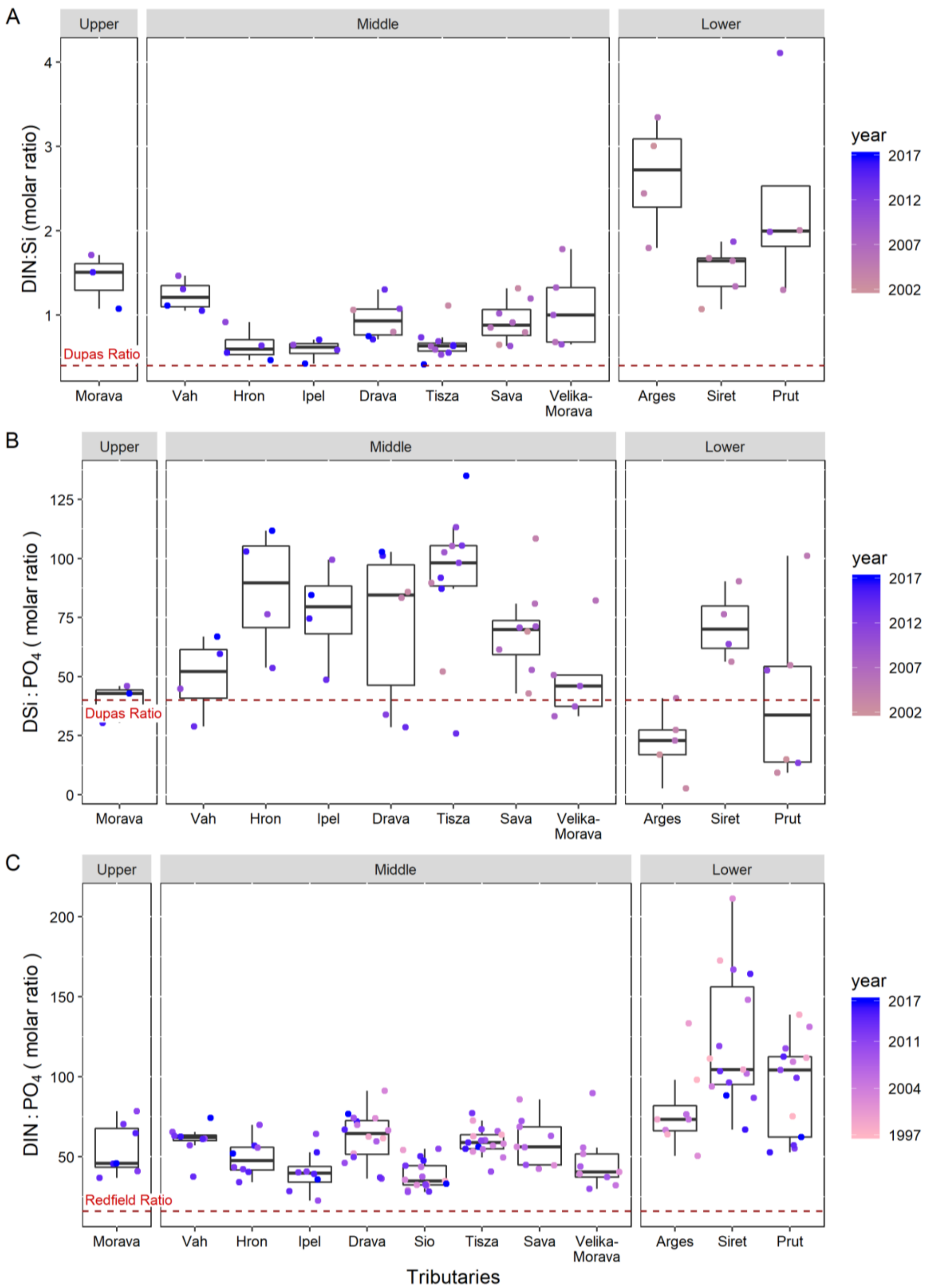

Figure 4.6. Nutrient ratios based on annual loads in 12 tributaries of the Danube River: A) DIN:DSi, B) DSi:PO_4, C) DIN:PO_4 in the tree sections.

*Table 4.1. Results of the best-fit regression models for nutrient ratios DIN:DSi, DSi:PO_4, DIN:PO_4 in the tributaries (n= 58, 60, 135 respectively). Nutrient ratios were calculated based on annual loads. Model 1 is the best-fit multiple regression model following the model-development procedure; Model 2 includes a variance structure for elevation class; Model 3 is a random intercept model for each elevation class; and Model 4 included both a variance structure and a random intercept. Significance of slopes are indicated with * ($p < 0.05$), ** ($p< 0.01$), and *** ($p< 0.001$). For more explanation, see Methods section.*

	Dependent variables					
	DIN:DSi		**DSi:PO_4**		**DIN:PO_4**	
Model comparison:						
R^2 (Model 1)	0.56		0.43		0.51	
AIC (Model 1)	-101.04		3.21		-150.26	
AIC (Model 2)	-104.46		**0.07**		-147.37	
AIC (Model 3)	**-114.33**		5.19		**-167.82**	
AIC (Model 4)	-111.04		1.75		-160.75	
Best-fit model result						
Fixed effects:						
- Intercept	0.11		1.86		1.56	
- Slopes						
logAgFo	0.60	*	-0.63	*	-0.11	
% Grasslands	-0.24		2.18	**	1.35	
% Metamorphic rock	0.27		-0.40			
Dam density	2.77		-3.02		-0.09	
WWTP density	-0.63		0.58		-1.82	*
% Artificial					6.73	**
Random effects:						
intercept s.d.[c]	0.074				0.086	
residual s.d.[d]	0.066				0.116	
Residual s.e.[e]			0.25			

[a]Predictor variables: log-transformed ratio of % agricultural land use and % forest land cover (logAgFo), % Grasslands, % Metamorphic rock, dam density (Dam/100 km^2), WWTP density (WWTP/100 km^2), and % Artificial as independent variables. [c]Intercept standard deviation; [d]Residual standard deviation; [e]Residual standard error

4.3.4 Controls of nutrient ratios: model results

The predictor variables that were retained in the multiple-linear regression model included the log-transformed (base 10) agriculture:forest ratio (AgFo), % grasslands, % metamorphic rock, dam density, and WWTP density. The best fit model for DIN:DSi ratio was Model 3 (AIC = -114.56), and for DSi:PO_4 it was Model 2 (AIC = 0.07). DIN:DSi was positively related to AgFo and negatively to DSi:PO_4. DSi:PO4 was positively related to the percent grassland area. Other predictor variables including dam density and WWTP were not significant (Table 4.1).

For DIN:PO_4, the model included ratio AgFo, % grasslands, % artificial, Dam density, and WWTP density (Model 1: R^2 = 0.51, AIC = -150.26). Model 2 and Model 4 had higher AIC values (-147.37 and -160.75, respectively); therefore, the best fit model was Model 3 (AIC = -167.82). In contrast to DSi ratios model, DIN:PO_4 was not significantly related to ratio AgFo (Table 4.1). However, WWTP density and % artificial showed to be negatively and positively related to DIN:PO_4 ratio, respectively.

4.3.5 Indicators of Eutrophication IFEP and ICEP

In the mainstem of the Danube, all stations show N-IFEP median values greater than 0 (0.10 – 5.7 kg C km^{-2} day^{-1}) (one-sample Wilcoxon sign test, $p < 0.05$), with the exception of three stations (Bazias the last station of the Middle section, and Radujevac and Dunare from the Lower section) (Figure 7A). In comparison, only four stations (Neu-Ulm in the Upper section, and Szob, Dunafoldvar, and Hercegszanto in the Middle section) showed N–ICEP median values greater than 0 (0.4 – 1.9 kg C km^{-2} day^{-1}) (Figure 8A). In contrast to N–IFEP and N–ICEP, there was no station with median P–IFEP and P–ICEP values greater than 0 (one sample Wilcoxon sign test, $p > 0.05$). P–IFEP and P–ICEP values ranged from -15 to 5.7 kg C km^{-2} day^{-1} and from -31 to 0.9 kg C km^{-2} day^{-1} respectively (Figure 7B and 8B). However, both P–IFEP and P–ICEP values increased from the Upper to the Middle section becoming closer to 0, which is an indication of higher PO_4 inputs (Figure 7B, 8B).

In the tributaries, the median N-IFEP values for Morava (Upper section), Vah and Drava (Middle section) and Arges, Siret, and Prut (all stations from the Lower section) were above 0 (ranging from 0.2 to 4.8 kg C km^{-2} day^{-1}) (Figure 7C), while Arges was the only station with a median N-ICEP values higher than 0 (1.17 kg C km^{-2} day^{-1}) (one sample Wilcoxon sign test, $p < 0.05$) (Figure 8C). Similar than in the mainstem, P–IFEP and P–ICEP values in the tributaries did not have median values greater than 0 (Figure 7D and 8D). However, P–ICEP values higher than 0 were found in Tisza (Middle section) and Arges, Siret and Prut (Lower section). The highest P–IFEP and P–ICEP values were found in Arges (30 and 28 kg C km^{-2} day^{-1} respectively) (Figure 7D and 8D).

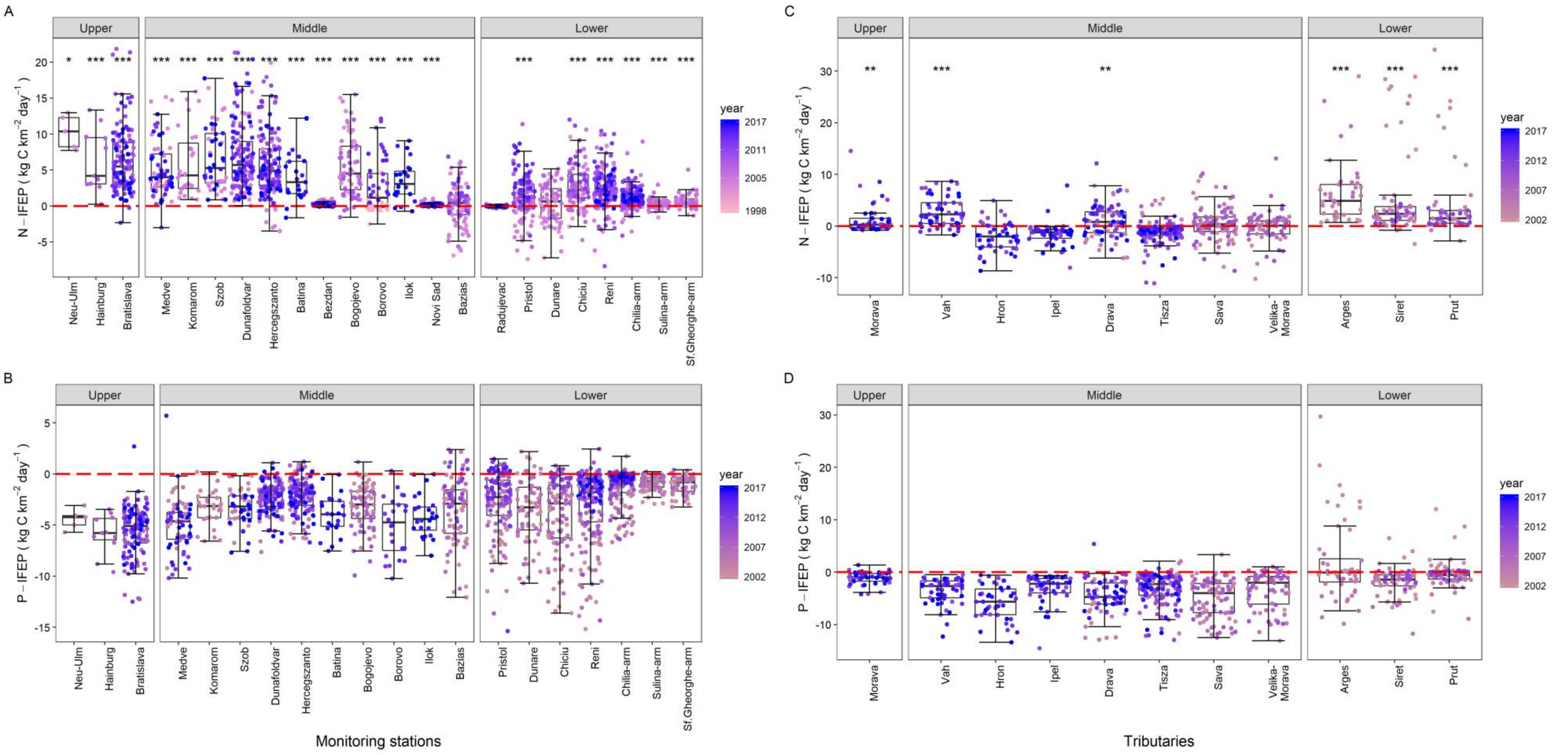

*Figure 4.7. Boxplots of N-IFEP and P-IFEP for the Danube River (A and B) and for its tributaries (C and D) from 1998 to 2017. For the N-IFEP and P-IFEP values > 0 Wilcoxon sign rank test, significance is indicated with * ($p < 0.05$), ** ($p < 0.01$), and *** ($p < 0.001$).*

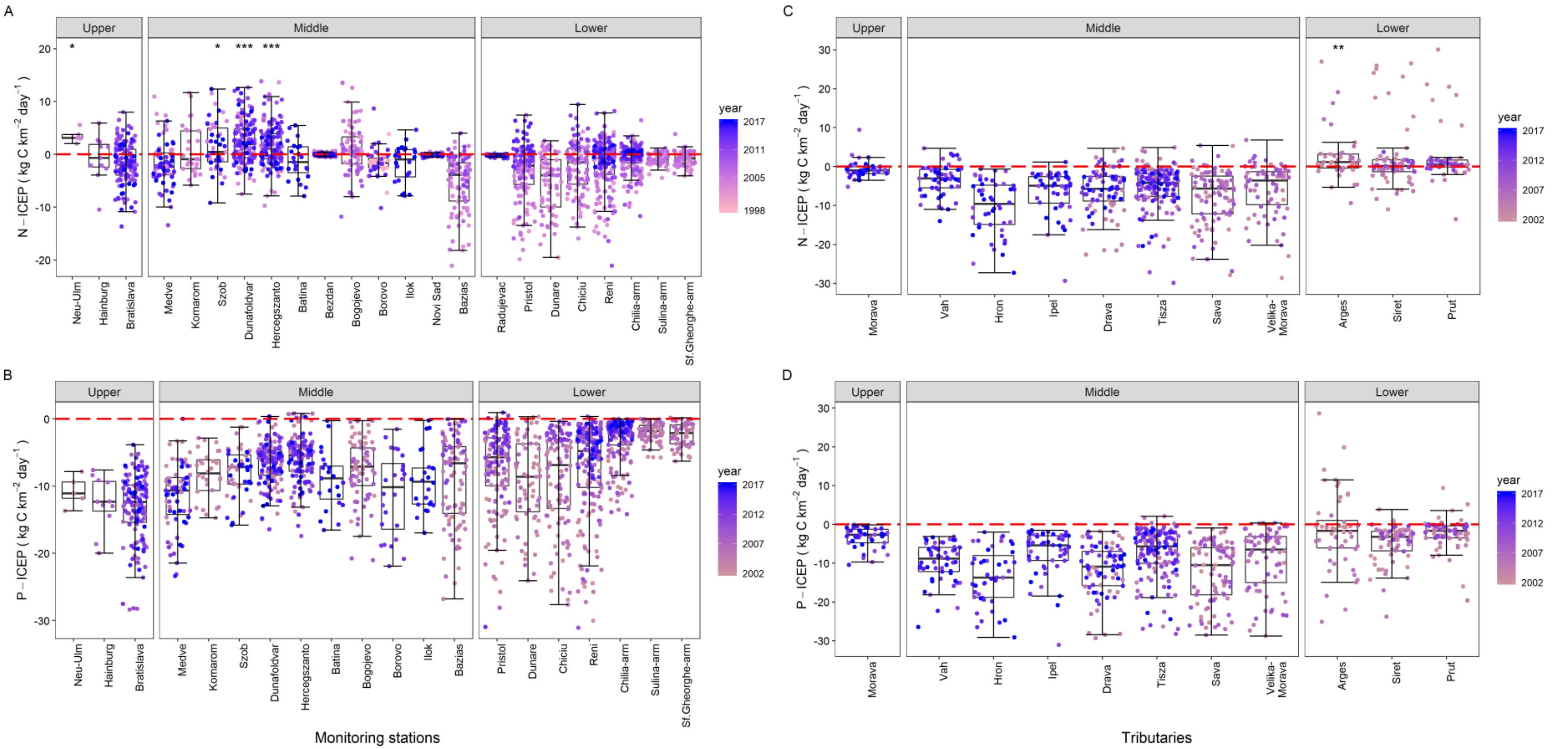

*Figure 4.8. Boxplots of N-ICEP and P-ICEP for the Danube River (A and B) and for its tributaries (C and D) from 1998 to 2017. For the N-ICEP and P-ICEP values > 0 Wilcoxon sign rank test, significance is indicated with * ($p < 0.05$), ** ($p < 0.01$), and *** ($p < 0.001$).*

4.4 DISCUSSION

4.4.1 Mainstem Danube

The gradually increasing loads of Si, N and P in the mainstem of the Danube River led to fluctuating DIN:DSi, DSi:PO_4 and DIN:PO_4 ratios, higher than Redfield and Dupas ratios, generally indicating Si and P limitation in the Danube River. There were some marked changes in loads and ratios related to the presence of large cities and to the contributions of tributaries. DIN:PO_4 ratio (116 to 244) was eleven times higher than the Redfield ratio in the Upper section of the Danube. This high ratio was likely caused by the high N loads in Germany, which has the highest N fertilizer application per cropland area (12,502 – 15,190 kg of N fertilizer km^{-2} $year^{-1}$) in the basin for the period 2002 – 2017 (Appendix 23) (Ritchie et al. 2022). DIN:PO_4 in the Upper section was higher than in the Middle and Lower sections, with strong reductions first at the Bratislava station, and then at the Bazias station which are both located downstream from large cities (Bratislava and Belgrade, respectively) (Figure 4.5C). The reduction on DIN:PO_4 is caused by jumps in P load from these cities which have WWTPs with low collection rate (< 80%), compared to WWTPs in Vienna and Budapest which collect over 80% of the wastewater (ICPDR 2015). Moreover, Bazias station is the first station after the confluence of the Sava tributary that carries water from Slovenia and Croatia, which both have the highest areal P fertilizer application rate (1,400 – 10,345 kg of P fertilizer km^{-2} $year^{-1}$) (Appendix 23) (Ritchie et al. 2022). Overall, the fertilizer applied in Germany has a higher N:P ratio (14:1); than Slovenia and Croatia where the N:P ratio is lower (5:1). Therefore, Slovenia and Croatia apply relatively more P than N in cropland areas compared to Germany. DIN:DSi and DSi:PO_4 were almost four times and two times higher than the Dupas ratio in the Upper and Middle sections until Bazias station, probably because the Sava and Tisza tributaries carry the highest loads of DSi to the Danube (Figure 4.4) and contribute to the drop in DIN:DSi and increase of DSi:PO_4 ratio in the mainstem.

4.4.2 Tributaries

To better understand the controlling factors on nutrient ratios, we used data from tributaries as they can be analysed as statistically independent, whereas the Danube mainstem stations cannot. The model results showed that nutrient ratios in the tributaries were influenced more by land use and land cover than by lithology or water infrastructure (Table 4.1). The ratio Ag:Fo was the most important predictor for DIN:DSi (positive) and DSi:PO_4 (negative), reflecting the importance of agricultural land use as a source of N and P. In contrast, agricultural land use leads to a reduction of Si export to rivers (Vandevenne et al. 2012). Si is taken up by crops at higher rates than by forest and grasslands ecosystems (Guntzer et al. 2012), and crop harvesting removes plant biomass (phytoliths) which leads to a subsequent reduction of soil recycling, and ultimately a depletion of the phytogenic Si pool (Keller et al. 2012). Every year, 210 – 224 million tons of Si are removed at global scale from cultivated soil (Matichenkov and Bocharnikova 2001). Similar to our results, Carey et al. (2019) found a positive effect of agriculture on DIN:DSi ratios in the Mississippi Basin due to high emissions of N from fertilizer application, and a reduction of Si through the loss of soil Si pool. As in our study, they also found a negative effect of forest cover on DIN:DSi ratios. In an earlier study in the Upper Danube basin, we found a significant negative effect of DIN:DSi from forest land cover, in contrast to this study, no effect from agricultural land use (Chapter 2). An explanation for this can be that the alpine areas in this study included small streams where agricultural land use was lower than 25%, and consisted mainly of alpine meadows used for livestock grazing where harvesting was not as important mechanism for reducing DSi export.

Our models showed a positive effect of grasslands on DSi:PO_4 ratios, suggesting the preferential sequestration of P over Si. This may be because grasslands require a high content of macronutrient P compared to micronutrient Si, and the influence of grass type may play a role (Hodson et al. 2005). We were not able to find statistical evidence from our data that can support this preferential sequestration. In previous study focused on DSi export in the Danube, we found that grasslands reduced Si fluxes in Danube tributaries (Chapter 3), and a similar result was reported for the Alzette basin in Luxembourg (Onderka et al. 2012); however, the preferential sequestration of one nutrient over other may influence the result on DSi:PO_4 ratio.

The LULC (ratio Ag:Fo and % grasslands) and dam density did not influence DIN:PO_4 ratios, but % artificial areas and density of WWTPs showed a positive and negative effect on the nutrient ratio. The contradictory effect of these control factors could be because in artificial areas, the main diffuse sources of nutrient emissions to surface waters are overland flow, tile drainage, and stormflow. Based on a US stormwater database from 20 metropolitan areas, Schueler (2003) identified that stormwater runoff had a high N:P ratio (>16), which supports this observation. Meanwhile, WWTP is considered a major source of P in comparison to N, due to a relative lack of effective treatment to remove. In the Danube basin, WWTPs remove N more effectively than P, with 14% and 29% of total emissions, in the Middle and Lower sections respectively (Popovici 2014).

The analysis showed that reservoirs did not have a significant effect on any of the nutrient ratios. Similarly, our earlier study on DSi in the Danube did not identify a significant effect of dams on DSi yields (Chapter 3). Some studies suggest that dams typically reduce P more than N and Si (Garnier et al. 1999; Maavara et al. 2020b), through rapid sorption to mineral surfaces which leads to sedimentation (Maranger et al. 2018). However, it has been hypothesized that the retention of nutrients by dams depends strongly on the reservoir's residence time (Maavara et al. 2020b). In the Three Gorge Dams (China), with a residence time < 27 days, Si was reduced more efficiently than N and P due to Si uptake by diatoms (Maavara et al. 2020b). This trend can also be observed in our study by comparing the Bazias and Pristol stations, which are upstream and downstream of the Iron Gate Dams, which has a short residence time of ∼ 6 days. There was a tendency for an increase of DIN:DSi from 0.9 ± 0.15 to 1.1 ± 0.1, while DSi:PO_4 showed a decrease from 51 ± 7 to 43 ± 6 (Figure 4.5A and 4.5B). This suggests preferential sequestration of Si over N and P in reservoirs with a short residence time. In alpine rivers, run-of-the-river reservoirs appear not to sequester Si (Chapter 2), which may because of their shorter residence time (< 1 day). In this study we used the "Major Dams" classification from the GRanD Database, which is defined by storage capacity (from 5 to 1230 million cubic meters). This may not necessarily be the best measure of residence time, as the Iron Gates Dam would fall into this category in the database, even though it has a short residence time, while the small hydropower long-residence time reservoirs in the alpine space do not, even though they have long residence times of >1 year. For this study, we conclude that compared with land use and WWTP, reservoirs have a smaller effect on nutrient ratios in the Danube system.

4.4.3 Basin eutrophication potential

The impact of land use on nutrient ratios in the tributaries and the mainstem of the Danube has increased the risk of eutrophication in recent years. The median values for N-IFEP and N-ICEP were greater than 0 but P-ICEP values were negative. Overall, the Danube Basin seems to show greater potential for eutrophication from N rather than P in the mainstem and its tributaries (Figure 4.7 and 4.8). However, P-IFEP and P-ICEP values have been increasing between 2002 and 2017 in the Lower section (Figure 4.7B nd 4.8B), possibly because of the decrease of Si loads since 2000s. This potentially leads to a eutrophication problem in the Lower section of the Danube if DSi continues to reduce. The IFEP and ICEP values had the same overall patterns in the mainstem and in the tributaries. However, the main difference between the IFEP and ICEP values is that IFEP results showed higher potential of eutrophication risk due to the higher Si requirement of freshwater diatoms.

Previous studies using data from the Global-NEWS model calculated a larger range of P–ICEP values from 2–5 for the period 1970–2000 (Garnier et al. 2010; Strokal and Kroeze 2013). The difference in results can be explained from the fact that we used only the dissolved inorganic forms of N and P for the ICEP calculations, whereas the other studies used total N and total P and, constrained by data availability, only the dissolved forms of Si (Garnier et al. 2010; Strokal and Kroeze 2013). The inorganic forms have higher bioavailability, but some organic forms can be available when they are rapidly recycled. However, this is the first study analysing the risk of eutrophication along the river and in the tributaries by using the IFEP equation established by freshwater systems. Recently studies developed in USA have used this indicator to accommodate the observation that diatoms in freshwater systems have a higher Si requirement (Dupas et al. 2015; Royer et al. 2020; Senath et al. 2022).

4.4.4 Danube Mouth

The reduction of Si has been highlighted as a cause of the eutrophication problems in the Danube and the Black Sea (Humborg et al. 1997). The data presented in this study support this, particularly with the time series analysis at Reni station, the last station of the Danube River before entering the Danube Delta and Black Sea. From 2000 to 2017, the annual DSi and DIN loads have decreased, but PO_4 load has been stable since 2000 (Figure 4.3). The reduction of the DIN can be a result of implementation of the EU-WFD, while agricultural activities in the Danube may have reduced Si as they account for around 50% of land use. Despite the DIN load reduction in recent years, DIN loads at the Reni station by 2017 were still 1.5 times higher than in the 1960s. In comparison, DSi and PO_4 loads are 1.5 and 1.6 times lower than in the 1960s, respectively. After the Reni station, the remaining stations located in the Danube Delta have lower loads, partly because the total load is divided among the Chilia (63% of the total flow of the Danube River), Sulina (16%) and Sf. Georghe (21%) branches. Based on a mass balance analysis the sum of nutrient loads on these three branches is lower than at Reni station, suggesting that there is retention of nutrients in the Danube Delta due to uptake by macrophytes and phytoplankton in the delta lakes that serve as a nutrient sink during the growing season (Friedrich et al. 2003; Oosterberg et al. 2000).

4.5 Conclusions

This study analyses nutrient stoichiometry in the Danube Basin using empirical data. Overall, the nutrient stoichiometry showed Si and P limitation in the Danube River and its tributaries, as the nutrient ratios were higher than the Redfield and Dupas ratios. The evidence in this study suggests that the high ratios of DIN with DSi and PO_4 are due the high N fertilizer application in the upper section of the Danube River (Germany). The nutrient ratios (DIN:DSi and DIN:PO_4) decrease along the mainstem of the Danube River as a result of the reduction of loads of DSi from the tributaries (Tisza and Sava), and high PO_4 inputs from the effluents of WWTPs from the cities Bratislava and Belgrade and from the fertilizer application in the eastern part of the basin (Slovenia, Croatia, Serbia).

The mixed model analyses of the data from the tributaries showed that the spatial pattern of nutrient stoichiometry is affected by LULC (relative proportion of agriculture to forest land, % grasslands, and % artificial areas) and the density of WWTPs. DIN:DSi and DSi:PO_4 were affected positively and negatively, respectively by the ratio of agriculture and forest land. These results highlight the importance of agriculture as a source of N and P and as a sink of Si. DIN:PO_4 ratios were influenced positively by % artificial areas (preferential source of N) and negatively by the density of WWTPs (preferential source of P).

Trends in nutrient loads were similar for Si, N and P, increasing from upstream to downstream, especially after the confluence of two main tributaries Tisza and Sava, which carry the largest nutrient loads, mainly because of their high discharge. Moreover, DIN and DSi loads have been decreasing since 2000; however, DIN loads from the Danube River Basin to the Black Sea are at present still higher than in the 1960s. As a consequence, IFEP and ICEP values showed potential risk of eutrophication due to DSi reduction in the mouth of the Danube River.

5
Discussion and Conclusions

5.1 SYNTHESIS OF MAIN FINDINGS

This thesis aimed to quantify Si export from the mainstem and major tributaries of the Danube River Basin and the effects of major controlling factors on nutrient yields and ratios for nitrogen (N), phosphorus (P), and silica (Si).

Chapter 1 presented the theoretical background of Si and nutrient export, identified main findings from the literature, highlighted the relevance of the research, defined the research objectives, and provided an overview of the structure of the thesis.

In Chapter 2, an analysis was made of the key controlling factors affecting nutrient concentration and yields in the upper Danube Basin (Austria and Germany), where reservoirs with long and short residence times are located. The controlling factors that were investigated included land use/land cover (LULC), catchment size, elevation, lithological class, and river discharge. In this chapter, the results of two fieldwork campaigns in 2015 and 2016 were presented, which included 11 reservoirs with long residence time (≥ 1 year), 25 reservoirs with short residence time (run-of-the-river-hydropower systems) (< 1 day), and 38 inlet sites. The results showed that dissolved silica (DSi) concentrations and yields in the headwater rivers located in the upper Danube basin are controlled by both lithology (% metamorphic rock) and coniferous forest land cover. No significant relationships of DSi export with other types of LULC, such as agriculture or grassland were found. However, total dissolved nitrogen (TDN) and phosphorus (TDP) concentrations and yields were positively related to agriculture, and only TDP was also positively related to coniferous land cover. Moreover, DSi concentrations were lower in reservoirs with long residence times compared with those with short residence times. The longitudinal analysis developed from upstream to downstream in two different sections of the rivers Lech and Inn, with presence of run-of-the-river-reservoirs, showed that DSi yields were not affected by the presence of these short-residence reservoirs. This contributed to the sparse data and understanding of DSi, N and P ratios in alpine systems (Austria), which are characterized by a large number of hydropower reservoirs and run-of-the-river hydropower systems.

While Chapter 2 focused on specific areas of the Danube River using data from synoptic surveys, Chapter 3 focused on DSi throughout the Danube Basin using empirical data from the International Commission for the Protection of the Danube River (ICPDR) database. Data were available from 43 monitoring stations (28 in the mainstem and in 15 tributaries) for the period 1998 to 2017. Analysis of DSi yields showed that the main controlling factors of DSi for the basin scale of the Danube River were LULC (ratio agriculture:forest, and % grassland). A doubling of the agriculture:forest ratio led to a decrease in DSi yield of about 1.2 tonnes km^{-2} year^{-1}. Such a reduction is similar to the DSi yield from the Seine River (France) (Billen et al. 2007). Grasslands were the other

Box 5.1: *Links and summary of the chapters published during the development of this thesis.*

Chapter 2: Controls of Si export and nutrient (N, P) stoichiometry in hydropower reservoirs and headwater rivers of the Danube River Basin

- Data collected from fieldwork in the headwater rivers (Austria and Germany) from 2015-2017.
- LULC (% coniferous) and lithology (% metamorphic rock) have a positive effect on DSi concentration, yields and its ratios with N and P.
- There is lower DSi concentration in reservoirs with long residence times compared with those with short residence times.
- Reservoirs with short residence time do not appear to reduce DSi yields along the river sections.
- The nutrient ratios DSi:TDP and DIN:PO_4 were above the threshold of Redfield and Dupas ratio (> 40 and >16 respectively) indicating an overall P limitation in the upper part of the Danube Basin, with evidence for DSi limitation and sequestration in the long-residence time reservoirs.

Chapter 3: Dissolved silica in the Danube Basin

- Data of DSi was provided from ICPDR, of the Danube River and its main tributaries from 1998 to 2017.
- LULC (ratio agriculture:forest and % grasslands) have a negative effect on DSi yields. The effect of the agriculture:forest ratio on DSi yield is of the same order of magnitude as the DSi yields in other rivers.
- Bivariate correlations showed that reservoirs (dam density) have a negative effect on DSi yield, consistent with Chapter 2. However, when it is included in a statistical mixed model analysis with LULC, WWTP, the effect of reservoirs on DSi is not visible.
- The highest contributions of DSi loads to the mainstem of the Danube were from Sava and Tisza tributaries located in the Middle section of the Danube Basin.

Chapter 4: Analysis of controlling factors of nutrient stoichiometry in the Danube River and its tributaries

- Nutrient export, yields and ratios were estimated for the Danube River and its tributaries using data from the ICPDR from 1998 to 2017.
- The nutrient ratios are above the threshold of Redfield and Dupas ratio (DIN:DSi > 0.4, DSi:PO_4 > 40 and DIN:PO_4 >16), indicating a prevalence of P and Si limitation in the Danube Basin.
- LULC variables in terms of the relative area of agriculture and forest lands, the proportion of grasslands and artificial land cover are stronger than lithology or water infrastructure (reservoirs or waste-water treatment plants) that affect nutrient stoichiometry in the Danube Basin. Reservoirs have a negative effect on DSi yield. Therefore they have a negative effect on DIN:DSi and positive effect on DSi:PO_4. However, these effects still small compared to LULC.

land use with a significant negative effect on DSi yield, with an increase of 10% grassland leading to a reduction in DSi yield of 1.1 tonnes km^{-2} $year^{-1}$. The tributaries with the highest loads in the Danube Basin were the Sava and Tisza tributaries, mainly due to their high discharge (mean 1042 m^3 s^{-1} ± 23) in comparison with other tributaries.

In Chapter 4, the ICPDR database was used to describe spatial and temporal variation in DSi, DIN, and PO_4 loads, concentrations and ratios within the Danube River, and analyse the influence of LULC, lithology, and water infrastructure (reservoirs, wastewater treatment plants) on these in the Danube mainstem and its major tributaries. The results showed that nutrient loads increase along the longitudinal gradient of the river. As a result, the nutrient ratios are above the threshold values for freshwater ecosystems (DIN:DSi >0.4, DSi:PO_4 > 40 and DIN:PO_4 >16). Based on the analysis using a mixed effects linear model, LULC variables (agriculture:forest ratio, % grasslands, and % artificial land use) strongly affected nutrient stoichiometry. Box 5.1 shows the links and summary of the papers published during the development of this thesis.

5.2 Importance of controlling factors

Previous studies found that the factors controlling the Si cycle in river basins included lithology, precipitation, temperature, latitude, land use and land cover, and water infrastructure (dams, wastewater treatment plants). However, these controlling factors influence Si in different ways. Most of the basin scale models have focused on lithology as the main controlling factor predicting riverine Si export due to the fact that it is the main natural source of Si in the environment (Dürr et al. 2011). Other studies have examined other controlling factors, including those that affect plant and soil cycling and runoff, such as LULC (Struyf et al. 2010; Vandevenne et al. 2012; Carey and Fulweiler 2011), or those that affect Si storage in river basins such as reservoirs (Humborg et al. 1997; Maavara et al. 2020b), or those that may comprise point-sources of Si export through human consumption (wastewater treatment plants Sferratore et al. 2005). In this study, all these controlling factors were assessed together to allow identification of the most important controls and their effect sizes.

The main conclusion of this thesis was that LULC is the main controlling factor of DSi yield and nutrient ratios in the Danube Basin. It was surprising that the effect of reservoirs was relatively weak in comparison to the effects of LULC, given the previous research that indicated that reservoirs were responsible for the reduction of DSi export to the Black Sea. This study showed an effect of reservoirs using simple bivariate correlation analysis indicate a significant but weak negative correlation of DSi yields (rho = -0.24), which also affected its stoichiometry with N and P (positive but weak correlation of DIN:DSi (Spearman rho correlation coefficient of 0.48), and negative correlation with DSi:PO_4

ratios (rho = -0.45) (Chapters 3 and 4). However, when included in the mixed models, these effects disappear with the strength of the LULC effect.

In the Danube River Basin, Si export has been predicted by using process-based models, such as the Riverstrahler model (Sferratore et al. 2005). In these models, the main source of Si inputs is lithology alone, while LULC determines N and P inputs. By ignoring the impact of land use on the Si cycle, this can result in underestimated Si export. The Global News-DSi model uses a multiple linear regression approach and showed that LULC was not significant for Si, while lithology (volcanic), slope, and precipitation were important predictors (Beusen et al. 2009). The News-DSi model used a dataset from 280 rivers from different continents which has uncertainties on how DSi values were measured. Based on the uncertainties of the underlying dataset, the Global News model is appropriate for regional and continental scales, but not for individual river basins (Beusen et al. 2009).

In this thesis, an empirical mixed-modelling approach was used to identify the controlling factors of DSi export to the Danube River, including lithology, LULC, and water infrastructure (reservoirs and wastewater treatment plants). The advantage of this approach is the use of the ICPDR dataset, which is an empirical dataset from field campaigns based on long-term monitoring in the Danube Basin. It covers spatial and temporal variables and includes more than 10,000 data points. This approach allows interpretation of the nested basin data representing different sub-basins and tributaries which does not violate the required assumption of independence in the statistical analysis. The mixed-effect linear models account for co-dependencies of data in space and/or time using random effects associated with e.g. sub-basins. This allowed the identification of main controls and effect sizes of controlling variables, which can be used in other analyses, e.g. process-based models that can incorporate more factors than are currently typically used. The current process-based Si models rely heavily on lithology as the main controlling variable, and do not represent other controlling variables (particularly LULC) well, and this research offers a potential way to include them.

The main challenges of using the empirical mixed-modelling approach were that data for discharge and nutrient concentrations were missing for some time periods (see Chapter 3). To address these gaps, some assumptions were made and some data had to be discarded. For example, the nutrient loads used in statistical analysis were calculated by assuming that one nutrient concentration measurement was representative of a whole month. Another main challenge for the model was inherent covariation among the predictor variables within the sub-basins, and the multi-collinearity between these variables. Multi-collinearity of predictor variables was avoided by not combining predictor variables with correlation coefficients greater than 0.5 and from the predictor variables, we systematically developed the most parsimonious models based on the lowest value of the Akaike Information Criterion (AIC) and the most homogeneous and normally distributed residuals. The mixed model approach could not be used to predict scenarios; however, this model has a dynamic element as we analysed the data using monthly and annual nutrient yields. Therefore, the outcomes from the application of the linear mixed models are helpful to determine main controls and effect-sizes that can be later used in other process-based models that rely on e.g. nutrient transfers as a function of land use or other landscape features.

5.3 DANUBE BASIN APPLICATION AND FUTURE OUTLOOK

5.3.1 Importance of ICPDR data reliability and availability

The monitoring of water quality is an important tool for the development of specific management policies both at regional and at national levels (Chapman et al. 2016; Grizzetti et al. 2016). Long-term monitoring provides information on specific, often slowly changing, variables in ecosystems (Lovett et al. 2007) and is useful for computational modelling that requires big datasets (Desouza and Lin 2011) and for validation of other types of models. In Europe, monitoring activities for the assessment of their waterbodies are required under the Water Framework Directive (WFD), the European Union (EU) water policy. The main objective of the WFD is to achieve good water quality as established in the Directive 2000/60/EC (European Commission 2000).

The riparian areas of the Danube River Basin are shared by 14 countries. Nine of these countries follow the WFD as they are members of the EU (Irvine et al. 2016). However, all the countries co-operating under the Danube River Protection Convention (DRPC), which was signed in 1996, have agreed to implement the WFD and their Directives in the Danube Basin through the ICPDR (Chapman et al. 2016). In the Danube River Basin, the ICPDR established the Transnational Monitoring Network (TNMN) which regularly monitors water quality. In 2000, the main objective of the TNMN was established to provide a structured and well-balanced overall view of the status and long-term development of quality and loads of priority pollutants in the major rivers of the Danube Basin.

Across the Danube Basin, the TNMN varies with respect to the spatial and temporal resolution. The data collection is carried out within the rules specified by the WFD by each country by the National Information Managers who receive the data from the national laboratories (Liska 2015). The TNMN Laboratories network guarantees high data quality by following an effective Analytical Quality Control (AQC) programme organized by the ICPDR. After collection, the data are checked and submitted to the TNMN data centre in Slovakia for additional checking and final processing and uploaded into the ICPDR database website (http://www.icpdr.org/wq-db). Therefore, the outputs of the Danube monitoring programmes have sufficient quality to evaluate the state of the whole river and can be used to inform planning and management at river basin level (ICPDR 2015).

TNMN comprises 133 monitoring stations, 49 on the mainstem of the Danube River and 84 on 20 of its main tributaries. While monitoring of N and P is done in all stations, DSi data have been collected only in 32 stations in the mainstem and 43 stations in 15 tributaries. DSi and discharge are available together with other physical and chemical variables for the period 1998 to 2017, in general with a monthly sampling frequency. However, there were stations in the mainstem and in the tributaries that showed gaps of discharge data for several years. These measurements are very important for the calculation of nutrients loads. Therefore, to improve the support of basin management and decision-making, the monitoring network should be strengthened in some stations: i) In the tributaries located in the Upper Section of the Danube (Inn, Lech, Isar Rivers), which did not show records of DSi. The Sava River, which is the tributary that carries water from Slovenia and Croatia, does not show records of discharge since 2010; ii) In the mainstem of the Danube River, the first station at Neu Ulm (Germany), which does not have discharge data since 2006. Stations with full information will be important in this part of the section as Germany, Slovenia, and Croatia have with the highest areal rates of fertilizer application (Ritchie et al. 2022).

5.3.2 Management/policy of the basin and reflection on land use importance in basin

A major concern in managing large river basins is the transfer of nutrients and pollutants from land-based activities to the deltas and coastal zones. Unfortunately, this is also a problem in the Danube basin, as diffuse sources of nutrients still dominate N and P contributions at the basin scale (ICPDR 2015). Nutrient pollution has led to historical patterns of eutrophication in the Black Sea over previous decades, alteration of nutrient ratios and food web structure, and continued elevated levels of nutrient inputs to the Black Sea from the Danube (as discussed in Chapter 4). This thesis identified the tributaries Sava (Slovenia, Croatia, Serbia) and Tisza (Ukraine, Hungary, Croatia) as the highest contributors of nutrients (Si, N, and P) to the Danube River. However, Si and N loads have been decreasing in the Danube River from 2000 to 2017, before reaching the Black Sea. However, as P loads have not decreased the reduction of Si (and the resulting shift in Si:nutrient ratios) can lead to a potential eutrophication problem in the Lower section of the Danube and in the Black Sea.

The results of this thesis show that LULC effects on river nutrients is bigger than the influence of reservoirs, lithology, or other wastewater treatment plants. To reach and maintain a good ecological status as established by the WFD (European Commission 2000), the main focus of future policies for the Danube basin should therefore be on reducing the effect of land use changes and management on river water quality. For example, urban areas are projected to increase by 10.5% in 2050 at the expense of the fraction of arable land, with the most pronounced increase in the western and southern parts of the basin (Bisselink et al. 2018). Even though agriculture areas are not projected to increase, their productivity is expected to increase, which may lead to higher nutrient inputs to rivers (Bouwman et al. 2009). However, the new European Green Deal policy aims at EU countries reducing the use of fertilizer by 20 % and decreasing nutrient losses by at least 50% in 2030 (European Commission 2019). The implementation of this new policy might lead to the decline of yields of agricultural crops and increase imports of agriculture products from outside Europe. However, this measure is not applicable for all countries of the Danube Basin, such as e.g. Ukraine which includes the upper part of the three main tributaries of the Danube River (Tisza, Siret and Prut) but is a non-EU country. Moreover, the current situation in Ukraine, where harvesting of planted crops, planting of new crops, and livestock production have been severely disrupted (FAO 2022), may also affect the impact on the Danube tributaries. Another crucial issue for Danube River Basin management in the future is the possible impact of climate change which can also affect the basin nutrient dynamics. For the coming years, climate change may lead to changes in snow accumulation, snow melt, and ultimately river discharge (Holzmann et al. 2008), with concomitant effects on nutrient loads.

REFERENCES

Ahearn DS, Sheibley RS, Dahlgren RA, Anderson M, Jonson J and Tate KW (2005). Land use and land cover influence on water quality in the last free-flowing river draining the western Sierra Nevada, California. Journal of Hydrology 313, 234–247.

Akbarzadeh Z, Maavara T, Slowinski S, Van Cappellen P (2019). Effects of Damming on River Nitrogen Fluxes: A Global Analysis. Global biogeochemical cycles, 33.

Amo YD, Brzezinski MA (1999). The Chemical form of dissolved Si taken up by marine diatoms. Journal of phycology 35(6):1162-1170.

Alexandre A, Meunier JD, Colin F, and Koud JM (1997). Plant impact on the biogeochemical cycle of silicon and related weathering processes. Geochim. Cosmochim. Ac., vol 61, pp 677–682.

Allan JD, Erickson DL, Fay J (1997). The influence of catchment land use on stream integrity across multiple spatial scales. Freshwater Biology 37, 149–161.

APHA (American Public Health Association) (1998). Standard Methods for the Examination of Water and Wastewater, 20th ed. APHA and the American Public Health Association, Washington, DC, USA.

Bartoli F, Wilding LP (1980). Dissolution of biogenic opal as a function of its physical and chemical properties, Soil Sci. Soc. Am. J., 44, 873–878.

Bartoli F (1983). The biogeochemical cycle of silica in two temperate forest ecosystems, Environ. Biogeochem. Ecol. Bull., 35, 469– 476.

Bartoli F (1985). Crystallochemistry and surface properties of biogenic opal, J. Soil Sci., 36, 335–350.

Belcher H, Swale E (1976). A Beginner's Guide to Freshwater Algae H.M. Stationery Office.

Bellinger EG, Sigee DC (2010). Freshwater Algae: Identification and Use as Bioindicators. John Wiley & Sons, Ltd.

van Bennekom AJ, Salomons W (1981). Pathways of nutrients and organic matter from land to ocean through rivers. In Review and Workshop on River Inputs to Ocean Systems. Rome (Italy). 26 Mar 1979.

Berman T, Bronk DA (2003). Dissolved organic nitrogen: a dynamic participant in aquatic ecosystems. Aquatic Microbial Ecology Vol. 31: 279–305.

Berner EK, Berner RA (1996). Global environment: water, air, and geochemical cycles. Prentice Hall, New Jersey.

Beusen AHW, Bouwman AF, Dürr HH, Dekkers ALM, Hartmann J (2009). Global patterns of dissolved silica export to the coastal zone: Results from a spatially explicit global model. Global Biogeochemical Cycles, 23(4).

Beusen AHW, Bouwman AF, Van Beek LPH, Mogollón JM, Middelburg JJ (2016). Global riverine N and P transport to ocean increased during the twentieth century despite increased retention along the aquatic continuum. Biogeosciences 2441-2451.

Billen G, Garnier J (2007). River basin nutrient delivery to the coastal sea: assessing its potential to sustain new production of non-siliceous algae. Mar. Chem. 106,148–160.138.

Billen G, Garnier J, Mouchel JM, Silvestre M (2007a). Human activity and material fluxes in a regional river basin: The Seine River watershed. Science of the total environment 375 (1-3).

Billen G, Garnier J, Némery J, Sebilo M, Sferratore A, Barles B, Benoit P, Benoît M (2007b). A long-term view of nutrient transfers through the Seine river continuum. Science of the Total Environment 375: 80–97.

Bisselink B, de Roo A, Bernhard J, Gelati E (2018). Future projections of water scarcity in the Danube River Basin due to land use, water demand and climate change. Journal of Environmental Geography, 11(3-4), 25-36.

Björkman KM, Karl DM (2003). Bioavailability of dissolved organic phosphorus in the euphotic zone at Station ALOHA, North Pacific Subtropical Gyre. Limnol. Oceanogr., 48(3), 1049–1057.

BMI (2019). Bundesministerium für Nachhaltigkeit und Tourismus, Hydrographisches Jahrbuch von Österreich 2016, 124. Band Hydrographischer Dienst in Österreich, Abteilung I/4 – Wasserhaushalt.

Bouwman AF, Beusen AH, Billen G (2009). Human alteration of the global nitrogen and phosphorus soil balances for the period 1970–2050. Global Biogeochemical Cycles, 23(4).

Boyer EW, Goodale CL, Jaworski NA and Howarth RW (2002). Anthropogenic nitrogen sources and relationships to riverine nitrogen export in the northeastern USA. Biogeochemistry 57–58:137–169.

Brown LE, Hannah DM, Milner AM (2003). Alpine stream habitat classification: an alternative approach incorporating the role of dynamic water source contributions. Arct. Antarct. Alp. Res., 35 (3) pp. 313-322.

Brzezinski MA (1985). The Si:C:N ratio of the marine diatoms: Interspecific variability and the effect of some environmental variables. J. Phycol. 1985. vol 21, pp 347-357.

Burnham KP, Anderson DR (2002). Model selection and multimodel inference: a practical information-theoretic approach, 2nd edn. Springer, New York.

Carey JC, Fulweiler RW (2012). Human activities directly alter watershed dissolved silica fluxes. Biogeochemistry. doi 10.1007/s10533-011-9671-2.

Carey JC, Fulweiler RW (2016). Human appropriation of biogenic silicon – the increasing role of agriculture. Functional Ecology 2016, 30, 1331–1339.

Carey JC, Jankowski K, Julian II P, Sethna LR, Thomas PK, and Rohweder J (2019). Exploring Silica Stoichiometry on a Large Floodplain Riverscape. Frontiers in Ecology and Evolution.

Carpenter SR, Caraco NF, Correll DL, Howarth RW, Sharpley AN, and Smith VH (1998). Nonpoint pollution of surface water with phosphorus and nitrogen. Ecological Applications 8:559–568.

Chapman DV, Bradley C, Gettel GM, Hatvani IG, Hein T, Kovács J, Liska I, Oliver DM, Tanos P, Trázy B, Várbíró G (2016). Developments in water quality monitoring and management in large river catchments using the Danube River as an example. Environmental Science & Policy, 64, 141-154.

Chen N, Wu Y, Wu J, Yan X, Hong H (2014). Natural and human influences on dissolved silica export from watershed to coast in Southeast China. J. Geophys. Res.: Biogeosci. 119 (1), 95−109.

Clymans W, Struyf E, Govers G, Vandevenne F, Conley DJ (2011). Anthropogenic impact on amorphous silica pools in temperate soils. Biogeosciences 8, 2281–2293.

Clymans W, Struyf E, Van den Putte A, Langhans C, Wang Z and Govers G (2015). Amorphous silica mobilization by inter-rill erosion: insights from rainfall experiments Earth Surf. Process. Landforms DOI: 10.1002/esp.3707.

Cociasu A, Dorogan L, Humborg C, Popa L (1996). Long-term ecological changes in Romanian coastal waters of the Black Sea. Marine Pollution Bulletin 32, 32–38.

Cociasu A, Popa L (2005). Significant changes in Danube nutrient loads and their impact on the Romanian Black Sea coastal waters. Cercet. Mar. 35, 25–37.

Commission of the European Communities (CEC) (2001). Communication from the Commission: Environmental Co-operation in the Danube – Black Sea Region. Brussels.

Conley D (2002). Terrestrial ecosystems and the global biogeochemical silica cycle. Global Biogeochemical Cycles Volume 16, Issue 4.

Conley DJ, Kilham SS, Theriot EC (1989). Differences in silica content between marine and freshwater diatoms, Limnol. Oceanogr., 34, 205 – 213.

Conley DJ, Schelske CL, Stoermer EF (1993). Modification of the biogeochemical cycle of silica with eutrophication. Marine Ecology Progress Series, 179-192.

Conley DJ, Stalnache P, Pitkanen H, Wilander A. (2000). The transport and retention of dissolved silicate by rivers in Sweden and Finland. Limnol Ocenogr, 2000, 45:1850–1853.

Cook PLM, Aldridge KT, Lamontagne S, Brooks JD (2010). Retention of nitrogen, phosphorus and silicon in a large semi-arid riverine lake system. Biogeochemistry 99: 49–63.

Cornelis JT, Delvaux B, Georg R, Lucas Y, Ranger J, Opfergelt S (2011). Tracing the origin of dissolved silicon transferred from various soil-plant systems towards rivers: a review.

Demmer W (1991). Österreichisches Nationalkomitee für Talsperren. Dams in Austria: prepared in commemoration of the Seventeenth Congress of the International Commission on Large Dams. Austrian National Committee on Large Dams.

Desouza K, Lin Y (2011). Towards evidence-driven policy design: Complex adaptive systems and computational modeling. The Innovation Journal, 16(1), Article-number.

van Dokkum H, Hulskotte JJ, Kramer KM, Wilmot JL (2004). Emission, Fate and Effects of Soluble Silicates (Waterglass) in the Aquatic Environment. Environ. Sci. Technol. 38, 515-521.

Dürr HH, Meybeck M, HartmannJ, Laruelle GG, Roubeix V (2011). Global spatial distribution of natural riverine silica inputs to the coastal zone. Biogeosciences, 8, 597–620.

Dupas R, Delmas M, Dorioz JM, Garnier J, Moatar F, Gascuel-Odoux C (2015). Assessing the impact of agricultural pressures on N and P loads and eutrophication risk. Ecological Indicators, 48, 396-407.

EEA (2000). Corine Land Cover 2000. European Environment Agency.

EEA (2006). Corine Land Cover 2006. European Environment Agency.

EEA (2012). Corine Land Cover 2012. European Environment Agency.

EEA (2018). Corine Land Cover 2018. European Environment Agency.

Ehrlich H, Demadis KD, Pokrovsky OS, Koutsoukos PG (2010). Modern views on desilicification: biosilica and abiotic silica dissolution in natural and artificial environments. Chemical reviews, 110(8), 4656-4689.

Elser JJ, Dobberfuhl DR, MacKay NA, Schampel JH (1996). Organism size, life history, and N: P stoichiometry: toward a unified view of cellular and ecosystem processes. BioScience, 46(9), 674-684.

Epstein E (1999). Silicon. Annual Review of Plant Physiology and Plant Molecular Biology, 50, 641–664.

Epstein E (2009). Silicon: its manifold roles in plants. Annals of applied Biology, 155(2), 155-160.

Esri (2017). ArcGIS Desktop: Release 10. Redlands, CA: Environmental Systems Research Institute.

European Commission (2019). The European green deal, COM/2019/640. Annex to the Communication from the Commission to the European Parliament, the European Council, the Council, the European Economic and Social Committee and the Committee of the Regions.

European Commission (2000). Directive 2000/60/EC of the European Parliament and of the Council of 23 October 2000 establishing a framework for community action in the field of water policy. Official journal of the European Communities L327(43), 1–72.

Farmer VC, Delbos E, Miller JD (2005). The role of phytolith formation and dissolution in controlling concentrations of silica in soil solutions and streams. Geoderma, 71–79.

FAO (Food and Agriculture Organization of the United Nations) (2022). Ukraine, Note on the Impact of the War on Food Security in Ukraine. FAO: Rome, Italy, 22, 1-9.

Fraysse F, Pokrovsky OS, Schott J, Meunier J-D (2009). Surface chemistry and reactivity of plant phytoliths in aqueous solutions. Chem Geol 258:197–206.

Friedl G, Teodoru C, Wehrli B (2004). Is the Iron Gate I reservoir on the Danube River a sink for dissolved silica?. Biogeochemistry 68: 21–32.

Friedrich J, Dinkel C, Friedl G, Pimenov N, Wijsman J, Gomoiu MT, Cociasu A, Popa L, Wehrli B. (2002). Benthic nutrient cycling and diagenetic pathways in the north-western Black Sea. Estuarine, Coastal and Shelf Science, 54(3), 369-383.

Friedrich J, Dinkel C, Grieder E, Radan S, Secrieru D, Steingruber S, Wehrli B (2003). Nutrient uptake and benthic regeneration in Danube Delta. Biogeochemistry 64, 373 – 398.

Fulweiler RW, Nixon SW (2005). Terrestrial vegetation and the seasonal cycle of dissolved silica in a southern New England coastal river. Biogeochemistry 74: 115–130.
Galloway JN (1998). The global nitrogen cycle: changes and consequences. Environ Pollut 102:15–24.

Garnier J, Beusen A, Thieu V, Billen G, Bouwman L (2010). N:P:Si nutrient export ratios and ecological consequences in coastal seas evaluated by the ICEP approach. Global Biogeochemical Cycles, vol 24.

Garnier J, Billen G, Hannon E, Fonbonne S, Videnina Y, Soulie M (2002). Modelling the transfer and retention of nutrients in the drainage network of the Danube River. Estuarine, Coastal and Shelf Science, 54(3), 285-308.

Garnier J, Leporcq B, Sanchez N, Philippon X (1999). Biogeochemical mass-balances (C, N, P, Si) in three large reservoirs of the Seine basin (France). Biogeochemistry 47, 119–146.

Garnier J, Sferratore A, Meybeck M, Billen G, Dürr H (2006). Modeling silicon transfer processes in river catchments. The silicon cycle. Human perturbations and impacts on aquatic systems, 66, 139-162.

Gérard F, Mayer KU, Hodson MJ (2008). Modelling the biogeochemical cycle of silicon in soils: application to a temperate forest ecosystem. Geochimica et Cosmochimica Acta 72: A304–A304.

Goolsby DA, Battaglin WA, Lawrence GB, Artz RS, Aulenbach BT, Hooper RP, Keeney, Dr, Stensland GJ (1999). Flux and Sources of Nutrients in the Mississippi–Atchafalaya River Basin Topic 3 Report for the Integrated Assessment on Hypoxia in the Gulf of Mexico.

Grizzetti B, Liquete C, Antunes P, Carvalho L, Geamănă N, Giucă R, Leone M, McConnell S, Preda E, Santos R, Turkelboom F, Vădineanu A, Woods H (2016). Ecosystem services for water policy: Insights across Europe. Environmental Science & Policy, 66, 179-190.

Guntzer F, Keller C, Poulton PR, McGrath SP, Meunier JD (2012). Long-term removal of wheat straw decreases soil amorphous silica at Broadbalk, Rothamsted. Plant Soil, 352, pp. 173-184.

Harrison JA, Frings PJ, Beusen AHW, Conley DJ, McCrackin ML (2012). Global importance, patterns, and controls of dissolved silica retention in lakes and reservoirs. Global Biogeochemical Cycles, Vol. 26, GB2037.

Harrison JA, Maranger RJ, Alexander RB, Giblin AE, Jacinthe PA, Mayorga E, Seitzinger SP, Sobota DJ, Wollheim WM (2009). The regional and global significance of nitrogen removal in lakes and reservoirs. Biogeochemistry 93, 143–157.

Harrison XA, Donaldson L, Correa-Cano ME, Evans J, Fisher DN, Goodwin CED, Robinson BS, Hodgson DJ, Inger R (2018). A brief introduction to mixed effects modelling and multi-model inference in ecology. PeerJ, 6, e4794.

Hartmann J, Dürr HH, Moosdorf N, Meybeck M, Kempe S (2012). The geochemical composition of the terrestrial surface (without soils) and comparison with the upper continental crust. Int J Earth Sci (Geol Rundsch) 101:365–376.

Hartmann J, Jansen N, Dürr HH, Harashima A, Okubo K, Kempe S (2010). Predicting riverine dissolved silica fluxes to coastal zones from a hyperactive region and analysis of their first-order controls. Int J Earth Sci (Geol Rundsch), 99:207–230.

Hartmann J, Moosdorf N (2012). The new global lithological map database GLiM: A representation of rock properties at the Earth surface. Geochemistry, Geophysics, Geosystems, 13, Q12004.

Hill AR (1981). Stream phosphorus exports from watersheds with contrasting land uses in southern Ontario. Water Resources Bulletin 17, 627–634.

Hodson MJ, White PJ, Mead A, Broadley MR (2005). Phylogenetic variation in the silicon composition of plants. Ann. Bot. 96, 1027– 1046.

Holzmann H, Lehmann T, Formayer H, Haas P (2008). Auswirkungen möglicher Änderungen der Schnee-, Regenanteile in Hinblick auf die Abflussbildung – Klimaänderung. Flood Risk II Vertiefung und Vernetzung zukunftsweisender Umsetzungsstrategien zum integrierten Hochwasserschutz. i.A. Bundesministerium für Land- und Forstwirtschaft, Umwelt und Wasserwirtschaft & Bundesministerium für Verkehr, Innovation und Technologie (117 pp).

Houlton B, Morford S, Dahlgren R (2018). Convergent evidence for widespread rock nitrogen sources in Earth's surface environment. Science, 360(6384), 58-62.

Howarth RW, Chan F, Conley DJ, Garnier J, Doney SC, Marino R and Billen G (2011). Coupled biogeochemical cycles: eutrophication and hypoxia in temperate estuaries and coastal Marine ecosystems. Front Ecol Environ 9(1): 18–26.

Howarth RW, Marino R, Lane J and Cole JJ (1998). Nitrogen fixation in freshwater, estuarine, and marine ecosystems. 1. Rates and importance. Limnol. Oceanogr. vol 33, pp 669-687.

Humborg C, Blomquist S, Avsan E, Bergensund Y, Smedberg E, Brink J, Morth CM (2002). Hydrological alterations with river damming in northern Sweden: Implications for weathering and river biochemistry. Global Biogeochemical Cycles, 16.

Humborg C, Conley DJ, Rahm L, Wulff F, Cociasu A, Ittekkot V (2000). Silicon Retention in River Basins: Far-reaching Effects on Biogeochemistry and Aquatic Food Webs in Coastal Marine Environments. Journal of the Human Environment, 29(1):45-50.

Humborg C, Ittekkot V, Cociasu A, Bodungen B (1997). Effect of Danube River dam on Black Sea biogeochemistry and ecosystem structure. Nature, Vol 386.

Humborg C, Pastuszak M, Aigars J, Siegmund H, Mörth CM, Ittekkot V (2006). Decreased silica land-sea fluxes through damming in the Baltic Sea catchment-significance of particle trapping and hydrological alterations. Biogeochemistry, 77(2), 265-281.

Humborg C, Smedberg E, Blomqvist S, Mörth CM, Brink J, Rahm L, Danielsson A, Sahlberg J. (2004). Nutrient variations in boreal and subarctic Swedish rivers: Landscape control of land–sea fluxes. Limnol. Oceanogr., 49 (5), 1871–1883.

Humborg C, Smedberg E, Medina MR, Mörth CM (2008). Changes in dissolved silicate loads to the Baltic Sea - the effects of lakes and reservoirs. Journal of Marine Systems, 73(3-4), 223-235.

ICPDR (2015). The Danube River Basin District Management Plan: Part A – Basin-wide overview.

ICPDR (2005). The Danube River Basin District WFD Roof Report.

ICPDR (2015). The update of the Danube Basin Analysis Report.

ICPDR (2017). Water quality in the Danube River Basin, TNMN yearbook report.

Irvine K, Weigelhofer G, Popescu I, Pfeiffer E, Păun A, Drobot R, Gettel G, Staska B, Stanica A, Hein T, Habersack H (2016). Educating for action: Aligning skills with policies for sustainable development in the Danube river basin. Sci. Total Environ. 543, 765–777.

Isles PDF (2020). The misuse of ratios in ecological stoichiometry. Ecology 101: e03153.

Jansen N, Hartmann J, Lauerwald R, Dürr HH, Kempe S, Loos S, Middelkoop H. (2010). Dissolved silica mobilization in the conterminous USA. Chemical Geology, 270(1-4), 90-109.

Johnson LB, Richards C, Host GE, Arthur JW (1997). Landscape influences on water chemistry in Midwestern stream ecosystems. Freshwater Biology 37, 193–208.

Keller C, Guntzer F, Barboni D, Labreuche J, Meunier JD (2012). Impact of agriculture on the Si biogeochemical cycle: input from phytolith studies. C. R. Geoscience 344, 739–746.

Kroiss H, Zessner M, Lampert C (2006). daNUbs: Lessons learned for nutrient management in the Danube Basin and its relation to Black Sea eutrophication. Chem Ecol 22:347–357.

Le TPQ, Billen G, Garnier J, Théry S, Ruelland D, Nghiem XA, Chau VM (2010). Nutrient (N, P, Si) transfers in the subtropical Red River system (China and Vietnam): modelling and budget of nutrient sources and sinks. Asian Earth Sci 37:259–274.

Lehner B, Grill G (2013). Global river hydrography and network routing: baseline data and new approaches to study the world’s large river systems. Hydrological Processes, 27(15): 2171–2186. Data is available at www.hydrosheds.org.

Lehner B, Liermann CR, Revenga C, Vörösmarty C, Fekete B, Crouzet P, Doll P, Endejan M, Frenken K, Magome J, Nilsson C, Robertson JC, Rodel R, Sindorf N, Wisser D (2011). High-resolution mapping of the world’s reservoirs and dams for sustainable river-flow manage-ment. Front. Ecol. Environ. 9, 494–502.

Liska I (2015). Managing an international river basin towards water quality protection: the Danube case. The Danube River Basin, 1-19.

Lovett GM, Burns DA, Driscoll CT, Jenkins JC, Mitchell MJ, Rustad L, Shanley JB, Likens GE, Haeuber R (2007). Who needs environmental monitoring?. Frontiers in Ecology and the Environment, 5(5), 253-260.

LfU-Bayern (2020). Bayrisches Landesamt für Umwelt, Gewässerkundlicher Dienst Bayern, Discharge data Bavaria, https://www.gkd.bayern.de/en/rivers/discharge, (access date: 2020-07-14).

Ludwig W, Dumont E, Meybeck M, Heussner S (2009). River discharges of water and nutrients to the Mediterranean and Black Sea: major drivers for ecosystem changes during past and future decades?. Progress in oceanography, 80(3-4), 199-217.

Lynam CP, Llope M, Möllmann C, Helaouët P, Bayliss-Brown GA, Stenseth NC (2017). Interaction between top-down and bottom-up control in marine food webs. Proceedings of the National Academy of Sciences: 201621037.

Lynn SG, Kilham SS, Kreeger DA, Interlandi SJ (2000). Effect of nutrient availability on the biochemical and elemental stoichiometry in the freshwater diatom Stephanodiscus minutulus (Bacillariophyceae). Journal of Phycology, 36(3), 510-522.

Maavara T, Akbarzadeh Z, Van Cappellen, P (2020a). Global dam-driven changes to riverine N: P: Si ratios delivered to the coastal ocean. Geophysical Research Letters, 47(15).

Maavara T, Chen Q, Van Meter K, Brown LE, Zhang J, Ni J, Zarfl C (2020b). River dam impacts on biogeochemical cycling. Nature Reviews Earth & Environment, 1, 103-116.

Maavara T, Dürr HH, Van Cappellen P (2014). Worldwide retention of nutrient silicon by river damming: From sparse data set to global estimate, Global Biogeochem. Cycles, 28, 842–855, doi:10.1002/ 2014GB004875.

Maavara T, Parsons CT, Ridenour C, Stojanovic S, Dürr HH, Powley HR, Van Cappellena P (2015) Global phosphorus retention by river damming. PNAS first published December 7.

Maguire TJ, Fulweiler RW (2016). Urban Dissolved Silica: Quantifying the Role of Groundwater and Runoff in Wastewater Influent. Environ. Sci. Technol. 50, 1, 54–61.

Maranger R, Jones SE, Cotner JB (2018). Stoichiometry of carbon, nitrogen, and phosphorus through the freshwater pipe. Limnology and Oceanography Letters 3, 89-101.

Matichenkov VV, Bocharnikova EA (2001). The relationship between silicon and soil physical and chemical properties. In: Datnoff LE, Snyder GH, Korndorfer GH (eds) Silicon in agriculture. Studies in plant science, 8. Elsevier, Amsterdam, pp 209–219.

McNaughton SJ, Tarrants JL, McNaughton MM, Davis RD (1985). Silica as a Defense against Herbivory and a Growth Promotor in African Grasses. Ecology, 66 (1985), pp. 528-535.

Melzer SE, Knapp AK, Kirkman KP, Smith MD, Blair JM, Kelly EF (2010). Fire and grazing impacts on silica production and storage in grass dominated ecosystems. Biogeochemistry 97:263–278.

Morée, A. L., Beusen, A. H. W., Bouwman, A. F., & Willems, W. J. (2013). Exploring global nitrogen and phosphorus flows in urban wastes during the twentieth century. Global biogeochemical cycles, 27(3), 836-846.

Nelson DM, Tréguer P, Brzezinski MA, Leynaert A., Queguiner B (1995). Production and dissolution of biogenic silica in the ocean: revised global estimates, comparison with regional data and relationship to biogenic sedimentation. Global Biogeochem. Cycl. 9:359–72.

Onderka M, Wrede S, Rodny M, Pfister L, Hoffmann L, Krein A (2012). Hydrogeologic and landscape controls of dissolved inorganic nitrogen (DIN) and dissolved silica (DSi) fluxes in heterogeneous catchments. Journal of Hydrology 450–451 36–47.

Oosterberg W, Staras M, Buijse AD, Bogdan L, Coops H, Constantinescu A, Ibelings BW, Hanganu J, Menting GAM, Navodaru I, Török L (2000). Ecological gradients in the Danube Delta lakes. Present state and man-induced changes. RIZA rapport 2000.015. Lelystad: RIZA. ISBN 903695309x, 167p.

Osborne LL and Wiley MJ (1988). Empirical relationships between land-use cover and stream water-quality in an agricultural watershed. Journal of Environmental Management 26, 9–27.

Paerl HW, Fulton RS, Moisander PH, Dyble J (2001). Harmful freshwater algal blooms, with an emphasis on cyanobacteria. The Scientific World Journal 1, 76-113.

Pardé M (1933). Fleuves et rivières. In: Revue de géographie alpine, tome 21, n°4, 1933. pp. 851-854.

Parsons ML, Dortch Q, Turner RE (2002). Sedimentological evidence of an increase in Pseudo-nitzschia (Bacillariophyceae) abundance in response to coastal eutrophication. Limnology and Oceanography, 47(2), 551-558.

Pinardi M, Soana E, Laini A, Bresciani M, Bartoli M (2018). Soil system budgets of N, Si and P in an agricultural irrigated watershed: surplus, differential export and underlying mechanisms. Biogeochemistry 140: 175–197.

Popa A (1993). Liquid and sediment inputs of the Danube River into the north-western Black Sea. Mitt. Geol.-Paläontol. Inst. Univ. Hamburg 74, 137–149.

Popovici M (2014). Nutrient Management in the Danube River Basin. In: Liska I. (eds) The Danube River Basin. The Handbook of Environmental Chemistry, vol 39. Springer, Berlin, Heidelberg.

Ptacnik R, Andersen T and Tamminen T (2010). Performance of the Redfield Ratio and a Family of Nutrient Limitation Indicators as Thresholds for Phytoplankton N vs. P Limitation Ecosystems vol 13, pp 1201–121.

R Core Team (2019). R: A language and environment for statistical computing. R Foundation for Statistical Computing, Vienna, Austria. URL https://www.R-project.org/.

R Studio Team (2015). RStudio: Integrated Development for R. RStudio, Inc., Boston, MA URL http://www.rstudio.com/.

Redfield AC (1958). The biological control of chemical factors in the environment. Am. Sci. vol 46, pp 205-221.

Ritchie H, Roser M, Rosado P (2022). "Fertilizers". Published online at OurWorldInData.org. Retrieved from: 'https://ourworldindata.org/fertilizers' (Online Resource).

Royer TV (2020). Stoichiometry of nitrogen, phosphorus, and silica loads in the Mississippi-Atchafalaya River basin reveals spatial and temporal patterns in risk for cyanobacterial blooms. Limnology and Oceanography, 65(2), 325-335.

Ryalls JMW, Moore BD, Johnson SN (2018). Silicon uptake by a pasture grass experiencing simulated grazing is greatest under elevated precipitation. BMC Ecology, 18, 53.

Scanlon TM, Raffensperger JP, Hornberger GM (2001). Modeling transport of dissolved silica in a forested headwater catchment: Implications for defining the hydrochemical response of observed flow pathways. Water Resources Research, 37(4), 1071-1082.

Schindler DW (1977). Evolution of phosphorus limitation in lakes. Sciences 195: 260-262.

Schueler T (2003). Impacts of Impervious Cover on Aquatic Systems. Center for Watershed Protection. Ellicott City, MD.

Seilheimer TS, Zimmerman PL, Stuevea KM, Perry CH (2013). Landscape-scale modeling of water quality in Lake Superior and Lake Michigan watersheds: How useful are forest-based indicators?. Journal of Great Lakes Research: volume 39, Issue 2, June 2013, Pages 211-223

Sethna LR, Royer TV, Speir SL, Trentman MT, Mahl UH, Hagemeier LP, Tank JL (2022). Silicon concentrations and stoichiometry in two agricultural watersheds: implications for management and downstream water quality. Biogeochemistry, 159 (2), 265-282.

Sferratore A, Billen G, Garnier J, Théry S (2005). Modeling nutrient (N, P, Si) budget in the Seine watershed: Application of the Riverstrahler model using data from local to global scale resolution. Global biogeochemical cycles, 19(4).

Sferratore A, Garnier J, Billen G, Conley DJ, Pinault S (2006). Diffuse and point sources of silica in the Seine River watershed. Environmental Science & Technology, 40: 6630–6635.

Sliva L and Williams DD (2001). Buffer zone versus whole catchment approaches to studying land use impact on river water quality. Water Research 35, 3462–3472.

Smart RP, Soulsby C, Neal C, Wade A, Cresser MS, Billett MF, Langan SJ, Edwards AC, Jarvie HP and Owen R (1998). Factors regulating the spatial and temporal distribution of solute concentrations in a major river system in NE Scotland. The Science of the Total Environment 221, 93–110.

Smetacek, V. (1999). Diatoms and the ocean carbon cycle. Protist, 150(1), 25-32.

Smil V (2000). Phosphorus in the environment: natural flows and human interferences. Ann Rev Energy Environ 25:53–88.

Stancik A, Jovanovic S, Sikora A, Urge L, Miklos D (1988). Hydrology of the River Danube – Publishing House Príroda, Bratislava, 271 pp.

Strokal M, Kroeze C (2013). Nitrogen and phosphorus inputs to Black Sea in 1970 – 2050. Reg Environ Change 13:179–192.

Struyf E, Conley DJ (2012). Emerging understanding of the ecosystem silica filter. Biogeochemistry 107(1):9-18.

Struyf E, Smis A, Van Damme S, Garnier J, Govers G, Van Wesemael B, Conley DJ, Batelaan O, Frot E, Clymans W, Vandevenne F, Lancelot C, Goos P, Meire P (2010). Historical land use change has lowered terrestrial silica mobilization (to the North Sea and the Scheldt Estuary). Nature Communications vol 1: pp 129.

Struyf E, Smis A, Van Damme S, Meire P, Conley DJ (2009). The global biogeochemical silicon cycle. Silicon, 1(4), 207-213.

Syvitski JPM, Vörosmarty CH, Kettner AJ, Green P (2005). Impact of Humans on the Flux of Terrestrial Sediment to the Global Coastal Ocean. Science, 308, 376.

Teodoru C, Dimopoulos A, Wehrli B (2006). Biogenic silica accumulation in the sediments of Iron Gate I Reservoir on the Danube River. Aquat. Sci. 68; 469 - 481.

Tiberti R, Tartari GA, Marchetto A (2010). Geomorphology and hydrochemistry of 12 Alpine lakes in the Gran Paradiso National Park, Italy. J. Limnol., 69(2): 242-256.

Tranter M, Sharp MJ, Lamb HR, Brown GH, Hubbard B P, Willis IC (2002). Geochemical weathering at the bed of Haut Glacier d'Arolla, Switzerland—a new model. Hydrol. Process. 16, 959–993.

Turner RE and Rabalais NN (2003). Linking landscape and water quality in the Mississippi River Basin for 200 years. Bioscience 53, 563–572.

Vandevenne FI, Barao AL, Schoelynck J, Smis A, Ryken N, Van Damme S, Meire P, Struyf E (2013). Grazers: biocatalysts of terrestrial silica cycling. Proceedings of the Royal Society B: Biological Sciences, 280(1772), 20132083.

Vandevenne F, Struyf E, Clymans W, Meire P (2012). Agricultural silica harvest: Have humans created a new loop in the global Silica cycle? Front Ecol Environ.10:243-248.

Vanni MJ, Renwick WH, Bowling AM, Horgan ML and Christian AD (2011). Nutrient stoichiometry of linked catchment-lake systems along a gradient of land use. Freshw. Biol. 56: 791–811.

Venohr M, Hirt U, Hofmann J, Opitz D, Gericke A, Wetzig A, Natho S, Neumann F, Hürdler J, Matranga M, Mahnkopf J, Gadegast M, Behrendt H (2011). Modelling of Nutrient Emissions in River Systems - MONERIS - Methods and Background. International Review of Hydrobiology, 96(5) 435-483.

Vilmin L, Mogollón JM, Beusen AHW, Bouwman AF (2018). Forms and subannual variability of nitrogen and phosphorus loading to global river networks over the 20th century. Global and Planetary Change 163, 67–85.

Vitousek PM, Aber JD, Howarth RW, Likens GE, Matson PA, Schindler DW, Schlesinger WH, Tilman DG (1997). Technical report: human alteration of the global nitrogen cycle: sources and consequences. Ecol Appl 7:737–750

Vörosmarty CJ, Meybeck M, Fekete B, Sharma K, Green P, Syvitski J (2003). Anthropogenic sediment retention: major global impact from registered river impoundment. Global and Planetary Change vol 39, pp 169–190.

Vörösmarty C, Lettenmaier D, Leveque C, Meybeck M, Pahl-Wostl C, Alcamo J, Cosgrove W, Grassl H, Hofe H, Kabat P, Lansigan F, Lawford R, Naiman R. (2004).

Humans transforming the global water system. Eos, Transactions American Geophysical Union, 85(48), 509-514.

World Wide Fund for Nature (WWF) (2002). Waterway Transport on Europe’s Lifeline, the Danube.

Wedepohl KH (1995). The composition of the continental crust. Geochimica et Cosmochimica Acta, Vol 59, pp 1217–1232.

Wetzel RG (2001). Limnology: Lake and River Ecosystems. Third edition. pp 1006.

Wilding LP, Drees LR (1974). Contributions of forest opal and associated crystalline phases to fine silt and clay fractions of soils. Clays and Clay Minerals 22: 295–306.

Zarfl C, Lumsdon AE, Berlekamp J, Tydecks L, Tockner K (2015). A global boom in hydropower dam construction. Aquatic Sciences, 77(1), 161-170.

Zinke A (1999). Dams and the Danube: Lessons from the Environmental Impact. World Commission on Dams, 26 March 1999, Prague. Published at: www.dams.org.

Zuur AF, Ieno EN, Smith GM (2007). Analysing ecological data. In: Gail, M., Krickeberg, K., Samet, J.M., Tsiatis, A., Wong, W. (Eds.), Statistics for Biology and Health. Springer Science and Business Media, New York, 672 p.

Zuur AF, Ieno EN, Walker NJ, Saveliev AA, Smith GM (2009). Mixed effects models and extensions in ecology with R. In: Gail, M., Krickeberg, K., Samet, J.M., Tsiatis, A., Wong, W. (Eds.), Statistics for Biology and Health. Springer Science and Business Media, New York, 574 p.

APPENDIXES

Appendix 1: Table showing the landscape variables used in regression analyses for each site, including elevation, catchment area and LULC classifications and % for each sampling site.

Code	River	Elevation (m)	Area km²	Land use and land cover types									
				Agriculture	**Artificial**	**Bare rock**	**Coniferous Forest**	**Deciduous Forest**	**Glacier**	**Grasslands**	**Sparse vegetation**	**Water Bodies**	**Wetlands**
IN1	Salzach	2030	10	0%	0%	71%	0%	0%	14%	6%	10%	0%	0%
IN2	Salzach	2030	1	0%	0%	73%	0%	0%	0%	27%	0%	0%	0%
IN3	Salzach	2030	3.2	0%	0%	57%	0%	0%	13%	30%	0%	0%	0%
IN4	Salzach	2257	1.2	0%	0%	61%	0%	0%	25%	0%	14%	0%	0%
IN5	Salzach	2257	1.3	0%	0%	73%	0%	0%	17%	0%	10%	0%	0%
IN6	Salzach	1463	12	0%	0%	38%	4%	0%	11%	14%	29%	4%	0%
IN7	Salzach	1463	1.8	1%	0%	0%	22%	0%	0%	45%	31%	1%	0%
IN8	Salzach	1463	23	0%	0%	56%	3%	0%	11%	18%	5%	8%	0%
IN9	Salzach	1463	0.2	0%	0%	0%	95%	0%	0%	5%	0%	0%	0%
IN10	Salzach	2024	0.3	0%	0%	44%	0%	0%	0%	22%	0%	34%	0%
IN11	Salzach	2024	2.7	0%	0%	80%	0%	0%	18%	0%	0%	2%	0%
IN12	Salzach	859	72	0%	1%	31%	10%	6%	13%	30%	6%	4%	0%
IN13	Salzach	859	0.9	0%	0%	0%	37%	6%	0%	27%	30%	0%	0%
IN14	Inn	1780	21	0%	0%	36%	0%	0%	26%	15%	22%	0%	0%
IN15	Inn	1780	21	0%	0%	36%	0%	0%	26%	15%	22%	0%	0%
IN16	Inn	1780	0.6	0%	0%	35%	0%	0%	0%	4%	57%	5%	0%
IN17	Inn	1780	0.6	0%	0%	35%	0%	0%	0%	4%	57%	5%	0%
IN18	Inn	1780	0.9	0%	0%	0%	0%	0%	0%	40%	47%	14%	0%
IN19	Inn	1780	0.9	0%	0%	0%	0%	0%	0%	40%	47%	14%	0%
IN20	Inn	1780	24	0%	0%	32%	1%	0%	9%	20%	38%	0%	0%
IN21	Inn	1780	24	0%	0%	32%	1%	0%	9%	20%	38%	0%	0%
IN22	Inn	1780	2.1	0%	0%	26%	9%	0%	0%	13%	50%	3%	0%
IN23	Inn	1780	2.1	0%	0%	26%	9%	0%	0%	13%	50%	3%	0%
IN24	Inn	1780	0.7	0%	0%	0%	28%	0%	0%	43%	13%	17%	0%
IN25	Inn	1140	51	0%	0%	39%	19%	0%	2%	21%	19%	0%	0%
IN26	Inn	1140	51	0%	0%	39%	19%	0%	2%	21%	19%	0%	0%
IN27	Inn	1140	4	0%	0%	29%	16%	0%	0%	53%	2%	0%	0%
IN28	Inn	1140	0.8	0%	0%	0%	55%	0%	0%	45%	0%	0%	0%

IN29	Inn	1140	0.5	0%	0%	0%	64%	0%	0%	35%	0%	1%	0%
IN30	Inn	1140	0.5	0%	0%	0%	64%	0%	0%	35%	0%	1%	0%
IN31	Inn	1870	2.1	0%	0%	56%	0%	0%	7%	16%	20%	0%	0%
IN32	Inn	1870	2.2	0%	0%	54%	0%	0%	26%	3%	17%	1%	0%
IN33	Inn	1870	5.1	0%	0%	66%	0%	0%	16%	0%	18%	0%	0%
IN34	Inn	1870	0.4	0%	0%	33%	0%	0%	0%	0%	66%	1%	0%
IN35	Inn	1870	0.4	0%	0%	34%	0%	0%	0%	0%	66%	0%	0%
IN36	Inn	1870	2.7	0%	0%	67%	0%	0%	0%	0%	33%	0%	0%
IN37	Inn	1870	11.3	0%	0%	62%	0%	0%	3%	0%	35%	0%	0%
IN38	Inn	1405	28	0%	0%	33%	14%	0%	7%	19%	27%	0%	0%
IN39	Inn	1405	28	0%	0%	33%	14%	0%	7%	19%	27%	0%	0%
IN40	Inn	1405	0.8	0%	0%	0%	84%	0%	0%	15%	0%	0%	0%
IN41	Inn	1405	0.7	0%	0%	0%	76%	0%	0%	24%	0%	0%	0%
IN42	Inn	1405	0.8	0%	0%	0%	44%	0%	0%	54%	0%	2%	0%
IN43	Inn	1405	0.8	0%	0%	0%	44%	0%	0%	54%	0%	2%	0%
IN44	Inn	1405	1.4	0%	2%	0%	34%	0%	0%	63%	0%	0%	0%
IN45	Inn	1405	1.4	0%	2%	0%	34%	0%	0%	63%	0%	0%	0%
IN46	Inn	1405	1.2	0%	0%	0%	50%	0%	0%	50%	0%	0%	0%
IN47	Inn	1405	1.2	0%	0%	0%	50%	0%	0%	50%	0%	0%	0%
IN48	Inn	1202	0.6	0%	0%	0%	74%	0%	0%	26%	0%	0%	0%
IN49	Inn	1202	142	0%	1%	12%	29%	0%	2%	40%	13%	1%	0%
IN50	Inn	1202	0.6	0%	0%	0%	74%	0%	0%	26%	0%	0%	0%
RE1	Salzach	2030	23	0%	0%	64%	0%	0%	13%	9%	6%	7%	0%
RE2	Salzach	2257	4.8	0%	0%	54%	0%	0%	28%	0%	12%	7%	0%
RE3	Salzach	1463	39	1%	0%	46%	6%	0%	10%	17%	14%	6%	0%
RE4	Salzach	1670	40	0%	0%	44%	0%	0%	20%	22%	7%	7%	0%
RE5	Salzach	2024	22	0%	0%	47%	0%	0%	32%	6%	8%	7%	0%
RE6	Salzach	859	74	0%	1%	31%	10%	6%	12%	30%	6%	4%	0%
RE7	Inn	1780	58	0%	0%	30%	2%	0%	13%	17%	34%	4%	0%
RE8	Inn	1780	58	0%	0%	30%	2%	0%	13%	17%	34%	4%	0%
RE9	Inn	1140	61	0%	0%	35%	22%	0%	2%	22%	18%	1%	0%
RE10	Inn	1405	45	0%	1%	22%	25%	0%	5%	26%	17%	4%	0%
RE11	Inn	1202	145	0%	1%	12%	30%	0%	2%	40%	13%	1%	0%
RRH1	Lech	780	1,609	1%	3%	7%	26%	6%	0%	30%	24%	2%	0%
RRH2	Lech	780	1,609	1%	3%	7%	26%	6%	0%	30%	24%	2%	0%
RRH3	Lech	743	1,703	2%	2%	7%	27%	6%	0%	29%	24%	2%	0%

RRH4	Lech	728	1,713	2%	2%	7%	27%	6%	0%	29%	24%	2%	0%
RRH5	Lech	722	1,771	2%	2%	7%	26%	6%	0%	31%	24%	2%	0%
RRH6	Lech	712	1,863	3%	2%	6%	27%	6%	0%	32%	22%	2%	1%
RRH7	Lech	694	1,903	3%	2%	6%	26%	6%	0%	32%	22%	2%	1%
RRH8	Lech	462	2,738	12%	5%	4%	24%	7%	0%	30%	15%	2%	1%
RRH9	Lech	457	4,032	17%	6%	3%	22%	5%	0%	34%	11%	1%	1%
RRH10	Lech	425	4,432	22%	6%	3%	21%	5%	0%	31%	10%	1%	1%
RRH11	Lech	415	4,451	22%	6%	3%	21%	5%	0%	31%	10%	1%	1%
RRH12	Lech	406	4,472	22%	6%	3%	21%	5%	0%	31%	10%	1%	1%
RRH13	Lech	398	4,479	22%	6%	3%	21%	5%	0%	31%	10%	1%	1%
RRH14	Inn	442	11,397	2%	3%	13%	27%	6%	2%	29%	16%	1%	0%
RRH15	Inn	431	12,084	3%	3%	12%	27%	7%	2%	30%	16%	1%	0%
RRH16	Inn	422	12,157	3%	3%	12%	27%	7%	2%	30%	15%	1%	0%
RRH17	Inn	415	12,310	4%	3%	12%	27%	7%	2%	30%	15%	1%	0%
RRH18	Inn	403	12,374	4%	3%	12%	27%	7%	2%	30%	15%	1%	0%
RRH19	Inn	398	12,616	5%	3%	12%	26%	7%	2%	29%	15%	1%	0%
RRH20	Inn	369	12,616	5%	3%	12%	26%	7%	2%	29%	15%	1%	0%
RRH21	Inn	350	23,000	9%	3%	9%	26%	10%	1%	29%	11%	1%	0%
RRH22	Inn	336	23,609	9%	4%	8%	26%	10%	1%	29%	10%	1%	0%
RRH23	Inn	326	24,069	10%	4%	8%	26%	10%	1%	28%	10%	1%	0%
RRH24	Inn	314	25,380	14%	4%	8%	26%	10%	1%	27%	9%	1%	0%
RRH25	Inn	302	26,253	15%	4%	8%	25%	10%	1%	27%	9%	1%	0%
RRH26	Inn	300	26,253	15%	4%	8%	25%	10%	1%	27%	9%	1%	0%

Appendix 2: Table showing the percentage of lithological classes used in regression analyses for each site for each sampling site.

Code	River	Lithological classes						
		Acid plutonic	Acid volcanic	Basic plutonic	Basic volcanic	Carbonate	Metamorphic rock	Mix sedimentary rock
IN1	Salzach	68.4%	0.0%	0.0%	0.0%	0.0%	31.6%	0.0%
IN2	Salzach	8.2%	0.0%	0.0%	0.0%	0.0%	91.8%	0.0%
IN3	Salzach	3.3%	0.0%	0.0%	0.0%	0.0%	96.7%	0.0%
IN4	Salzach	100.0%	0.0%	0.0%	0.0%	0.0%	0.0%	0.0%
IN5	Salzach	100.0%	0.0%	0.0%	0.0%	0.0%	0.0%	0.0%
IN6	Salzach	100.0%	0.0%	0.0%	0.0%	0.0%	0.0%	0.0%
IN7	Salzach	100.0%	0.0%	0.0%	0.0%	0.0%	0.0%	0.0%
IN8	Salzach	57.3%	0.0%	0.0%	0.0%	0.0%	42.7%	0.0%
IN9	Salzach	25.8%	0.0%	0.0%	0.0%	0.0%	74.2%	0.0%
IN10	Salzach	0.0%	0.0%	0.0%	0.0%	0.0%	100.0%	0.0%
IN11	Salzach	0.0%	0.0%	0.0%	0.0%	0.0%	100.0%	0.0%
IN12	Salzach	0.0%	0.0%	0.0%	0.0%	0.1%	99.9%	0.0%
IN13	Salzach	0.0%	0.0%	0.0%	0.0%	72.8%	27.2%	0.0%
IN14	Inn	46.6%	0.0%	0.0%	0.0%	9.7%	43.7%	0.0%
IN15	Inn	46.6%	0.0%	0.0%	0.0%	9.7%	43.7%	0.0%
IN16	Inn	23.6%	0.0%	0.0%	0.0%	0.0%	76.4%	0.0%
IN17	Inn	23.6%	0.0%	0.0%	0.0%	0.0%	76.4%	0.0%
IN18	Inn	0.0%	0.0%	0.0%	0.0%	0.0%	100.0%	0.0%
IN19	Inn	0.0%	0.0%	0.0%	0.0%	0.0%	100.0%	0.0%
IN20	Inn	81.8%	0.0%	0.0%	0.0%	2.9%	15.3%	0.0%
IN21	Inn	81.8%	0.0%	0.0%	0.0%	2.9%	15.3%	0.0%
IN22	Inn	100.0%	0.0%	0.0%	0.0%	0.0%	0.0%	0.0%
IN23	Inn	100.0%	0.0%	0.0%	0.0%	0.0%	0.0%	0.0%

IN24	Inn	100.0%	0.0%	0.0%	0.0%	0.0%	0.0%	0.0%
IN25	Inn	81.1%	0.0%	0.0%	0.0%	0.0%	18.9%	0.0%
IN26	Inn	81.1%	0.0%	0.0%	0.0%	0.0%	18.9%	0.0%
IN27	Inn	65.2%	0.0%	0.0%	0.0%	0.0%	34.8%	0.0%
IN28	Inn	8.5%	0.0%	0.0%	0.0%	0.0%	91.5%	0.0%
IN29	Inn	0.0%	0.0%	0.0%	0.0%	0.0%	100.0%	0.0%
IN30	Inn	0.0%	0.0%	0.0%	0.0%	0.0%	100.0%	0.0%
IN31	Inn	100.0%	0.0%	0.0%	0.0%	0.0%	0.0%	0.0%
IN32	Inn	100.0%	0.0%	0.0%	0.0%	0.0%	0.0%	0.0%
IN33	Inn	100.0%	0.0%	0.0%	0.0%	0.0%	0.0%	0.0%
IN34	Inn	100.0%	0.0%	0.0%	0.0%	0.0%	0.0%	0.0%
IN35	Inn	100.0%	0.0%	0.0%	0.0%	0.0%	0.0%	0.0%
IN36	Inn	100.0%	0.0%	0.0%	0.0%	0.0%	0.0%	0.0%
IN37	Inn	100.0%	0.0%	0.0%	0.0%	0.0%	0.0%	0.0%
IN38	Inn	85.0%	0.0%	0.0%	0.0%	8.8%	6.2%	0.0%
IN39	Inn	85.0%	0.0%	0.0%	0.0%	8.8%	6.2%	0.0%
IN40	Inn	0.0%	0.0%	0.0%	0.0%	23.8%	76.2%	0.0%
IN41	Inn	0.0%	0.0%	0.0%	0.0%	0.0%	100.0%	0.0%
IN42	Inn	0.0%	0.0%	0.0%	0.0%	0.0%	100.0%	0.0%
IN43	Inn	0.0%	0.0%	0.0%	0.0%	0.0%	100.0%	0.0%
IN44	Inn	0.0%	0.0%	0.0%	0.0%	0.3%	99.7%	0.0%
IN45	Inn	0.0%	0.0%	0.0%	0.0%	0.3%	99.7%	0.0%
IN46	Inn	0.0%	0.0%	0.0%	0.0%	0.0%	100.0%	0.0%
IN47	Inn	0.0%	0.0%	0.0%	0.0%	0.0%	100.0%	0.0%
IN48	Inn	0.0%	0.0%	0.0%	0.0%	100.0%	0.0%	0.0%
IN49	Inn	26.2%	0.0%	0.0%	0.0%	14.9%	58.9%	0.0%
IN50	Inn	0.0%	0.0%	0.0%	0.0%	100.0%	0.0%	0.0%
RE1	Salzach	57.9%	0.0%	0.0%	0.0%	0.0%	42.1%	0.0%
RE2	Salzach	100.0%	0.0%	0.0%	0.0%	0.0%	0.0%	0.0%

RE3	Salzach	73.6%	0.0%	0.0%	0.0%	0.0%	26.4%	0.0%
RE4	Salzach	0.0%	0.0%	0.0%	0.0%	0.0%	100.0%	0.0%
RE5	Salzach	0.0%	0.0%	0.0%	0.0%	0.0%	100.0%	0.0%
RE6	Salzach	0.0%	0.0%	0.0%	0.0%	1.1%	98.9%	0.0%
RE7	Inn	67.7%	0.0%	0.0%	0.0%	4.9%	27.4%	0.0%
RE8	Inn	67.7%	0.0%	0.0%	0.0%	4.9%	27.4%	0.0%
RE9	Inn	77.3%	0.0%	0.0%	0.0%	0.0%	22.7%	0.0%
RE10	Inn	54.9%	0.0%	0.0%	0.0%	7.2%	37.9%	0.0%
RE11	Inn	25.9%	0.0%	0.0%	0.0%	16.1%	58.0%	0.0%
RRH1	Lech	0.0%	0.0%	0.0%	0.0%	87.8%	0.0%	4.5%
RRH2	Lech	0.0%	0.0%	0.0%	0.0%	87.8%	0.0%	4.5%
RRH3	Lech	0.0%	0.0%	0.0%	0.0%	84.4%	0.0%	7.6%
RRH4	Lech	0.0%	0.0%	0.0%	0.0%	83.9%	0.0%	7.7%
RRH5	Lech	0.0%	0.0%	0.0%	0.0%	81.1%	0.0%	8.9%
RRH6	Lech	0.0%	0.0%	0.0%	0.0%	77.1%	0.0%	10.3%
RRH7	Lech	0.0%	0.0%	0.0%	0.0%	75.5%	0.0%	10.8%
RRH8	Lech	0.0%	0.0%	0.0%	0.0%	52.5%	0.0%	10.3%
RRH9	Lech	0.0%	0.0%	0.0%	0.0%	36.6%	0.0%	14.5%
RRH10	Lech	0.0%	0.0%	0.0%	0.0%	33.3%	0.0%	16.5%
RRH11	Lech	0.0%	0.0%	0.0%	0.0%	33.1%	0.0%	16.5%
RRH12	Lech	0.0%	0.0%	0.0%	0.0%	33.0%	0.0%	16.4%
RRH13	Lech	0.0%	0.0%	0.0%	0.0%	32.9%	0.0%	16.4%
RRH14	Inn	4.9%	0.2%	0.4%	0.5%	29.7%	50.2%	2.9%
RRH15	Inn	4.6%	0.2%	0.4%	0.5%	28.0%	47.4%	3.0%
RRH16	Inn	4.6%	0.2%	0.4%	0.5%	27.9%	47.1%	3.0%
RRH17	Inn	4.6%	0.2%	0.4%	0.5%	27.5%	46.5%	2.9%
RRH18	Inn	4.5%	0.2%	0.4%	0.5%	27.4%	46.2%	3.0%
RRH19	Inn	4.4%	0.2%	0.4%	0.5%	26.8%	45.4%	3.3%
RRH20	Inn	4.4%	0.2%	0.4%	0.5%	26.8%	45.4%	3.3%

RRH21	Inn	4.6%	0.3%	0.2%	0.6%	29.5%	36.3%	8.7%
RRH22	Inn	4.5%	0.2%	0.2%	0.6%	28.9%	35.4%	10.9%
RRH23	Inn	4.4%	0.2%	0.2%	0.6%	28.3%	34.7%	12.5%
RRH24	Inn	4.2%	0.2%	0.2%	0.6%	26.9%	32.9%	16.2%
RRH25	Inn	4.1%	0.2%	0.2%	0.6%	26.0%	32.3%	18.3%
RRH26	Inn	4.1%	0.2%	0.2%	0.6%	26.0%	32.3%	18.3%

Appendix 3: Physical-chemical characteristics and nutrient concentrations and ratios for each of the sampling sites.

Code	River	Temp	DO	EC	pH	Flow	DCl	DOC	TDN-N	NO_3-N	NH_4-N	TDP-P	PO_4-P	DSi
		°C	mg/L	μs/cm		m^3/s	mg/L	mg/L	mg/L	mg/L	mg/L	μg/L	μg/L	mg/L
IN1	Salzach	8	10	22	8	0.49	1.25	0.22	0.21	0.18	0.003	9.35	5.00	0.59
IN2	Salzach	13	9	47	8	0.05	1.15	0.10	0.18	0.15	0.003	11.22	4.17	0.84
IN3	Salzach	13	7	56	8	0.16	1.22	0.25	0.12	0.12	0.003	5.34	4.46	1.07
IN4	Salzach	5	10	5	9	0.06	1.16	0.07	0.18	0.16	0.021	6.68	3.95	2.90
IN5	Salzach	5	10	16	9	0.07	1.31	0.06	0.25	0.25	0.003	6.15	3.13	0.85
IN6	Salzach	13	8	14	7	0.59	1.39	1.84	0.12	0.11	0.003	5.34	4.91	0.76
IN7	Salzach	6	11	37	7	0.09	1.23	0.70	0.18	0.18	0.003	9.09	4.02	1.48
IN8	Salzach	11	9	36	7	1.16	1.31	3.27	0.28	0.27	0.008	12.29	5.13	3.44
IN9	Salzach	11	9	62	7	0.01	1.25	2.33	0.14	0.12	0.003	10.96	5.00	3.05
IN10	Salzach	6	9	113	8	0.01	1.41	0.14	0.17	0.15	0.016	6.41	5.24	0.14
IN11	Salzach	6	9	118	8	0.14	1.18	0.12	0.14	0.13	0.003	4.28	3.71	0.57
IN12	Salzach	11	9	178	8	3.69	1.47	0.56	0.27	0.26	0.009	3.74	3.64	1.51
IN13	Salzach	16	8	349	8	0.05	1.53	0.43	0.50	0.49	0.010	5.61	3.43	3.83
IN14	Inn	9	10	39	8	0.91	1.18	0.03	0.27	0.26	0.003	6.68	2.25	0.79
IN15	Inn		10	68	8	0.48	1.58	3.45	0.26	0.24	0.005	5.50	1.72	0.96
IN16	Inn	9	10	11	8	0.03	1.22	0.16	0.20	0.19	0.013	5.34	5.15	0.70
IN17	Inn	16		31	8	0.01	1.07	0.46	0.20	0.17	0.030	4.80	0.97	1.65
IN18	Inn	9	10	168	8	0.04	1.17	0.09	0.27	0.23	0.003	7.48	3.61	2.01
IN19	Inn			300		0.02	1.02	0.53	0.28	0.25	0.032	6.92	0.47	1.82
IN20	Inn	11	9	26	8	1.07	1.17	0.12	0.27	0.18	0.003	7.75	7.12	0.87
IN21	Inn	9	9	31	8	0.56	1.17	0.78	0.27	0.24	0.026	4.66	2.50	0.61
IN22	Inn	11	9	14	8	0.09	1.19	0.49	0.15	0.12	0.003	6.95	6.48	1.24
IN23	Inn	9	9	16	8	0.05	1.18	2.18	0.22	0.18	0.038	4.03	1.47	0.59
IN24	Inn	8	10	71	8	0.03	1.79	0.57	0.20	0.18	0.011	6.95	5.43	1.19

IN25	Inn	7	12	12	7	1.74	1.22	0.67	0.26	0.26	0.003	5.34	5.20	1.28
IN26	Inn	10	9	22	8	1.21	1.07	0.75	0.25	0.22	0.030	5.12	1.94	0.93
IN27	Inn	6	11	10	8	0.14	1.18	1.01	0.09	0.09	0.003	4.63	4.50	0.70
IN28	Inn	7	11	31	7	0.03	1.17	2.36	0.12	0.04	0.005	5.88	2.92	2.40
IN29	Inn	8	11	42	7	0.02	1.17	2.05	0.12	0.08	0.006	3.74	3.45	1.67
IN30	Inn	12	8	83	8	0.01	1.07	1.85	0.15	0.09	0.033	4.92	0.84	2.21
IN31	Inn	4	11	8	8	0.06	1.18	0.32	0.11	0.11	0.003	2.85	2.82	0.89
IN32	Inn	5	10	16	7	0.07	1.25	0.47	0.13	0.12	0.003	6.15	6.02	0.76
IN33	Inn	5	11	15	7	0.15	1.18	0.26	0.14	0.13	0.003	2.60	2.60	1.11
IN34	Inn	5	10	10	7	0.01	1.19	0.37	0.18	0.18	0.003	4.10	4.08	1.20
IN35	Inn	5	11	6	7	0.01	1.18	1.00	0.16	0.11	0.003	3.38	3.38	0.50
IN36	Inn	5	10	13	7	0.08	1.17	0.28	0.12	0.11	0.003	2.14	2.06	0.95
IN37	Inn	5	11	15	7	0.34	1.19	0.23	0.18	0.18	0.003	5.88	4.64	1.17
IN38	Inn	9	10	28	8	0.91	1.25	0.86	0.24	0.18	0.005	5.99	5.98	1.90
IN39	Inn	8	7	39	8	0.63	1.06	0.94	0.21	0.18	0.029	6.27	1.86	1.61
IN40	Inn	9	10	74	8	0.02	1.24	0.46	0.18	0.13	0.003	10.42	5.09	5.46
IN41	Inn	14	9	149	8	0.02	1.40	0.47	0.12	0.11	0.003	4.81	4.71	4.20
IN42	Inn	14	9	47	8	0.03	1.39	1.04	0.14	0.06	0.032	10.15	8.41	4.25
IN43	Inn	8	7	299	8	0.02	1.32	0.84	0.19	0.14	0.050	8.16	1.38	2.76
IN44	Inn	14	9	151	8	0.04	1.40	0.66	0.13	0.10	0.003	9.09	4.86	4.22
IN45	Inn	8	7	288	8	0.03	1.56	1.13	0.32	0.30	0.023	7.90	1.16	2.74
IN46	Inn	16	9	124	8	0.04	5.55	1.31	0.28	0.16	0.020	11.22	3.24	2.88
IN47	Inn	8	7	273	8	0.03	1.47	1.20	0.14	0.11	0.031	7.13	0.22	2.59
IN48	Inn	10	7	34	7	0.01	1.15	12.71	0.19	0.03	0.010	10.56	3.84	2.72
IN49	Inn	11	10	59	8	4.49	1.47	3.60	0.25	0.13	0.016	12.29	12.25	1.83
IN50	Inn	12	10	22	7	0.02	1.39	18.32	0.33	0.02	0.012	12.56	11.62	3.93
RE1	Salzach	10	8	38	8	NA	1.38	0.81	0.27	0.18	0.019	9.79	4.84	1.10
RE2	Salzach	5	8	8	8	NA	1.20	0.22	0.23	0.20	0.020	9.22	4.43	0.47
RE3	Salzach	9	10	34	7	NA	1.26	1.21	0.18	0.17	0.009	13.15	4.90	1.68

RE4	Salzach	9	9	182	3	NA	1.28	0.29	0.21	0.18	0.019	3.79	3.08	0.72
RE5	Salzach	9	9	90	8	NA	1.28	0.51	0.20	0.17	0.020	4.10	2.89	0.65
RE6	Salzach	10	9	213	8	NA	1.73	0.28	0.36	0.35	0.008	4.65	3.19	1.60
RE7	Inn	10	10	25	8	NA	1.19	0.26	0.31	0.24	0.016	5.98	3.55	0.99
RE8	Inn	10	7	34	8	NA	1.09	0.41	0.21	0.18	0.025	4.95	1.23	0.66
RE9	Inn	8	16	17	7	NA	1.27	0.79	0.26	0.25	0.007	5.26	4.93	1.56
RE10	Inn	14	8	51	8	NA	1.67	0.84	0.21	0.15	0.013	7.56	5.33	2.00
RE11	Inn	11	10	73	8	NA	1.69	3.23	0.27	0.15	0.037	12.88	9.74	1.92
RRH1	Lech	18	9	272	8	58.67	3.52	1.14	0.40	0.32	0.030	6.31	5.35	1.33
RRH2	Lech	19	9	303	8	34.22	3.52	1.38	0.28	0.23	0.019	4.89	1.34	0.68
RRH3	Lech	18	9	273	8	62.10	2.88	0.89	0.44	0.37	0.014	5.34	5.26	1.54
RRH4	Lech	15	10	244	8	62.47	2.83	1.08	0.42	0.36	0.022	5.00	5.00	1.83
RRH5	Lech	17	10	257	8	64.62	3.03	0.84	0.42	0.34	0.071	5.34	5.00	1.70
RRH6	Lech	15	10	260	8	67.94	3.14	0.94	0.37	0.35	0.016	5.00	5.00	1.90
RRH7	Lech	19	10	281	8	69.39	3.49	1.13	0.41	0.32	0.015	8.02	5.10	2.01
RRH8	Lech	17	7	347	8	162.49	4.93	1.09	0.58	0.52	0.012	12.29	5.00	3.32
RRH9	Lech	17	3	406	7	239.34		5.00	2.00	1.92	0.060	60.13	19.64	1.89
RRH10	Lech	18	9	414	8	263.08	10.60	2.02	1.33	1.28	0.048	44.63	35.16	3.01
RRH11	Lech	18	9	385	8	264.21	8.44	1.50	1.05	1.02	0.029	20.04	17.92	2.50
RRH12	Lech	18	9	386	8	265.46	8.38	1.52	1.07	1.04	0.031	20.31	14.96	2.63
RRH13	Lech	18	9	387	8	265.87	8.22	1.46	1.21	1.01	0.032	17.90	12.74	2.78
RRH14	Inn	15	10	198	8	1102.27	4.85	0.76	0.51	0.49	0.016	8.55	8.41	3.44
RRH15	Inn	16	10	280	8	1140.00	7.36	1.83	1.06	1.04	0.016	17.64	16.94	4.61
RRH16	Inn	15	10	217	8	1158.74	5.45	1.03	0.62	0.61	0.012	12.29	12.05	4.00
RRH17	Inn	16	10	217	8	1173.32	5.70	1.05	0.63	0.62	0.011	9.89	5.82	4.16
RRH18	Inn	17	10	224	8	1179.42	5.41	1.04	0.59	0.58	0.010	6.68	6.34	3.67
RRH19	Inn	15	10	231	8	1164.95	5.60	1.00	0.57	0.55	0.012	7.48	7.46	4.12
RRH20	Inn	15	11	223	8	1164.95	5.65	1.01	0.64	0.62	0.014	8.02	7.54	3.75
RRH21	Inn	15	10	224	8	2110.98	5.99	1.16	0.73	0.70	0.014	13.63	10.78	4.14

RRH22	Inn	15	10	249	8	2166.97	7.17	1.18	0.77	0.75	0.017	12.74	12.50	3.68
RRH23	Inn	15	11	230	8	2209.10	6.55	1.14	0.79	0.75	0.011	12.47	11.21	3.92
RRH24	Inn	15	10	243	8	2329.42	6.91	1.12	0.79	0.78	0.012	17.64	14.23	4.04
RRH25	Inn	15	10	232	8	2390.00	6.75	1.29	0.76	0.74	0.015	15.14	14.22	3.69
RRH26	Inn	15	11	232	8	2390.00	6.66	1.10	0.88	0.76	0.011	24.32	13.79	3.60

Appendix 4: Mean and standard error for the nutrient concentrations and ratios by system types.

		TDN mg/L	TDP µg/L	DSi mg/L	TDN:TDP molar	TDN:DSi molar	DSi:TDP molar
Inlets	mean	0.2	6.7	1.8	74	0.8	143
	SE	0.01	0.4	0.2	4	0.1	11
Reservoirs	mean	0.3	7.4	1.2	96	1.3	102
	SE	0.02	1.0	0.2	14	0.3	15
RRHs	mean	0.7	14	3.0	133	1.2	144
	SE	0.07	2.5	0.2	6	0.2	14

Appendix 5: Pearson correlation coefficients between the predictor variables used in the model-building process (see methods). Predictor variables that had a correlation about 0.5 were not included in the multivariate models. Elevation was included as random effect (Model 2).

	Elevation	% Metamorphic rock	% Artificial	% Agriculture	% Coniferous	% Deciduous	% Grasslands	Cl
Elevation	1.00							
% Metamorphic rock	0.14	1.00						
% Artificial areas	-0.82	-0.26	1.00					
% Agriculture	-0.66	-0.28	0.90	1.00				
% Coniferous	-0.40	0.22	0.11	0.06	1.00			
% Deciduous	-0.87	-0.21	0.81	0.65	0.12	1.00		
% Grasslands	-0.46	0.36	0.29	0.16	0.45	0.21	1.00	
Cl	-0.80	-0.20	0.93	0.88	0.14	0.80	0.24	1.00

*Appendix 6: Relationship between DSi, DCl concentrations, and DSi:DCl molar ratios and the main controlling factors (% coniferous, % agriculture, %metamorphic rock and elevation) for the three system types: inlets, reservoirs, and run-of-the-river hydropower systems (RRH). Numbers indicate Spearman rank correlation coefficients for each system type. Significance is indicated with * (p < 0.05), ** (p < 0.01), *** (p < 0.001) or NS (not significant).*

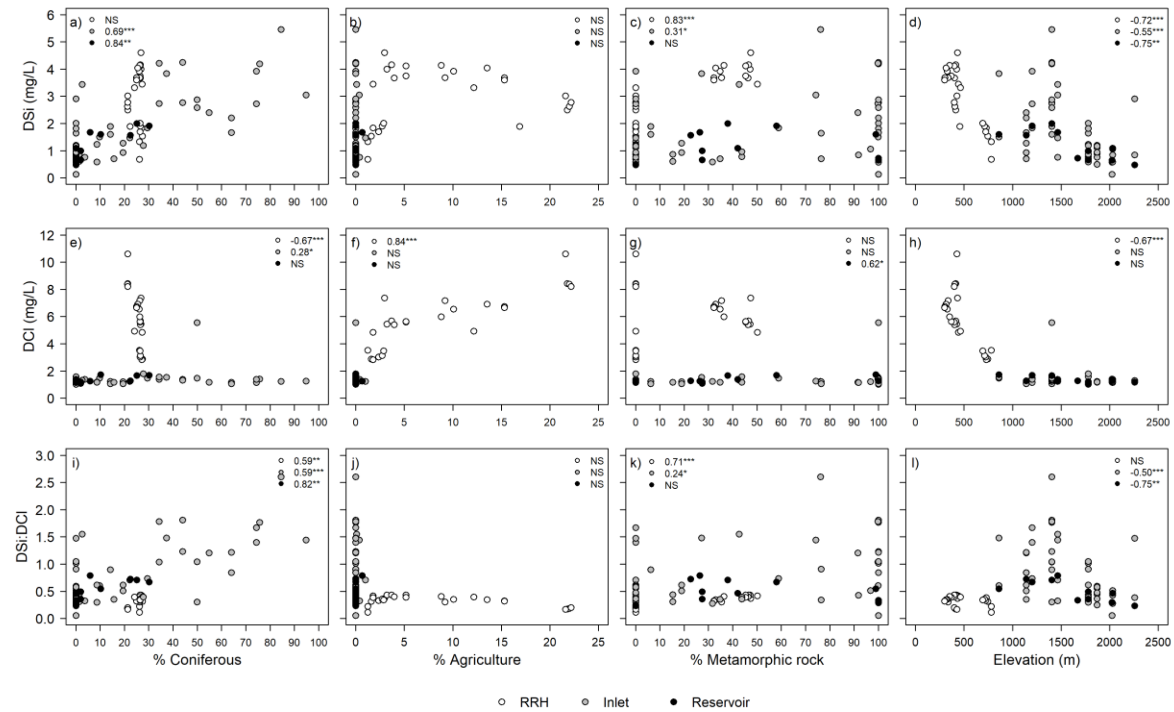

*Appendix 7: Relationship between TDN, TDP concentrations, and TDN:DCl, TDP:DCl molar ratios and the main controlling factors (% coniferous, % agriculture, and elevation) for the three system types: inlets, reservoirs, and run-of-the-river hydropower systems (RRH). Numbers indicate Spearman rank correlation coefficients for each system type. Significance is indicated with * (p < 0.05), ** (p < 0.01), *** (p < 0.001) or NS (not significant).*

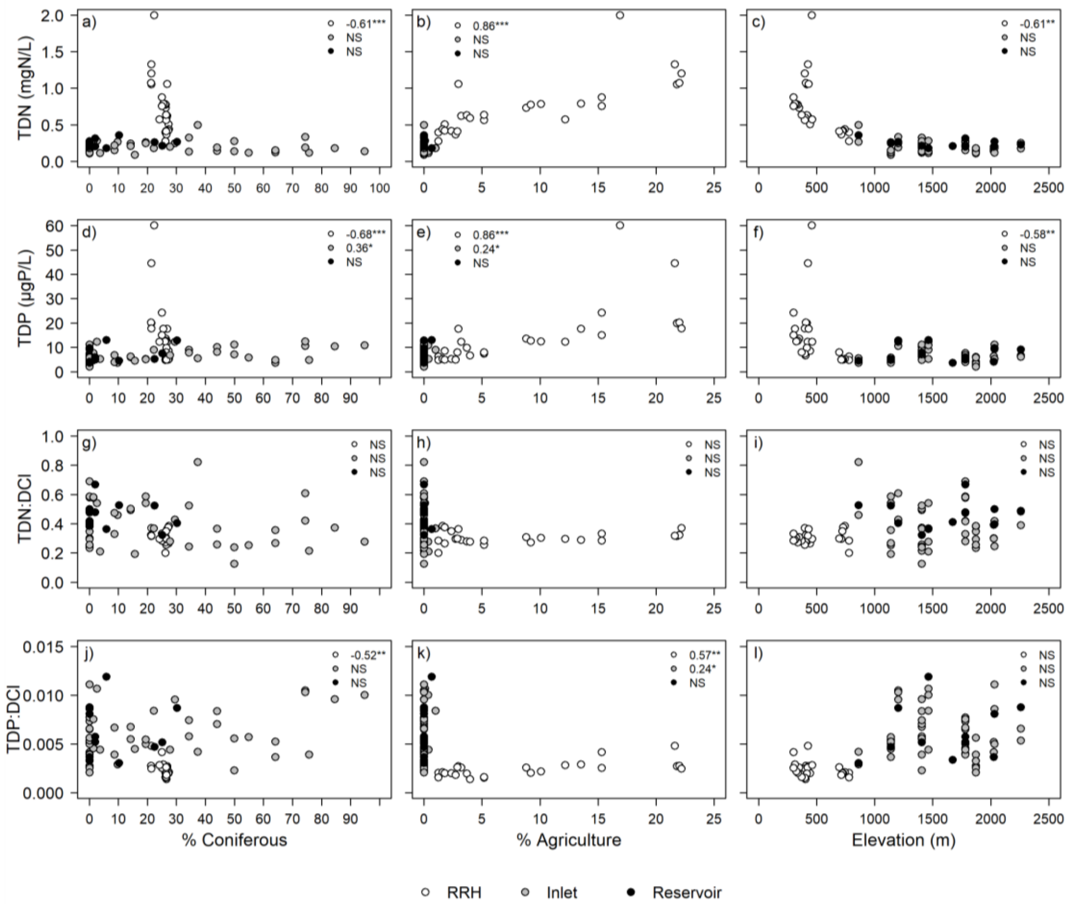

Appendix 8: Characteristics of the monitoring stations located in the mainstem of the Danube River

Location name	Station code	Country	Distance from the mouth (km)	Elevation (m.a.s.l.)	Area (km^2)
Neu-Ulm	DE1	Germany	2581	460	6450
Hainburg	AT6	Austria	1879	136	131516
Bratislava	SK1	Slovak Republic	1869	128	132027
Medve/Medvedov	HU1SK2	Hungary	1806	108	133851
Komarom/Kedvedov	HU2	Hungary	1768	101	152154
Szob	HU3	Hungary	1708	100	183544
Szob	SK5	Slovak Republic	1707	100	183542
Dunafoldvar	HU4	Hungary	1560	89	189123
Hercegszanto	HU5	Hungary	1435	82	209645
Batina	HR1	Croatia	1429	82	210434
Bezdan	RS1	Republic of Serbia	1426	81	210680
Bogojevo	RS2	Republic of Serbia	1367	80	252179
Borovo	HR2	Croatia	1337	78	252359
Ilok	HR11	Croatia	1302	78	256255
Backa Palanka	RS9	Republic of Serbia	1299	77	253737
Novi Sad	RS3	Republic of Serbia	1255	74	257619
Zemun	RS4	Republic of Serbia	1173	71	412762
Pancevo	RS5	Republic of Serbia	1155	71	520081
Banatska Palanka	RS6	Republic of Serbia	1077	70	564648
Bazias	RO1	Romania	1071	70	565896
Tekija	RS7	Republic of Serbia	954	68	574307
Radujevac	RS8	Republic of Serbia	851	32	577085
Pristol/Novo Selo	RO2	Romania	834	31	578734
Dunare	RO3	Romania	432	16	666224
Chiciu/Silistra	RO4	Romania	375	13	684150
Reni-	RO5UA1	Romania-Ukraine	132	4	787517
Vilkova	RO6UA2	Romania-Ukraine	18	1	800174
Sulina - Sulina arm	RO7	Romania	0	1	794016
Sf. Gheorghe arm	RO8	Romania	0	1	793983

Appendix 9: Characteristics of the monitoring stations located in the tributaries of the Danube Basin

River	Location name	Station code	Country	Distance from the confluence (km)	Elevation (m.a.s.l.)	Area (km^2)
Morava	Bratislava	SK6	Slovak Republic	1880	145	27414
Vah	Komarno	SK4	Slovak Republic	1766	106	17786
Horn	Kamenica	SK7	Slovak Republic	1716	114	5460
Ipel	Salka	SK8	Slovak Republic	1708	110	5074
Sio	Szekszard-Palank	HU6	Hungary	1498	85	14884
Drava	D. Miholjac	HR5HU7	Hungary	1382	92	36762
Tisza	Tiszasziget	HU9	Hungary	1214	74	138786
Sava	Sremska Mitrovica	RS14	Republic of Serbia	1170	75	87851
Velika Morava	Ljubicevski Most	RS17	Republic of Serbia	1103	71	37460
Jiu	Zaval	RO19	Romania	694	31	9883
Olt	Islaz	RO20	Romania	604	32	24278
Arges	Clatesti	RO9	Romania	432	14	12489
Ialomita	Downstream Tandarei	RO21	Romania	244	9	10779
Siret	Sendreni	RO10	Romania	155	4	46010
Prut	Giurgiulesti	RO11	Romania	132	5	28738

Appendix 10: Summary of data available for each monitoring station in the mainstem of the Danube River for Si.

Location name	Station code	DSi		Discharge	
		Number of observations*	Data available (Years)	Number of Observations*	Data available (Years)
Neu-Ulm	DE1	5	2004	3653	1996-2000/2002-2006
Hainburg	AT6	11	2008	4383	2006-2017
Bratislava	SK1	132	2007-2017	7669	1996-2000/2002-2017
Medve/Medvedov	HU1SK2	71	2003-2005/2012-2017	7668	1996-2000/2002-2017
Komarom/Kedvedov	HU2	28	2003-2005	6959	1996-2000/2002-2017
Szob	HU3	50	2003-2005/2016-2017	6971	1996-2000/2002-2017
Szob	SK5	51	2011/2014-2017	0	-
Dunafoldvar	HU4	150	2003-2005/2008-2017	6846	1996-2000/2002-2017
Hercegszanto	HU5	154	2003-2005/2007-2017	6619	1996-2000/2002-2017
Batina	HR1	119	2008-2017	828	1998-2001/2003-2007/2016-2017
Bezdan	RS1	175	2002-2005/2007-2017	251	2011-2017
Bogojevo	RS2	159	2002-2005/2007-2017	2922	2002-2009
Borovo	HR2	118	1998-1999/2007-2013/2015	1592	1998-2000/2013-2016
Ilok	HR11	24	2016-2017	731	2016-2017
Backa Palanka	RS9	80	2002-2005/2007-2011	0	-
Novi Sad	RS3	167	2002-2005/2007-2017	191	2005-2017
Zemun	RS4	172	2002-2017	12	2001
Pancevo	RS5	85	2002-2005/2007-2011	20	2001-2002
Banatska Palanka	RS6	163	2002-2005/2007-2017	0	-
Bazias	RO1	106	2001-2008/2011-2012	6582	1996-2000/2002-2007/2009-2016
Tekija	RS7	148	2002-2017	9	2001

Radujevac	RS8	154	2002-2017	99	2001/2004/2009/2012-2017
Pristol/Novo Selo	RO2	142	2001-2008/2011-2015	7314	1996-2000/2002-2017
Dunare	RO3	99	2001-2008/2010-2011	3653	1996-2000/2002-2007
Chiciu/Silistra	RO4	108	2001-2008/2011-2013	7311	1996-2000/2002-2017
Reni-	RO5UA1	193	2001-2017	7316	1996-2000/2002-2017
Vilkova	RO6UA2	190	2001-2017	7312	1996-2000/2002-2017
Sulina - Sulina arm	RO7	97	2001-2008/2011	3973	1996-2000/2002-2007/2009
Sf. Gheorghe arm	RO8	95	2001-2008/2011	3597	1996-2000/2002/2004-2007/2009

(*) The MS has consistent measurements during the years

Appendix 11: Summary of data available for each monitoring station in the tributaries of the Danube Basin

River	Location name	Station code	DSi		Discharge	
			Number of observations*	**Data available (Years)**	**Number of Observations***	**Data available (Years)**
Morava	Bratislava	SK6	41	2011/2015-2017	2922	2010-2017
Vah	Koma¡rno	SK4	54	2011/2014-2017	2922	2010-2017
Horn	Kamenica	SK7	52	2011/2014-2017	2891	2010-2017
Ipel	Salka	SK8	52	2011/2014-2017	2922	2010-2017
Sio	Szekszard-Palank	HU6	42	2003-2005/2009-2011	6964	1996-2000/2002-2017
Drava	D. Miholjac	HR5HU7	161	2003-2005/2007-2017	6971	1996-2000/2002-2017
Tisza	Tiszasziget	HU9	151	2003-2005/2007-2017	6965	1996-2000/2002-2017
Sava	Sremska Mitrovica	RS14	112	2002-2011	3287	2002-2010
Velika Morava	Ljubicevski Most	RS17	131	2002-2017	3287	2002-2010
Jiu	Zaval	RO19	34	2007-2008/2011	8	2007
Olt	Islaz	RO20	36	2007-2008/2010/2012/2014	37	2007-2009/2012
Arges	Clatesti	RO9	97	2001-2008/2010-2011	3291	1996-2000/2002-2006
Ialomita	Downstream Tandarei	RO21	21	2007-2008	71	2007-2010
Siret	Sendreni	RO10	96	2001-2008/2011-2012	6215	1996-2000/2002-2006/2010-2017
Prut	Giurgiulesti	RO11	103	2001-2008/2011-2012	5845	1996-2000/2002-2005/2010-2017

(*) Monitoring station has consistent measurements during the years

Appendix 12: Lithological classes in the tributaries

Tributary	Station code	PA	VA	PB	VB	SC	PI	MT	SM	PY	SS	SU
Morava	SK6	5%	0%	0%	0%	2%	2%	23%	19%	0%	22%	27%
Vah	SK4	5%	0%	0%	3%	14%	0%	2%	16%	0%	16%	44%
Hron	SK7	8%	10%	0%	24%	8%	0%	10%	4%	0%	7%	29%
Ipel	SK8	6%	1%	0%	38%	2%	0%	1%	6%	11%	14%	22%
Sio	HU6	0%	0%	0%	1%	8%	0%	0%	8%	2%	1%	80%
Drava	HR5HU7	2%	0%	0%	1%	12%	0%	38%	14%	0%	10%	22%
Tisza	HU9	0%	4%	0%	2%	9%	0%	6%	13%	2%	31%	33%
Sava	RS14	0%	1%	4%	0%	46%	1%	1%	6%	0%	38%	4%
Velika	RS17	6%	5%	2%	1%	32%	0%	13%	6%	0%	35%	0%
Arges	RO9	0%	0%	0%	0%	1%	0%	11%	4%	0%	85%	0%
Siret	RO10	0%	1%	0%	0%	11%	0%	7%	17%	0%	61%	3%
Prut	RO11	0%	0%	0%	0%	0%	0%	0%	45%	0%	49%	5%

PA: Acid plutonic; VA: Acid Volcanic; PB: Basic Plutonic; VB: Basic Volcanic; SC: Carbonates sedimentary;

PI: Intermediate plutonic rocks; MT: Metamorphic rock; MS: Mix Sedimentary; PY: Pyroclastics;

SS: Siliciclastic sedimentary; SU: unconsolidated sediments

Appendix 13: Percentage of Land use and land cover types for the 15 tributaries for the years 2000, 2006, 2012, 2018.

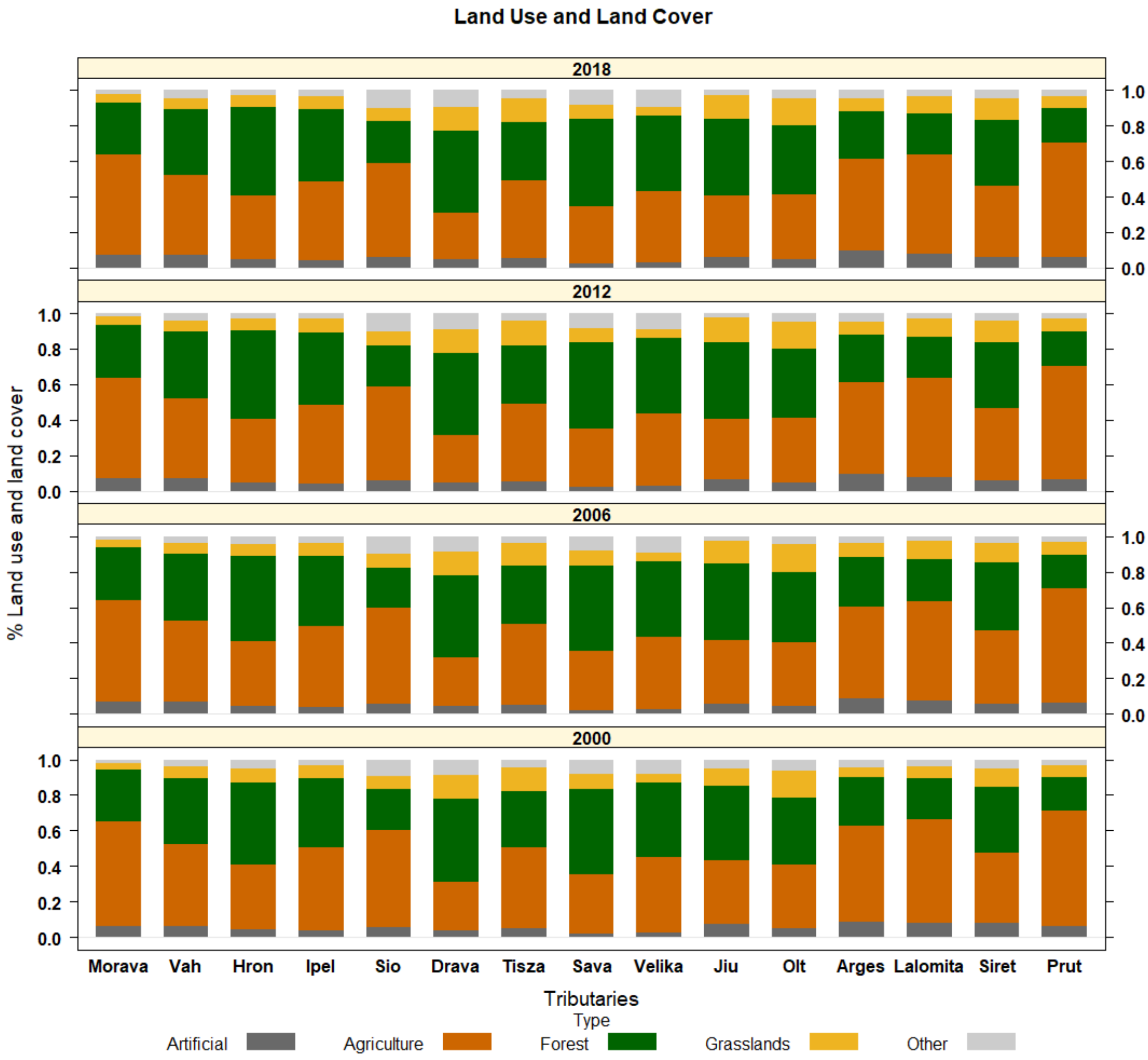

Appendix 14: Percentage of land use and land cover types for the mainstem of the Danube River for the years 2000, 2006, 2012, 2018.

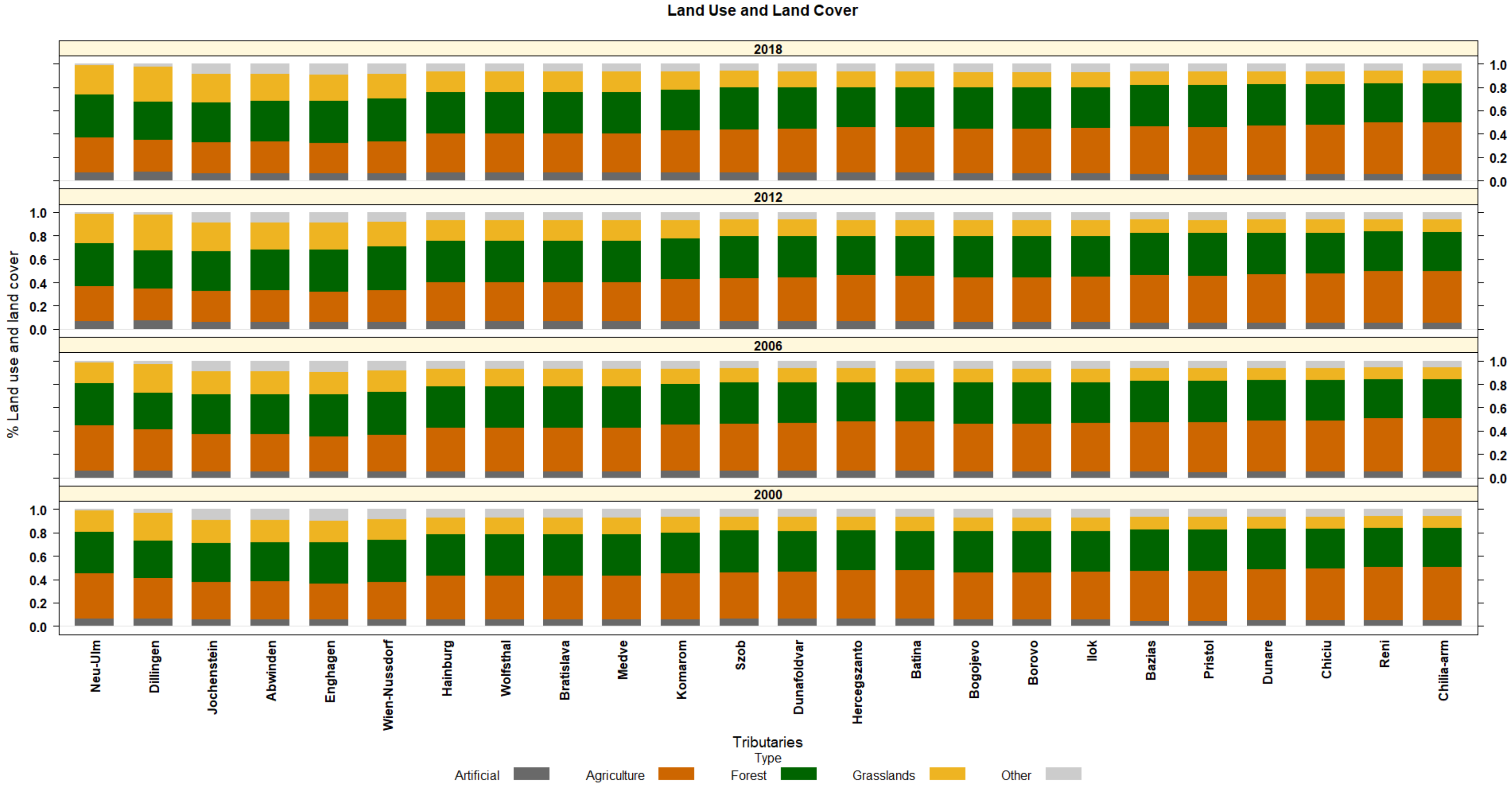

Appendix 15: DSi concentration on the Danube River (A) and its tributaries (B) over time, in the three sections of the Danube Basin.

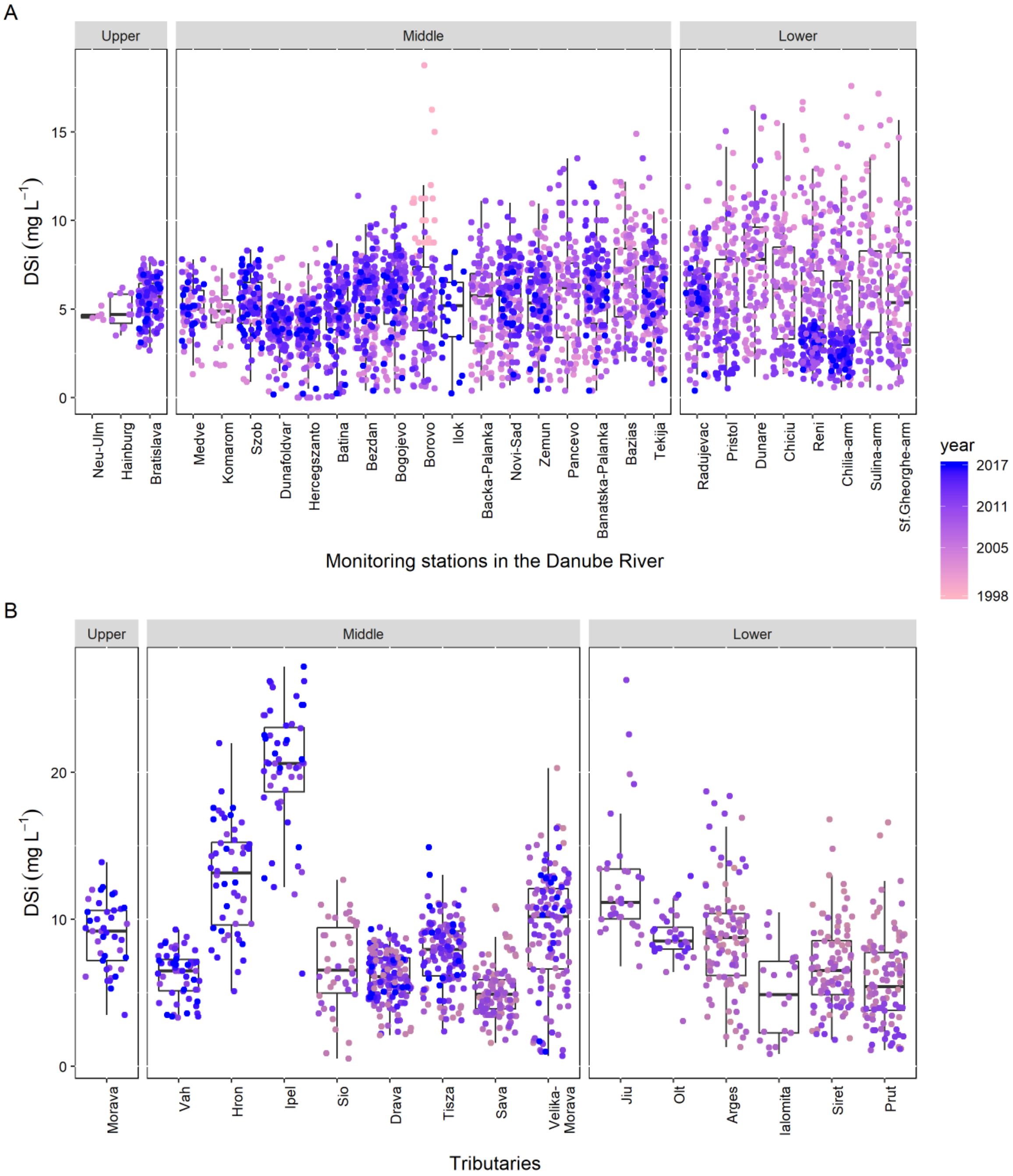

Appendix 16: Monthly flow average ($m^3\ s^{-1}$) in A) the mainstem of the Danube River and B) tributaries.

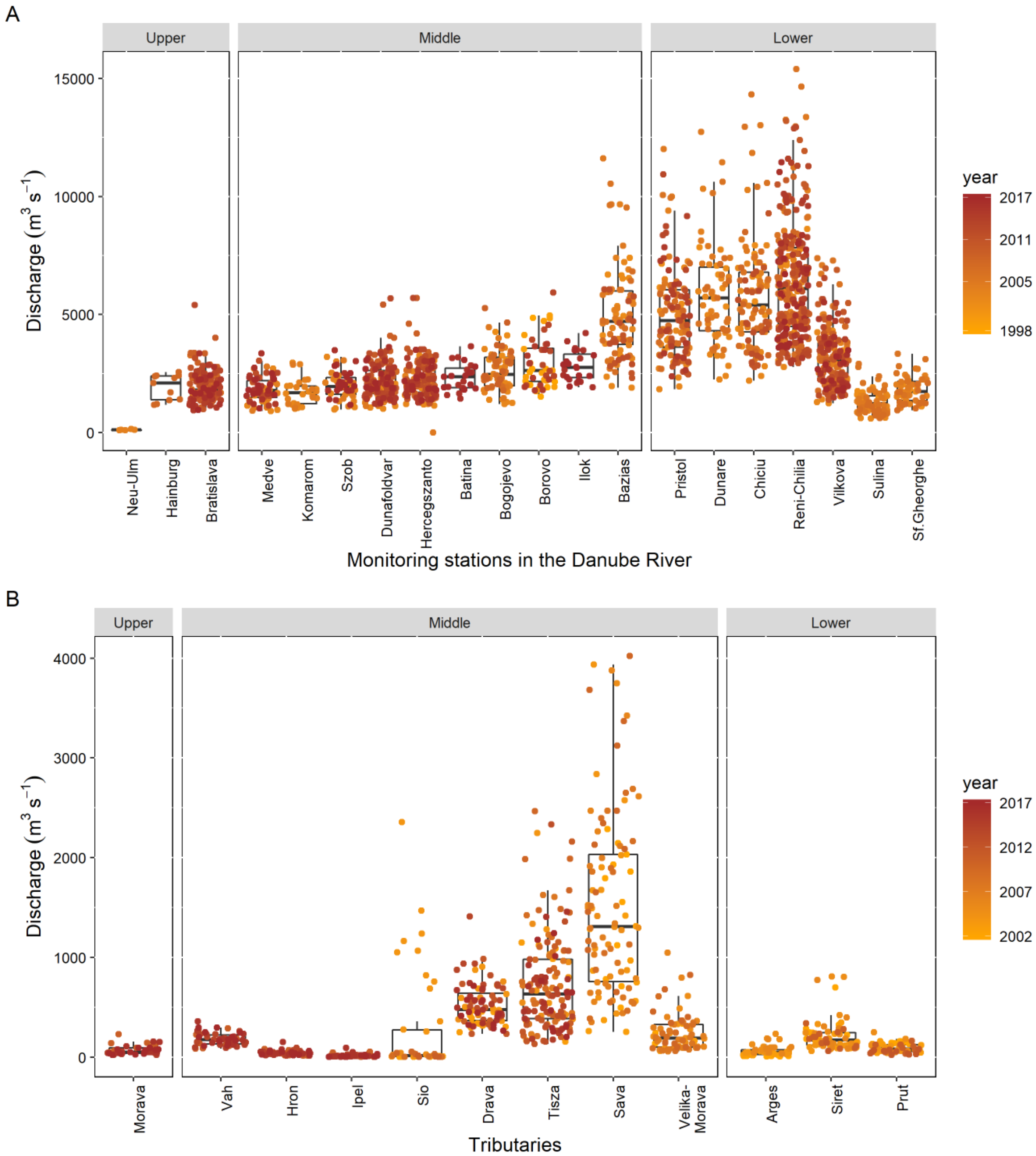

*Appendix 17: Relationship between annual DSi yields and the main controlling factors. Numbers indicate Spearman rank correlation coefficients. Significance is indicated with * (p < 0.05), ** (p < 0.01), *** (p < 0.001) or NS (not significant).*

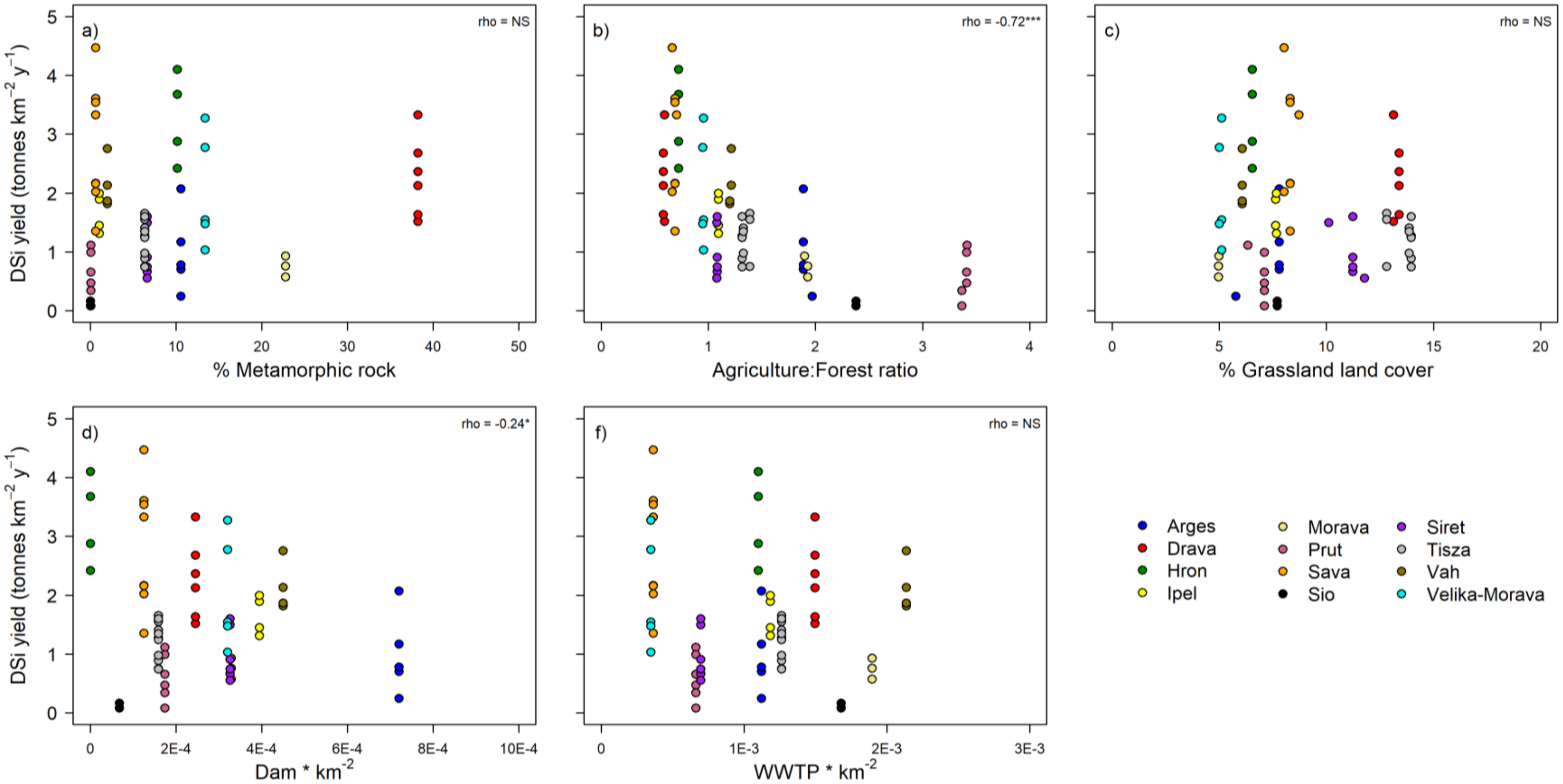

Appendix 18: Summary of data available for each monitoring station in the mainstem of the Danube River for Si.

Location name	Station code	DSi		Discharge	
		Number of observations*	**Data available (Years)**	**Number of Observations***	**Data available (Years)**
Neu-Ulm	DE1	5	2004	3653	1996-2000/2002-2006
Hainburg	AT6	11	2008	4383	2006-2017
Bratislava	SK1	132	2007-2017	7669	1996-2000/2002-2017
Medve/Medvedov	HU1SK2	71	2003-2005/2012-2017	7668	1996-2000/2002-2017
Komarom/Kedvedov	HU2	28	2003-2005	6959	1996-2000/2002-2017
Szob	HU3	50	2003-2005/2016-2017	6971	1996-2000/2002-2017
Szob	SK5	51	2011/2014-2017	0	-
Dunafoldvar	HU4	150	2003-2005/2008-2017	6846	1996-2000/2002-2017
Hercegszanto	HU5	154	2003-2005/2007-2017	6619	1996-2000/2002-2017
Batina	HR1	119	2008-2017	828	1998-2001/2003-2007/2016-2017
Bezdan	RS1	175	2002-2005/2007-2017	251	2011-2017
Bogojevo	RS2	159	2002-2005/2007-2017	2922	2002-2009
Borovo	HR2	118	1998-1999/2007-2013/2015	1592	1998-2000/2013-2016
Ilok	HR11	24	2016-2017	731	2016-2017
Backa Palanka	RS9	80	2002-2005/2007-2011	0	-
Novi Sad	RS3	167	2002-2005/2007-2017	191	2005-2017
Zemun	RS4	172	2002-2017	12	2001
Pancevo	RS5	85	2002-2005/2007-2011	20	2001-2002
Banatska Palanka	RS6	163	2002-2005/2007-2017	0	-
Bazias	RO1	106	2001-2008/2011-2012	6582	1996-2000/2002-2007/2009-2016
Tekija	RS7	148	2002-2017	9	2001

Radujevac	RS8	154	2002-2017	99	2001/2004/2009/2012-2017
Pristol/Novo Selo	RO2	142	2001-2008/2011-2015	7314	1996-2000/2002-2017
Dunare	RO3	99	2001-2008/2010-2011	3653	1996-2000/2002-2007
Chiciu/Silistra	RO4	108	2001-2008/2011-2013	7311	1996-2000/2002-2017
Reni-	RO5UA1	193	2001-2017	7316	1996-2000/2002-2017
Vilkova	RO6UA2	190	2001-2017	7312	1996-2000/2002-2017
Sulina - Sulina arm	RO7	97	2001-2008/2011	3973	1996-2000/2002-2007/2009
Sf. Gheorghe arm	RO8	95	2001-2008/2011	3597	1996-2000/2002/2004-2007/2009

(*) The MS has consistent measurements during the years

Appendix 19: Summary of data available for each monitoring station in the tributaries of the Danube Basin

River	Location name	Station code	DSi		Discharge	
			Number of observations*	**Data available (Years)**	**Number of Observations***	**Data available (Years)**
Morava	Bratislava	SK6	41	2011/2015-2017	2922	2010-2017
Vah	Koma¡rno	SK4	54	2011/2014-2017	2922	2010-2017
Horn	Kamenica	SK7	52	2011/2014-2017	2891	2010-2017
Ipel	Salka	SK8	52	2011/2014-2017	2922	2010-2017
Sio	Szekszard-Palank	HU6	42	2003-2005/2009-2011	6964	1996-2000/2002-2017
Drava	D. Miholjac	HR5HU7	161	2003-2005/2007-2017	6971	1996-2000/2002-2017
Tisza	Tiszasziget	HU9	151	2003-2005/2007-2017	6965	1996-2000/2002-2017
Sava	Sremska Mitrovica	RS14	112	2002-2011	3287	2002-2010
Velika Morava	Ljubicevski Most	RS17	131	2002-2017	3287	2002-2010
Jiu	Zaval	RO19	34	2007-2008/2011	8	2007
Olt	Islaz	RO20	36	2007-2008/2010/2012/2014	37	2007-2009/2012
Arges	Clatesti	RO9	97	2001-2008/2010-2011	3291	1996-2000/2002-2006
Ialomita	Downstream Tandarei	RO21	21	2007-2008	71	2007-2010
Siret	Sendreni	RO10	96	2001-2008/2011-2012	6215	1996-2000/2002-2006/2010-2017
Prut	Giurgiulesti	RO11	103	2001-2008/2011-2012	5845	1996-2000/2002-2005/2010-2017

(*) Monitoring station has consistent measurements during the years

*Appendix 20: Monthly nutrient concentration in 11 tributaries of the Danube River. Kruskal-Wallis results that showed significant differences between months is indicated with * (p < 0.05), ** (p < 0.01), and *** (p < 0.001).*

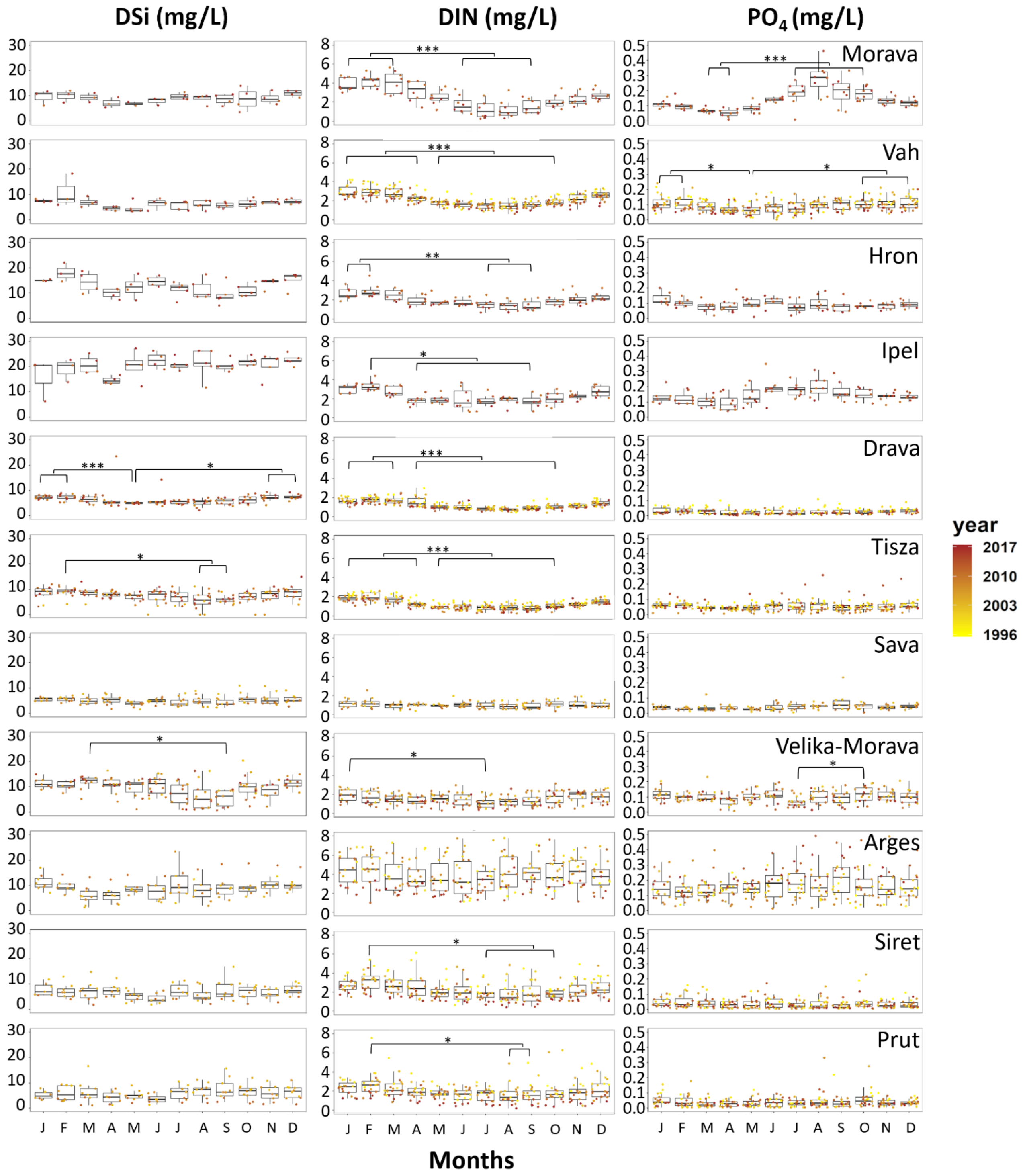

*Appendix 21: Monthly nutrient ratios in 11 tributaries of the Danube River. Kruskal-Wallis results that showed significant differences between months is indicated with * (p < 0.05), ** (p < 0.01), and *** (p < 0.001).*

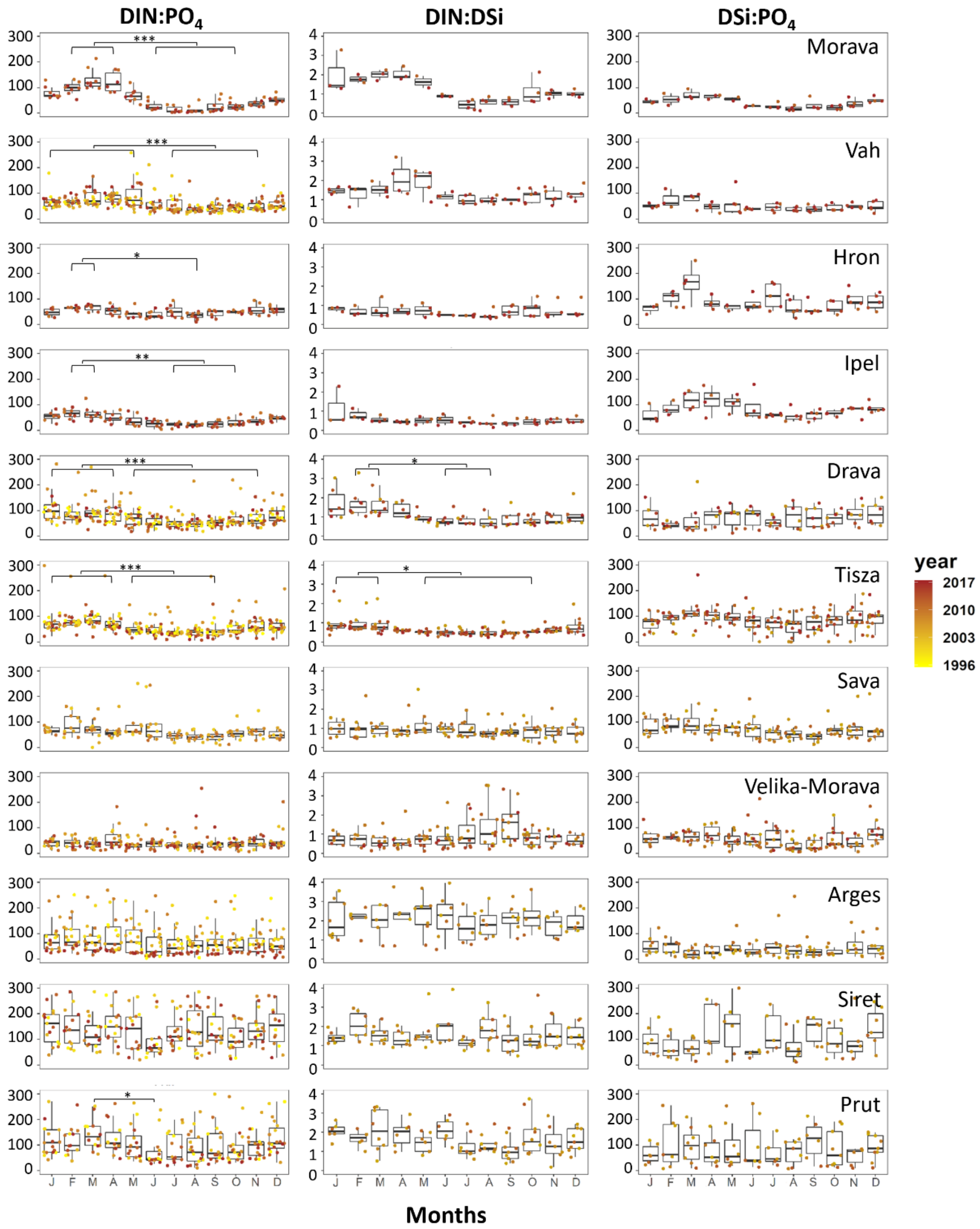

*Appendix 22: Relationship between annual nutrient ratios and the main controlling factors in the tributaries. Numbers indicate Spearman rank correlation coefficients. Significance is indicated with * (p < 0.05), ** (p < 0.01), *** (p < 0.001) or NS (not significant).*

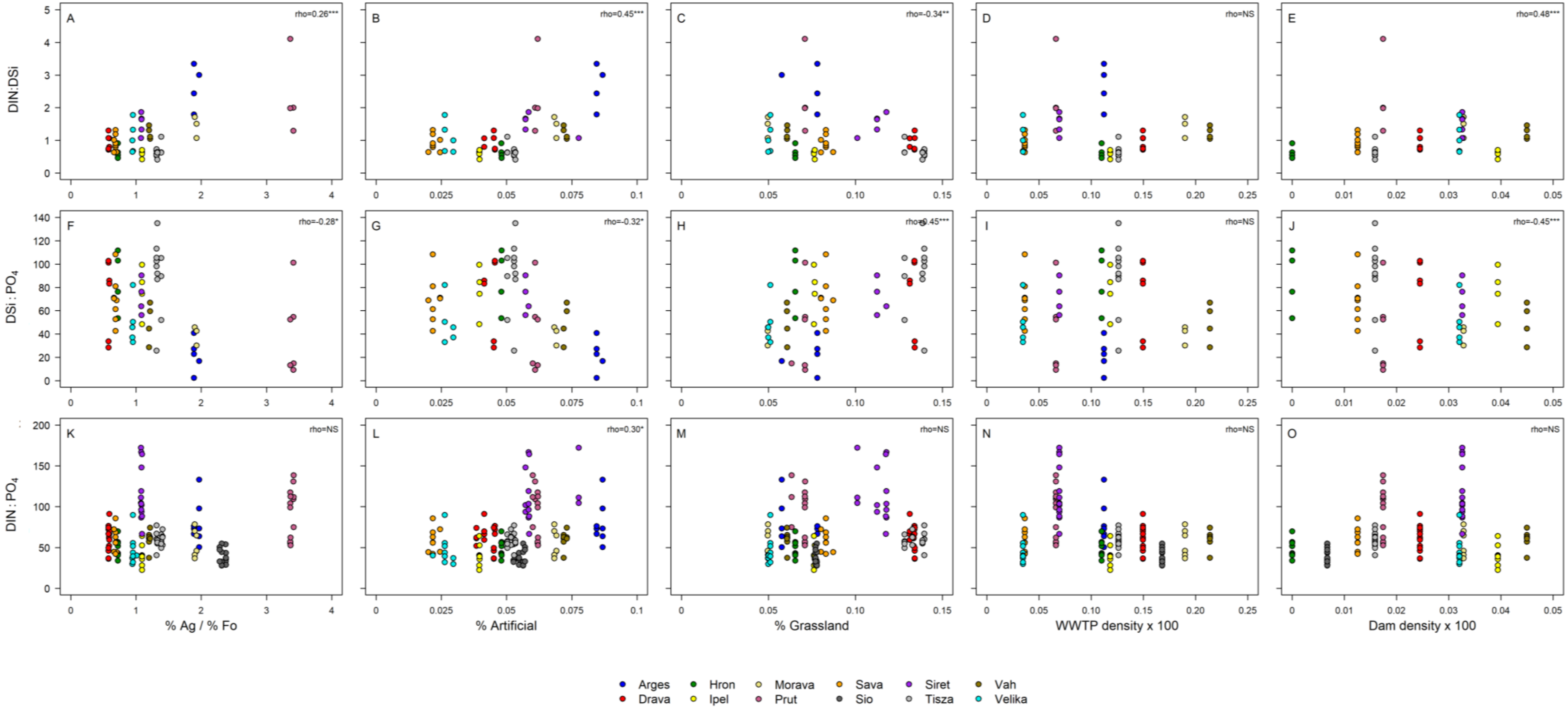

Appendix 23: Nitrogen(A) and Phosphorus(B) Fertilizer application per area cropland from 2002 to 2017. Data source from Ritchie et al. 2022 and download from *www.ourworldindata.org.*

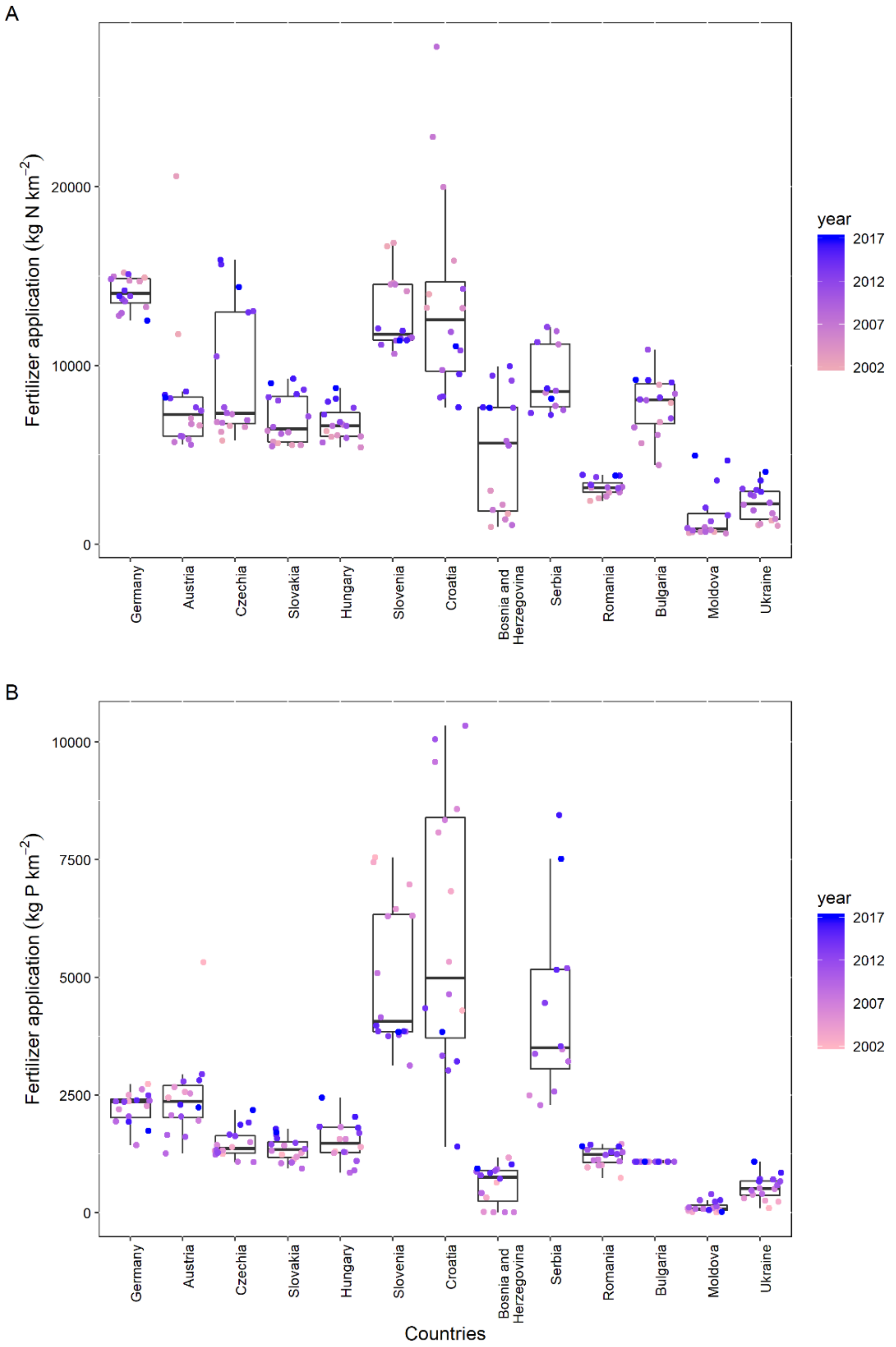

LIST OF ACRONYMS

AIC	Akaike Information Criterion
ANOVA	Analysis of Variance
APHA	American Public Health Association
DCl	Dissolved Chloride
DEM	Digital Elevation Model
DO	Dissolved Oxygen
DOC	Dissolved Organic Carbon
DSi	Dissolved Silica
EC	Electrical Conductivity
EEA	European Environment Agency
ESRI	Environmental Systems Research Institute
GLiM	Global Lithological Map
GRanD	Global Reservoir and Dam
GPS	Global Positioning System
ICPDR	International Commission for the Protection of the Danube River
IN	Inlet
KT	metric tonnes
LULC	Land use and land cover
MT	metamorphic rocks
PA	Acid Plutonic
RR	Reservoir
RRH	Run-of-the-river

Si	Silicon
SRTM	Shuttle Radar Topography Mission
SS	siliciclastic sedimentary
TDN	Total Dissolved Nitrogen
TNMN	TransNational Monitoring Network
TDP	Total Dissolved Phosphorus
VA	Acid Volcanic
SU	unconsolidated sediments
WWTPs	wastewater treatment plants

LIST OF TABLES

*Table 2.1. Results of the best-fit regression models for silica concentration (DSi), and silica ratios with Cl, N, P (n = 87 for RRH, Reservoirs and Inlets) and for DSi yield (n= 76 for RRH and Inlets). Model 1 is the best-fit multiple regression model following the model-development procedure (see Methods), which includes % coniferous, % metamorphic rock and system type; Model 2 includes a covariance structure for elevation class; and Model 3 is a random intercept model for each elevation class. Significance of slopes are indicated with * (p < 0.05), ** (p< 0.01), and *** (p< 0.001), and differences among system types (intercepts) are represented by different letters.* 28

*Table 2.2. Results of the regression models for nitrogen (TDN) and phosphorus (TDP) concentration and their ratios with Cl with total no. of observations was 87 (RRH, Reservoirs and Inlets); TDN and TDP yield with total no. of observations was 76 (RRH and Inlets). Detailed results of the best fit model, with the lowest AIC-value (indicated in bold) are presented. Significance of intercepts are indicated with * (p < 0.05), ** (p< 0.01), and *** (p< 0.001).* 32

Table 2.3. Overview of published literature and monitoring stations reporting the DSi (mg /L) for the Danube River. DSi values represent medians for the period reported with the range in parentheses. [a]Mean. [b]Statndard error... 39

Table 2.4. Summary of peer-reviewed literature that statistically examined landscape controls on DSi, with studies showing either a positive (+), negative (-) or no relationship (nr). Blanks show that the study didn't consider the variable........................................ 41

Table 3.1. ***Results of the regression models for DSi annual yield (DSi, in tonnes km^{-2} year^{-1}) as dependent variable and land use, geology, dam density and wastewater treatment plant density as explanatory variables (see footnote). Significance of intercepts are indicated with ns (not significant, p > 0.10), ms (marginally significant, p < 0.10), * (p < 0.05), ** (p < 0.01), and *** (p < 0.001). Total no. of observations was 64.*................ 60

Table 3.2. Summary of DSi yields, modelling methods and controlling factors from the literature for other river basins worldwide. 67

*Table 4.1. Results of the best-fit regression models for nutrient ratios DIN:DSi, DSi:PO_4, DIN:PO_4 in the tributaries (n= 58, 60, 135 respectively). Nutrient ratios were calculated based on annual loads. Model 1 is the best-fit multiple regression model following the model-development procedure; Model 2 includes a variance structure for elevation class; Model 3 is a random intercept model for each elevation class; and Model 4 included both a variance structure and a random intercept. Significance of slopes are indicated with **

*($p < 0.05$), ** ($p< 0.01$), and *** ($p< 0.001$). For more explanation, see Methods section.* 92

LIST OF FIGURES

Figure 1.1. Schematic view of Si cycle and its forms (adapted from Struyf et al. 2009). ASi (Amorphous Silica), DSi (Dissolved Silica), and BSi (Biogenic Silica). 3

Figure 1.2. Map of the Danube River Basin, with its tributaries.................................... *6*

Figure 1.3. Reservoir in the Danube River Basin. *7*

Figure 1.4. Reservoir in the Danube River Basin. *7*

Figure 1.5. Agriculture activities in the upper part of the Danube River Basin............. *8*

Figure 1.6. Nitrogen(A) and Phosphorus(B) Fertilizer application per area cropland from 2002 to 2017 10

Figure 2.1. Location of sampling sites in the upper Danube River basin...................... *21*

Figure 2.2. Temperature (a), electrical conductivity (b), dissolved oxygen (b) and pH (d) of inlets (n = 50), reservoirs (n = 11) and run-of-river hydropower systems (n = 26). System types sharing the same letter were not significantly different (Kruskal-Wallis ANOVA and post-hoc test, p < 0.001).... 26

Figure 2.3. Dissolved silica (DSi) concentration (a), DSi:DCl ratio (b), TDN:DSi ratio (c), DSi:TDP ratio (d), total dissolved nitrogen TDN (e), TDN:DCl ratio (f), total dissolved phosphorus TDP (g), TDP:DCl ratio (h), TDN:TDP ratio (i), and dissolved chloride (DCl) concentration (j) of inlets (n = 50), reservoirs (n = 11) and run-of-river hydropower systems-RRH (n = 26). All nutrients ratios are expressed in molar units. System types sharing the same letter were not significantly different (Kruskal-Wallis ANOVA and post-hoc test, p < 0.001).... 27

*Figure 2.4. Relationship between DSi yield and the ratios of DSi with TDN and TDP and the main controlling factors (% coniferous, % agriculture, % metamorphic rock and elevation) for the three system types: inlets, reservoirs, and run-of-the-river hydropower systems (RRH). Numbers indicate Spearman rank correlation coefficients for each system type. Significance is indicated with * (p < 0.05), ** (p < 0.01), *** (p < 0.001) or NS (not significant).* 30

Figure 2.5. Relationship between nutrient yields and their ratio (TDN, TDP and TDN:TDP) and the main controlling factors (% coniferous, % agriculture and elevation)

*for the three system types: inlets, reservoirs, and run-of-the-river hydropower systems (RRH). Numbers indicate Spearman rank correlation coefficients for each system type. Significance is indicated with * (P < 0.05), ** (p < 0.01), *** (p < 0.001) or NS (not significant).* 31

Figure 2.6. Longitudinal trend of DSi yield for two rivers Inn and Lech with presence of RRH. The two rivers were divided in four sections: Inn 1 - upstream (y_1) (R^2= 0.03), Inn 2 – downstream (y_2) (R^2= 0.4), Lech 1 – upstream (y_3) (R^2= 0.6), Lech 2 – downstream (y_4) (R^2= 0.001). 34

Figure 2.7. a) Relationship between DSi and diatom abundance in the reservoirs (n = 9). The estimated regression line equation is y = 130.7x + 438.4. b) Relationship between DSi and chlorophyll a concentration in the reservoirs (n = 11) and the estimated regression line equation is y = x + 0.30. Lines indicate linear regression relationships. 34

Figure 3.1. Schematic location of the tributaries and the monitoring station from the Trans-National Monitoring Network (TNMN) of the International Commission for the Protection of the Danube River (ICPDR) in the Upper, Middle, and Lower sections of the Danube Basin. 51

Figure 3.2. Monthly DSi loads on the Danube River (A) and its tributaries (B) for 2002 - 2017 in the Danube Basin. Dashed red lines on plot A indicates the presence of tributaries. 56

Figure 3.3. Contribution of the monthly DSi loads from upstream and tributaries, in six river sub basins over time. The bar plots showed contribution from the upstream and tributaries, while the dots showed the downstream load. 58

Figure 3.4. Annual DSi yields on the tributaries of the Danube Basin for different periods in the Danube Basin. 59

Figure 3.5. Effect plots for the effects of land use on the annual DSi yield (tonnes km^{-2} $year^{-1}$) in the Danube river basin. A) Agriculture:Forest ratio; and B) % Grassland. The colored bands indicate 95% confidence levels calculated using Model 4 (see Table 3.1). 61

*Figure 4.1. Schematic location of the monitoring stations in the tributaries and in the mainstem of the Danube River in the three sections of the basin. The detailed information of the monitoring stations from the mainstem and tributaries are in Appendix 8 and 9.*79

Figure 4.2. Annual nutrient loads: A) DSi from 2002 to 2017, B) DIN, and C) PO_4, from 1996 to 2017, in the three sections of the mainstem of the Danube River. 86

*Figure 4.3. Nutrients loads at Reni station, before entering the Danube Delta, from 1997 to 2017. Numbers indicate Spearman rank correlation coefficients (rho). Significance is indicated with * ($p < 0.05$), ** ($p < 0.01$), *** ($p < 0.001$) or NS (not significant). DIN (y_1) (R^2= 0.31), DSi (y_2) (R^2= 0.67), PO_4 (y_3) (R^2= 0.005).* 87

Figure 4.4. Annual nutrient loads: A) DSi from 2002 to 2017, B) DIN, and C) PO_4, from 1996 to 2017, of 11 tributaries located in the three sections of the Danube Basin. 88

Figure 4.5. Nutrient ratios based on annual loads in the tree sections of the mainstem of the Danube River: A) DIN:DSi, B) DSi:PO_4 from 2002 to 2017, C) DIN:PO_4 from 1996 to 2017. Location of main cities are in red lyrics. 90

Figure 4.6. Nutrient ratios based on annual loads in 12 tributaries of the Danube River: A) DIN:DSi, B) DSi:PO_4, C) DIN:PO_4 in the tree sections. 91

*Figure 4.7. Boxplots of N-IFEP and P-IFEP for the Danube River (A and B) and for its tributaries (C and D) from 1998 to 2017. For the N-IFEP and P-IFEP values > 0 Wilcoxon sign rank test, significance is indicated with * ($p < 0.05$), ** ($p < 0.01$), and *** ($p < 0.001$).* 94

*Figure 4.8. Boxplots of N-ICEP and P-ICEP for the Danube River (A and B) and for its tributaries (C and D) from 1998 to 2017. For the N-ICEP and P-ICEP values > 0 Wilcoxon sign rank test, significance is indicated with * ($p < 0.05$), ** ($p < 0.01$), and *** ($p < 0.001$).* 95

ABOUT THE AUTHOR

Jessica obtained a BSc in Geographic Engineering, with specialization in Environment and Natural Resources, in 2006 from the National University of San Marcos (UNMSM), Peru. She then worked as an Environmental Specialist at National Environmental Fund by evaluating and superving the remediation work of mining environmental legacies in Peru. In 2010 she received a scholarship from the Joint Japan/World Bank Graduate Scholarship Program (JJ/WBGSP) to pursue a MSc in Environmental Science and Technology at the IHE Delft Institute for Water Education, The Netherlands. As part of her master thesis, Jessica worked on the Mara River, which starts in the Mau Forest of Kenya and runs across the Tanzanian border into Lake Victoria. Her fieldwork in tropical rivers and subsequent laboratory work sparked her curiosity for a deeper understanding of aquatic ecosystems.

After obtaining her MSc degree, Jessica worked as a lecturer in the UNMSM and as environmental evaluator of environmental projects at the Ministry of Energy and Mines in Peru. During this period, she was part of a team of professionals that evaluate the implementation and construction of reservoirs in the Peruvian Amazons. After working in this group, Jessica developed an interest in the understanding of the effects of the construction of reservoirs in the aquatic ecosystems.
Jessica was awarded with research grants from FINCyT Program, Peru and from the Schlumberger Foundation Faculty for the Future, in order to developed her PhD at IHE Delft. Over the course of the PhD, Jessica organized and developed many fieldwork campaigns in Austria, and Germany. During these fieldwork campaigns, she had collected and analyzed more than 4000 water samples from streams and reservoirs. During this work she developed laboratory expertise that helped her to become a very meticulous professional.

Peer review paper

Salcedo-Borda JS, van Dam AA, Gayraud J., Islam H., Irvine K and Gettel GM (2022). Controls of Si export and nutrient (N, P) stoichiometry in hydropower reservoirs and headwater rivers of the Danube River Basin. Submitted Biogeochemistry Journal.

Salcedo-Borda J.S., van Dam A.A., Irvine K. and Gettel G.M. (2022). Dissolved silica in the Danube Basin. Under Review.

Salcedo-Borda J.S., van Dam A.A., Irvine K. and Gettel G.M. (2022). Analysis of controlling factors on nutrient stoichiometry on the Danube River and its tributaries. Under Review.

Masese, F.O., Salcedo-Borda, J.S., Gettel, G.M., Irvine, K., McClain, M.E., 2017. Influence of catchment land use and seasonality on dissolved organic matter composition and ecosystem metabolism in headwater streams of a Kenyan river. Biogeochemistry 132: 1-22. https://doi.org/10.1007/s10533-016-0269-6.

Conference proceedings

Effects of reservoirs on Nutrient Concentrations and Ratios along the Longitudinal Gradient of Danube River Basin, American Geophysical Union – AGU 2015, San Francisco, USA.

Effects of reservoirs on nutrient stoichiometry and phytoplankton community. PhD Seminar 2016, at IHE-Delft, The Netherlands.

Effects of reservoirs on nutrient stoichiometry, PhD Seminar 2016 Institute of Meteorology and Climate Research Atmospheric Environmental Research (IMK-IFU), Garmisch-Partenkirchen, Germany.

Effect of reservoirs with long and short residence time on nutrient concentrations in the upper part of the Danube River Basin, Aquatic Sciences Meeting ASLO 2017, Hawaii, USA.

The research described in this thesis was financially supported by FINCyT Program, Peru (Agreement Nº 077- FINCyT-BDE-2014) and the Schlumberger Foundation Faculty for the Future.

SENSE

Netherlands Research School for the
Socio-Economic and Natural Sciences of the Environment

D I P L O M A

for specialised PhD training

The Netherlands research school for the
Socio-Economic and Natural Sciences of the Environment
(SENSE) declares that

Jessica Sara Salcedo Borda

born on 6 January 1983 in Lima, Peru

has successfully fulfilled all requirements of the
educational PhD programme of SENSE.

Delft, 3 April 2023

Chair of the SENSE board

Prof. dr. Martin Wassen

The SENSE Director

Prof. Philipp Pattberg

The SENSE Research School has been accredited by the Royal Netherlands Academy of Arts and Sciences (KNAW)

KONINKLIJKE NEDERLANDSE
AKADEMIE VAN WETENSCHAPPEN

The SENSE Research School declares that **Jessica Sara Salcedo Borda** has successfully fulfilled all requirements of the educational PhD programme of SENSE with a work load of 38.7 EC, including the following activities:

SENSE PhD Courses

- Environmental research in context (2014)
- Research in context activity: 'Co-organizing SENSE 'Summer Academy 2014'

Other PhD and Advanced MSc Courses

- Watershed Ecology and Biogeochemistry, Swedish University of Agricultural Sciences (2015)

External training at a foreign research institute

- Training on safe handling of electrical equipment and hazardous substances, and Hydrolabs for depth profiles, Institute of Meteorology and Climate Research Atmospheric Environmental Research (IMK-IFU), Garmisch-Partenkirchen, Germany (2016)

Management and Didactic Skills Training

- Young Professional (YP) of the 36th IAHR World Congress, support the organizations of different workshops and co-chairing in several sessions (2015)
- Supervising four MSc students with thesis (2014-2017)
- Teaching in the MSc course 'International Fieldtrip Water Chemistry' (2014)

Oral Presentations

- *Effects of reservoirs on nutrient stoichiometry and phytoplankton community*. PhD symposium at UNESCO-IHE, 29 September to 3 October, 2014, Delft, The Netherlands
- Effects of reservoirs on nutrient concentrations and ratios along the longitudinal gradient of Danube River Basin. American Geophysical Union, 14-18 December 2015, San Francisco, United States of America
- *Effects of reservoirs on nutrient stoichiometry*, PhD Seminar 2016 Institute of Meteorology and Climate Research Atmospheric Environmental Research (IMK-IFU), 20 July 2016, Garmisch-Partenkirchen, Germany
- *Effect of reservoirs with long and short residence time on nutrient concentrations in the upper part of the Danube River Basin*. Aquatic Sciences Meeting ASLO, 26 February– 3 March 2017, Hawaii, United States of America

SENSE coordinator PhD education

Dr. ir. Peter Vermeulen

IHE DELFT

Institute for
Water Education
under the auspices
of UNESCO

WAGENINGEN
UNIVERSITY & RESEARCH

Changes in Silica (Si) delivery to coastal systems, caused by human activities (e.g. reservoir construction and agricultural development) can cause shifts in phytoplankton community structure with impacts through the whole aquatic food web. Although nutrient exports of nitrogen (N) and phosphorous (P) and the impacts of human activity on these are relatively well understood, the extent and potential impact on the combined effects on Si, N, and P ratios are rarely evaluated simultaneously in one basin. I assessed the effects of natural and human controlling factors on nutrient loads and stoichiometry for Si, N, P in the Danube River and its tributaries. The overall findings of this thesis indicate that land use and land cover is the major controlling factor for Si export and its ratios with N and P at a basin scale, and that this factor tends to maintain overall P limitation in the basin. Moreover, analysis of data at Reni monitoring station just upstream from the Danube Delta showed that there has been a decrease in dissolved inorganic nitrogen (DIN) and dissolved Silica (DSi) loads from the entire Danube over time (since 2000), indicating a high risk of eutrophication in the Black Sea due to DSi reduction.

This book is printed on paper from sustainably managed forests and controlled sources

9 789073 445499

2023_IHE_COVER_PHD_SALCEDO.indd 1